Stan C.

NATIONAL COOPERATIVE HIGHWAY RESEARCH PROGRAM
REPORT 154

DETERMINING PAVEMENT SKID-RESISTANCE REQUIREMENTS AT INTERSECTIONS AND BRAKING SITES

TRANSPORTATION RESEARCH BOARD
NATIONAL RESEARCH COUNCIL

NATIONAL COOPERATIVE HIGHWAY RESEARCH PROGRAM
REPORT 154

DETERMINING PAVEMENT SKID-RESISTANCE REQUIREMENTS AT INTERSECTIONS AND BRAKING SITES

E. FARBER, M. S. JANOFF, S. CRISTINZIO,
J. G. BLUBAUGH, W. REISENER, AND W. DUNNING
THE FRANKLIN INSTITUTE
PHILADELPHIA, PA

RESEARCH SPONSORED BY THE AMERICAN ASSOCIATION OF STATE HIGHWAY AND TRANSPORTATION OFFICIALS IN COOPERATION WITH THE FEDERAL HIGHWAY ADMINISTRATION

AREAS OF INTEREST:

PAVEMENT DESIGN
PAVEMENT PERFORMANCE
HIGHWAY SAFETY
MAINTENANCE, GENERAL

TRANSPORTATION RESEARCH BOARD
NATIONAL RESEARCH COUNCIL
WASHINGTON, D.C. 1974

NATIONAL COOPERATIVE HIGHWAY RESEARCH PROGRAM

Systematic, well-designed research provides the most effective approach to the solution of many problems facing highway administrators and engineers. Often, highway problems are of local interest and can best be studied by highway departments individually or in cooperation with their state universities and others. However, the accelerating growth of highway transportation develops increasingly complex problems of wide interest to highway authorities. These problems are best studied through a coordinated program of cooperative research.

In recognition of these needs, the highway administrators of the American Association of State Highway and Transportation Officials initiated in 1962 an objective national highway research program employing modern scientific techniques. This program is supported on a continuing basis by funds from participating member states of the Association and it receives the full cooperation and support of the Federal Highway Administration, United States Department of Transportation.

The Transportation Research Board of the National Research Council was requested by the Association to administer the research program because of the Board's recognized objectivity and understanding of modern research practices. The Board is uniquely suited for this purpose as: it maintains an extensive committee structure from which authorities on any highway transportation subject may be drawn; it possesses avenues of communications and cooperation with federal, state, and local governmental agencies, universities, and industry; its relationship to its parent organization, the National Academy of Sciences, a private, nonprofit institution, is an insurance of objectivity; it maintains a full-time research correlation staff of specialists in highway transportation matters to bring the findings of research directly to those who are in a position to use them.

The program is developed on the basis of research needs identified by chief administrators of the highway and transportation departments and by committees of AASHTO. Each year, specific areas of research needs to be included in the program are proposed to the Academy and the Board by the American Association of State Highway and Transportation Officials. Research projects to fulfill these needs are defined by the Board, and qualified research agencies are selected from those that have submitted proposals. Administration and surveillance of research contracts are responsibilities of the Academy and its Transportation Research Board.

The needs for highway research are many, and the National Cooperative Highway Research Program can make significant contributions to the solution of highway transportation problems of mutual concern to many responsible groups. The program, however, is intended to complement rather than to substitute for or duplicate other highway research programs.

NCHRP Report 154

Project 1-12 FY '70
ISBN 0-309-02306-8
L. C. Catalog Card No. 75-1795

Price: $4.40

Notice

The project that is the subject of this report was a part of the National Cooperative Highway Research Program conducted by the Transportation Research Board with the approval of the Governing Board of the National Research Council, acting in behalf of the National Academy of Sciences. Such approval reflects the Governing Board's judgment that the program concerned is of national importance and appropriate with respect to both the purposes and resources of the National Research Council.

The members of the advisory committee selected to monitor this project and to review this report were chosen for recognized scholarly competence and with due consideration for the balance of disciplines appropriate to the project. The opinions and conclusions expressed or implied are those of the research agency that performed the research, and, while they have been accepted as appropriate by the advisory committee, they are not necessarily those of the Transportation Research Board, the National Research Council, the National Academy of Sciences, or the program sponsors.

Each report is reviewed and processed according to procedures established and monitored by the Report Review Committee of the National Academy of Sciences. Distribution of the report is approved by the President of the Academy upon satisfactory completion of the review process.

The National Research Council is the principal operating agency of the National Academy of Sciences and the National Academy of Engineering, serving government and other organizations. The Transportation Research Board evolved from the 54-year-old Highway Research Board. The TRB incorporates all former HRB activities but also performs additional functions under a broader scope involving all modes of transportation and the interactions of transportation with society.

Published reports of the

NATIONAL COOPERATIVE HIGHWAY RESEARCH PROGRAM

are available from:

Transportation Research Board
National Academy of Sciences
2101 Constitution Avenue, N.W.
Washington, D.C. 20418

(See last pages for list of published titles and prices)

Printed in the United States of America.

FOREWORD

By Staff
Transportation
Research Board

The findings of the experimental program described in this report add substantially to the body of knowledge concerning driver-vehicle-pavement interaction as it relates to safe automobile maneuverability on wet pavements. Instrumentation and procedures for determining pavement skid-resistance requirements at intersections and other braking sites are described, and they can be used by highway agencies (1) to determine the relative skid-resistance requirements (normal, intermediate, or high) for specific braking sites, and (2) to study existing problem sites in terms of probable causes of accidents and the influence of proposed corrective measures. Additional research and field evaluation efforts are necessary to further develop and verify procedures for determining skid-resistance requirements at curves and other types of sites in a more precise manner. Personnel involved in highway safety programs and concerned with reducing accidents will find this document useful because it reports on research findings having immediate applicability to practice in some degree. It will also be useful and of interest to researchers in the fields of driver behavior, vehicle and tire influences on automobile maneuverability, and pavement surface characteristics.

A crucial question in the highway safety problem area is the level of skid resistance that should be available on highway pavements to provide for safe operation of motor vehicles. Dry pavements are usually quite adequate in this regard, but the skid resistance of wet pavements, which is one of the critical factors of traffic safety, is often of questionable adequacy for traffic conditions. The construction and maintenance of all pavements with wet skid-resistance properties comparable to those of dry pavements would not in most cases result in best use of available materials and funds because of the extremely high cost in relation to possible benefits. Realistic pavement skid-resistance requirements should be dictated by actual traffic needs at a particular site. Thus, the objective of the research described herein was to provide highway departments with methods for determining pavement skid-resistance requirements for any given set of roadway and traffic conditions.

The Franklin Institute Research Laboratories' approach to development of procedures for determining skid-resistance requirements was based on the premise that measurable empirical relationships exist between the longitudinal and lateral accelerations resulting from vehicle maneuvers and pavement skid-resistance requirements. To evaluate this premise, it was first necessary to develop instrumentation to measure vehicle acceleration values at highway sites without influencing the driver behavior and vehicle operation. This was followed by skid studies using instrumented vehicles performing braking, cornering, and combination maneuvers on pavement surfaces with measured skid resistance and the correlation of the data with field-measured accelerations.

The research was successful in that instrumentation for measuring acceleration values of vehicles at highway sites was developed and field tested. Furthermore, procedures were developed and shown to be feasible for converting, in a relative manner, measured longitudinal accelerations at intersections braking sites

to skid-resistance requirements. The report also describes a simplified Intersection Demand Model (IDM) for estimating skid-resistance requirements at intersections on the basis of speed, traffic count, and stopping distance data collected at the site. Additional field evaluation is necessary to determine more precisely the skid-resistance requirements at intersections and to evaluate ability of the procedure to identify hazardous locations before they become high-accident sites. When it is not feasible to use either the Tapeswitch system or the Intersection Demand Model to determine pavement skid-resistance requirements, the information in Table 5 can provide general guidelines for minimum requirements. It must be recognized that *these guidelines are very tentative because they are based on extremely limited field data* (12 intersections in the eastern Pennsylvania and New Jersey area).

The limited study of cornering maneuvers indicates that not enough is presently known about the relationship between lateral accelerations and pavement surface characteristics to permit development of procedures for determining skid-resistance requirements for highway curves. The problem is made particularly complex by the rather extreme, and yet undetermined, influence of vehicle tires.

Other recent NCHRP publications concerned with the reduction of wet-pavement skidding accidents are *NCHRP Synthesis 14,* "Skid Resistance," and *NCHRP Research Results Digest 61,* "Wear-Resistant and Skid-Resistant Pavement Skid Tester Correlation and Calibration Techniques."

CONTENTS

1 SUMMARY

PART I

3 CHAPTER ONE Introduction and Research Approach
Problem Statement
Research Approach

5 CHAPTER TWO Findings
Research Plan
Vehicle Acceleration Measurement System
Research on Driver Demand
Skid Studies
Skid Resistance Required to Accommodate the Measured Deceleration Profiles

25 CHAPTER THREE Interpretation and Applications
Introduction
Development of the Intersection Demand Model
Application of the Intersection Demand Model
Tentative Skid-Resistance Requirements for Intersections

32 CHAPTER FOUR Conclusions and Recommendations
Conclusions
Recommendations
Recommendations for Further Research

33 REFERENCES

PART II

34 APPENDIX A Literature Review

40 APPENDIX B Required Skid Number, Deceleration, and Speed Profile Plots for Study Intersections

53 APPENDIX C Measuring Lateral Acceleration Profiles on Curves

ACKNOWLEDGMENTS

The research reported herein was conducted by the Operations Research Laboratory of the Systems Science Department, The Franklin Institute Research Laboratories (FIRL), with Eugene Farber, Senior Research Scientist, as Principal Investigator. (Mr. Farber is currently with the Ford Motor Co., Dearborn, Mich.) He was assisted by Michael S. Janoff, Suzanne Cristinzio, John G. Blubaugh, William Reisener, and Warren Dunning.

Appreciation is expressed to Professor W. A. Myers, Pennsylvania State University, and Dr. Bernard Siskind, Temple University, for their advice and consultation, and to Dr. Don Ivey and staff members of the Texas Transportation Institute who aided in performing skid tests at that facility.

Credit also is extended to Kenneth Fertner and John Price of the FIRL staff who conducted the Tapeswitch experiments and to others of the project staff who participated in the design of the research program, the data collection and analysis, and preparation of the final report.

DETERMINING PAVEMENT SKID-RESISTANCE REQUIREMENTS AT INTERSECTIONS AND BRAKING SITES

SUMMARY

The objective of the research reported here was to provide highway agencies with methods for determining minimum skid-resistance requirements for any given set of roadway conditions. Because wet-pavement skidding accidents occur most frequently at intersections and on curves, the study was primarily concerned with such situations. The experiments to determine skid-resistance requirements at intersections were successful, whereas similar experiments related to curves were only partially so. Therefore, this report is primarily concerned with the development of a measuring system and procedure for determining skid-resistance requirements at intersections. The work related to curves is reported in Appendix C.

A pavement can be considered deficient in skid resistance only in relation to the demand of traffic upon it. Skidding can occur on a dry pavement when one attempts a sufficiently violent maneuver, such as braking to a stop from 60 mph in 100 ft or negotiating a 200-ft radius curve at 60 mph. Such demands can arise in an emergency or as a consequence of extremely poor driving, but the resulting skids cannot be blamed on the pavement. It is only when skidding occurs as a consequence of maneuvers that are within the range of normal demand (accelerations, braking, and cornering by a majority of drivers under normal traffic conditions) or intermediate demand (last-minute brake or steering corrections caused by inattention, misjudgment, or unusual incidents) that the pavement skid resistance should be considered inadequate. Realistic skid-resistance requirements are those that will accommodate all normal demand and a great majority of intermediate demand for the prevailing conditions of the site. Data gathered during this study indicate that 99 percent of the observed drivers are in the normal or intermediate demand categories.

The approach to the determination of skid-resistance requirements for a site involves three steps:

1. Measure the longitudinal and lateral accelerations (g forces) developed by automobiles using the site. Assume that these in situ measurements are a reasonable representation of driver demand.
2. Conduct skid studies to develop approximate empirical relationships between maximum accelerations at skidding on standard pavement surfaces when wet and the skid resistance (SN_{40}) of the surfaces.
3. Combine the results of measurements in steps 1 and 2 to determine the skid numbers of surfaces that would accommodate driver demand.

The system developed for measurement of longitudinal acceleration at intersections is based on the use of a series of Tapeswitch * event detectors to determine

* Tapeswitch is a trade name for a pressure-sensitive electrical strip switch that can be placed on the pavement as a vehicle detector in the same manner as a pneumatic tube.

the time-position signature of a vehicle over a known distance, from which acceleration values can be computed. A series of 16 lengths of Tapeswitch were accurately placed on a street pavement at prescribed intervals for a distance of about 400 ft in advance of the stop point and the recorded data were collected and processed by electronic equipment. A study was conducted to determine the accuracy of the acceleration values computed from the time-position data by driving an instrumented vehicle over an installed Tapeswitch system and comparing the computed values with data from the accelerometer installed on the vehicle. Over a range of 0.03 *g* to 0.48 *g*, the computed values were within 0.02 *g* of the measured values. Studies were conducted to evaluate the influence of the Tapeswitch installation on driver behavior and the relationship between data collected on wet versus dry pavements. Although the results were based on limited data, it was concluded that the influence of these factors is of no practical significance, particularly in view of the accuracy of various other parts of the over-all procedure. Consequently, most data collected at the 12 intersection sites were from dry pavements with the full 16-section system. Regarding the wet versus dry pavement data collection, an important consideration is that many drivers attempting to brake at or near peak demand on a wet pavement are likely to skid; thus, the highest deceleration values measured would be the maximum permitted by the wet pavement rather than the actual driver demand.

Data were collected for an average of 350 vehicles at each of the 12 intersection sites located in eastern Pennsylvania and New Jersey, and longitudinal accelerations were computed for various distances from the stop line.

Controlled skid studies to determine the relationships between longitudinal acceleration and pavement skid-resistance requirements were conducted by FIRL personnel at the Texas Transportation Institute using seven skid pads of varying surface characteristics. Two instrumented automobiles, a 1970 Plymouth Fury and a 1971 Ford Mustang, were used for the skid tests. Three sets of tires (conventional bias ply, belted bias ply, and radial) were used on the Plymouth, and belted bias-ply tires only were used on the Ford. All tires were relatively new. For the purpose of developing correlations, the skid resistance of each test pad was measured as a skid number (SN) at 20, 40, and 60 mph using a locked-wheel skid tester in general conformance with ASTM E 274.

It is apparent from analysis of the braking data that complex interactions exist between pavement surface characteristics, speeds, tires, and vehicles. No tire/vehicle combination produced the highest longitudinal acceleration for all surfaces and all speeds. However, a plot of maximum deceleration (negative longitudinal acceleration) versus skid number (see Fig. 22) was developed in which each point is the worst case from among the four tire/vehicle combinations at each of the speeds for each of the seven skid pads used for the correlation. Each point represents the average of six skid tests. This plot was used to convert the measured accelerations to skid-resistance requirements.

The measured accelerations for the 12 intersection sites studied during the project were converted to required skid resistance using the FIRL procedure. The 99th percentile computed skid-resistance requirements ranged from SN_{40} values of 32 to 57. The procedure can be useful in determining whether a particular site is in a category requiring normal, intermediate, or high skid resistance (see Table 10).

It appears that the observation of driver demand in traffic is a rational basis for establishing skid-resistance requirements. The Tapeswitch system does show promise for measuring in situ acceleration profiles, at least at intersections. The equipment and procedure can be used immediately to measure the *relative* demand

for skid resistance at various sites. For example, the recommended measurements can be used to identify unsafe conditions at a given site before that site becomes a high-accident site. Anomalously, high acceleration demand at one site relative to others indicates a need for skid-resistance improvement. The approximate relationships between measured acceleration demand and required skid resistance given herein are valuable as design guidelines in making such improvements. Points of peak demand can be isolated and regarded as the bases for beneficial spot improvements at minimum cost.

Although the procedures developed during this project are based on limited data collected in one locality, they have undergone limited field evaluation and represent the best currently available approach for estimating skid-resistance requirements at braking sites. Pilot implementation of the procedures is encouraged so that potential users have firsthand knowledge of their ability to recognize both potential high-accident sites and relative needs for wet-pavement skid resistance.

CHAPTER ONE

INTRODUCTION AND RESEARCH APPROACH

PROBLEM STATEMENT

In driving, the forces required to maintain speed against wind, rolling resistance and grades, and to effect controlled changes of speed and direction are transmitted between tire and pavement. The maximum force that can be transmitted depends on tire/pavement friction. The lower the coefficient of friction between tire and pavement, the greater likelihood that the forces associated with normal maneuvering will exceed the capacity of the interface to transmit them, and hence the greater the likelihood of a skid. With few exceptions, the skid resistance * of dry pavements is adequate for normal maneuvers. It is generally only on wet pavement that skid resistance becomes low enough to be a serious problem. Under any given set of circumstances, the likelihood of a skid depends not only on pavement surface properties but also on the characteristics of the tires and the vehicle as well as the nature of the maneuver as determined and constrained by road geometry, control features, and traffic conditions.

Although systematic and comprehensive accident data bearing on this problem are lacking, it is clear that skidding accident rate increases as pavement skid resistance decreases (*1-3*). In areas of high annual rainfall, wet-pavement skidding accidents account for up to 30 percent of all wet-pavement accidents and 6 percent of all accidents (*1*). These findings cannot be explained by the poorer visibility that frequently accompanies wet pavements. One study revealed a correlation coefficient of —0.92 between wet-pavement skid-resistance values and the frequency of accidents. Further, a number of before-and-after studies have shown substantial decreases in wet-pavement skidding accident frequencies following grooving or resurfacing (*4-7*). As indicated by these and other studies, the problem is amenable to remediation. While techniques and materials exist for improving the skid-resistance performance of pavements, the arbitrary application of this technology does not constitute a meaningful solution to the problem. A wet pavement is deficient in skid resistance only in relation to the demands of traffic. Prior research concerning driver demand is discussed in Appendix A.

* The characteristic of a pavement surface that contributes to tire/pavement friction.

RESEARCH APPROACH

The Franklin Institute Research Laboratories (FIRL) approach is based on the relationship between vehicle acceleration and tire/pavement friction. The coefficient of friction required to transmit the forces associated with a given maneuver under a given set of conditions is termed the friction number (FN) given by

$$FN = 100(F/W) \tag{1}$$

where F is the sum of all horizontal forces acting on all vehicle wheels and W is vehicle weight. Since

$$F = ma = \frac{W}{g}a \tag{2}$$

where m is the mass; a is acceleration, in feet per second squared; and g is the gravitational constant (32.2 ft/sec^2), it follows that

$$FN = 100(a/g) = 100G \quad (3)$$

which states that the friction required to accommodate a given level of acceleration is equivalent to the acceleration, G, expressed in units of the gravitational constant (i.e., $G = a/g$).

The term *acceleration* is used generically to denote any change in vehicle velocity vector produced by braking, cornering, or forward acceleration. In addition, any external force, such as wind or gravity (on grades and crowns), that requires a brake, throttle, or steering wheel adjustment to maintain steady-state speed or track can be expressed as a component of acceleration. Note that the acceleration arising from all these components is a vector sum, or

$$G = \sqrt{G_L^2 + G_R^2} \quad (4)$$

where G_L is the sum of all longitudinal components, and G_R is the sum of all radial (lateral) components. The effect of grade, expressed as G, is given simply by the slope, expressed as the tangent of the grade (i.e., the acceleration required to maintain constant velocity on a 4-percent grade is 0.04 g). The effects of wind and rolling resistance can be similarly expressed. These considerations are discussed in more detail in subsequent sections.

The longitudinal acceleration (observed from outside the vehicle) associated with braking and forward acceleration is

$$G_L = \underset{\Delta t \to 0}{\text{limit}}\ \Delta V/32.2\ \Delta t \quad (5)$$

where ΔV is the change in speed, in miles per hour, over the time interval Δt. In cornering, the lateral acceleration is

$$G_R = V^2/15R \quad (6)$$

where V is speed, in miles per hour; and R is the radius of the curve, in feet.

Up to this point, the terms skid resistance, pavement friction, and tire/pavement friction have been used somewhat interchangeably. Actually, the term pavement friction is a misnomer because the coefficient of friction is a property of two surfaces—in the present case, the pavement and the tires—influenced by a variety of other conditions. Thus, when the expressions pavement friction or skid resistance are used, they are meaningful only when the tire and other conditions of measurement are specified. Or, to put it another way, skid resistance can be considered to be a property of the pavement only when all other conditions of measurement are held constant. The various expressions for skid resistance used herein refer to the friction between the road and a given tire measured under given sets of conditions.

Many methods exist for quantifying skid resistance. These include automobile stopping distance, skid trailers, and static testers, such as the British Pendulum Tester. Note that, according to Eq. (3), the maximum acceleration achievable on a given surface is also a definition of pavement friction. The method of skid-resistance measurement in widest use in this country as a standard is the skid trailer. A standard trailer and tire and a standard set of procedures is specified by ASTM (*11*). The pavement friction coefficient measured in this way is termed the skid number (SN). The skid number is a sliding (locked-wheel) coefficient and is usually measured at 40 mph. The value thus obtained is designated SN_{40} and is roughly equivalent to the friction number defined in Eq. (1).

Because values of skid numbers observed at a given location vary with speed and the measurement conditions, the relationship between SN and FN is not on a one-to-one basis; the relationship must be established empirically. Nevertheless, the equivalence of FN and G provides a convenient definition of driver demand on pavement friction (i.e., acceleration at a given speed). For a more thorough and comprehensive discussion and review of vehicular acceleration and skid resistance, the reader is urged to consult *NCHRP Report 37* (*1*).

In most driving situations, typical levels of lateral as well as positive and negative longitudinal acceleration are well within the capabilities of the driver/vehicle/roadway system. In normal braking and cornering behavior, a driver is governed by what seems comfortable and prudent rather than by his car's physical limits of adhesion. The problem arises when a driver attempts to execute a maneuver that requires a greater friction coefficient than is instantaneously available. When this occurs, the vehicle skids and the driver partially or completely loses directional control and stopping power.

Situations in which the demand on tire/pavement friction exceeds the supply arise in normal driving as well as under emergency conditions. Drivers probably are at least partially sensitive to the braking and cornering capabilities of their own vehicles, and vehicle characteristics probably influence normal maneuvering behavior. However, drivers are probably less sensitive to pavement skid-resistance levels. Wet-pavement skid resistance varies considerably from road to road and in the same road from time to time (*1*). Beyond anticipating that a wet pavement provides less control than a dry pavement, drivers have no way of knowing how much pavement friction is available in a given situation. To the extent that a driver is insensitive to time-to-time and point-to-point changes in skid resistance, his demand on skid resistance will be independent of the supply. The prevalence of wet-pavement skidding accidents and the generally high correlation between wet-pavement friction coefficients and skidding accidents strongly suggest that this is often the case; that is, for some percentages of "normal" maneuvers, the friction forces available will be less than what is demanded. Ultimately, the prevalence of normal driving skids depends on the frequency distribution in the driver population of the peak values of acceleration that occur in normal wet-weather driving and on the range and distribution of wet-pavement friction levels. Kummer and Meyer (*1*) have used analytically derived estimates of such distributions to project an estimate of 100 skids per 10,000 vehicle-miles arising out of normal demand on roads with a skid number of 20; these estimates are based on observations of the braking performance of a single driver whose model deceleration demand in coming to a full stop was 0.2 g. Fewer than 5 percent of these driver braking maneuvers exceeded a deceleration value of 0.4 g, and this value (multiplied by $100 = 40$) was recommended as a minimum skid number of normal driving.

However, some drivers brake and corner harder than

others in normal driving, and a skid number of 40 is not necessarily adequate for all, or even most, drivers and situations. Further, different driving situations impose different friction requirements. The forces transmitted by a tire of a vehicle traveling at 60 mph on a tangent roadway are substantially less than the forces transmitted when the same vehicle brakes for a traffic signal. It is probably economically unfeasible to establish a single high skid number to meet every possible driver need on all primary rural highways. Designing or treating pavements for high levels of skid resistance is expensive, as is the cost of maintaining the design level. Local skid numbers should thus reflect local demands, which, as will be shown vary both with maneuver mode (braking, cornering, and forward acceleration done singly and in combination) and with factors such as approach speeds, traffic volume, road configuration, and traffic controls. For any given site, therefore, the skid resistance required for normal driving is that which will accommodate the demand associated with some substantial percentage (99 percent, for example) of the traffic maneuvers at that site.

The project requires that the research address "emergency" as well as normal skid-resistance needs of traffic. This is a difficult requirement to comply with because there is no systematic basis for defining emergency requirements. To specify an emergency level of skid resistance, it would be necessary to specify the longitudinal and/or lateral acceleration demanded by the driver. This in turn is a function of the speed and distance relationships between the driver's vehicle and the other vehicles or objects that gave rise to the emergency. For example, consider a situation in which a driver, who has not been paying attention to the road and who is traveling at 60 mph, suddenly finds himself 200 ft from the rear of a stationary vehicle on an expressway in which all other lanes are blocked. In order to stop in time, he must brake at an average deceleration of 0.6 *g* (neglecting reaction time). However, if the closing distance were 100 ft, the pavement would have to accommodate 1.2 *g*'s, which is simply beyond the state of the art for anything but a racing car on dry pavement. If the distance were only 50 ft, the required deceleration would be 2.4 *g*'s, which is beyond the capability of any tire/road/vehicle combination present or contemplated. Thus, whatever level of deceleration is specified, it is always possible to define an emergency situation which requires more. Because there is no basis for selecting any one emergency demand as more likely than any other, emergency avoidance situations provide no basis for establishing an emergency level of skid resistance.

The only meaningful specification for emergency friction levels is whatever is theoretically feasible with due consideration given to the economics of implementation. A reasonable alternative, proposed in this report, is to "provide adequate skid resistance for all normal driving maneuvers and 99 percent of measurable, intermediate demand-type maneuvers."

In order to establish skid-resistance requirements for a given site, two sets of data are needed. First, because demand on pavement friction is defined as acceleration, it is necessary to determine that level of lateral or longitudinal acceleration that constitutes the controlling or reasonable worst-case demand. The most convenient meaning that can be attached to "controlling or reasonable worst-case demand" is that level of acceleration arising out of normal driving behavior below which the great majority of acceleration values fall (i.e., the *p*th percentile acceleration level). Second, data are required that will permit specification of the minimum skid-resistance level that will accommodate the controlling demand. This is necessary because, as pointed out earlier, acceleration and the level of skid resistance expressed as a skid number required to accommodate it are not numerically equivalent and the relationship must be established empirically.

RESEARCH OBJECTIVES

These requirements are the basis of the research program carried out by FIRL. Most of the research was devoted to (1) developing and collecting data with a vehicle acceleration measuring system, and (2) establishing empirical relationships between acceleration and the minimum accommodating pavement friction levels.

The procedures used in achieving the research objectives are discussed in Chapter Two.

CHAPTER TWO

FINDINGS

RESEARCH PLAN

The research program was accomplished in three phases. During the first phase, the requirements for a system to measure in situ vehicle acceleration were defined. Candidate systems to meet these requirements were developed and tested. The most promising system was one utilizing Tapeswitch event detectors. Although this system is discussed, highly technical information concerning the Tapeswitch data recording system and computer programs can be found elsewhere.*

* Appendix B, "Tapeswitch Data Recording System," and Appendix C, "Computer Programs for Reduction of Tapeswitch Data," of the agency's final report are not published with this report. However, copies of the original report are available on request to the Program Director, NCHRP.

During the second phase, the Tapeswitch system was used to measure the acceleration profiles of drivers in actual traffic situations. A total of 24 sites of five different types were instrumented. These included:

- Twelve intersections.
- Five two-lane highway curves.
- One freeway curve.
- Four freeway entrance curves.
- Two deceleration lanes.

The measurement procedure for intersections is discussed herein. Figures B-1 through B-12 of Appendix B show summary data for required skid number, deceleration, and speed profiles for intersections. Measurements for curves are discussed in Appendix C.

During the third phase, FIRL conducted skid tests at the Texas Transportation Institute (TTI) skid pad facility. The purpose of the tests was to establish the wet-pavement skid resistance required to accommodate various levels of vehicular acceleration. Those tests applicable to intersections are discussed herein, and other tests are discussed in Appendix C.

VEHICLE ACCELERATION MEASUREMENT SYSTEM

Acceleration is most easily and accurately measured internally by vehicle-mounted accelerometers. This method has several distinct advantages. It is easily developed, presents a minimum of operational problems in the field, measures instantaneous values of acceleration, and can be used to record maneuvers under traffic and geometric conditions that are not amenable to external instrumentation. Although an instrumented vehicle was developed and used throughout the program for various purposes, most of the demand data was recorded by an external system.

The advantages of an external system are two. First, economic constraints preclude the instrumentation of enough vehicle/driver combinations to obtain a statistically reliable sample. An external measurement system is much less expensive to implement on a per-vehicle basis. Second, it is extremely difficult to perform meaningful experiments with an instrumented vehicle and, at the same time, prevent subject drivers from knowing that their behavior is being observed. As in any behavioral study, the extent and direction of the effect of this knowledge on performance is unpredictable. Thus, conclusions about pavement skid-resistance requirements that rely solely on data obtained from subject-driven, instrumented vehicles may be susceptible to considerable bias. An external, passive measurement system allows the collection of data relatively free from driver bias. For these reasons, it was concluded that an objective, empirical, and economical determination of driver demand for pavement skid resistance is best accomplished by passively measuring the acceleration behavior of traffic as it passes through a site.

Before describing the external measurement system developed by FIRL, it will be useful to discuss additional performance requirements.

Acceleration Measurement Requirements

Average longitudinal acceleration (negative, or braking deceleration, as well as positive) can be determined by measuring changes in speed over some interval of time (see Eq. 5). Lateral acceleration is defined by speed and radius of curvature (see Eq. 6). Although cornering speed can be measured instantaneously by radar, the curvature of a vehicle's path must be determined by measurements made over some finite interval. Hence, values of both lateral and longitudinal acceleration computed from external time, speed, and distance measurements will be average values. However, average acceleration when measured over an interval exceeding a few seconds is a poor representation of demand because a maneuvering automobile's profile of acceleration over time is not smooth. Peaks may occur whose amplitudes are considerably greater than the average. Because it is the peak value and not the average that constitutes the controlling demand, it is evident that the system must be capable of measuring acceleration over sufficiently brief intervals to permit resolution of major peaks in an acceleration trace. Results of pilot studies with an instrumented vehicle indicate that, in both braking and cornering, a time resolution of from 1.5 to 2.0 sec is adequate. Inspection of cornering and braking acceleration traces recorded under actual traffic conditions (see Fig. 1) revealed that, over a 2-sec interval with an average acceleration in excess of 0.25 *g*, peak values of acceleration were generally within 0.02 *g* of the average. Over intervals of 5 sec, peak values are as much as three times the average. Thus, it is clear that time resolution on the order of 1.5 to 2.0 sec or better is required for an adequate representation of demand.

However, it is not sufficient to measure acceleration over a single interval. Both braking deceleration and cornering acceleration can vary with location in the site. Further, the pavement skid resistance required to accommodate a given level of acceleration depends on speed. Hence, both acceleration and speed must be measured at a number of points in the site to provide acceleration and speed profiles. Pilot data recorded in traffic from the instrumented vehicle show that braking for an intersection generally begins within 400 ft of the stop line and the heaviest braking occurrs within the last 250 ft. These data indicate that braking deceleration at intersections should be sampled at a number of points over a 400-ft interval.

Another important consideration is the required accuracy of the system. It is believed that the measurement accuracy provided by the system should be at least twice as good as current state-of-the-art skid trailers to allow for future improvements in trailer performance. Although skid trailer performance varies widely, standard deviations of SN_{40} values for the better instruments in recent tests range from 2.0 to 5.0 with between-trailer 95-percent confidence limits of about ten (*11*). More recent tests with the National Bureau of Standards' (NBS) trailer (Texas Transportation Institute, March, 1971)* resulted in 95-percent confidence limit of SN_{40} values of approximately ± 5. On the basis of these data, it was decided that measurements of acceleration should be accurate to within $\pm$ 0.025 *g*.

* Personal communication: A. Niel, National Bureau of Standards.

Two other considerations strongly influenced the approach to the development of the system: (1) that the system's data output be amenable to rapid processing, and (2) that the system be simple to set up, use, and remove.

In summary, the performance requirements established for the system were:

1. Accuracy of ± 0.025 g.
2. Resolution of 1.5 to 2.0 sec.
3. Area of coverage (braking sites) was 400 ft to the stopping point.
4. Capability for measuring speed and acceleration at a number if different points in the interval.
5. Raw data amenable to rapid processing.
6. Simplicity in application.

The FIRL vehicle acceleration measuring system and its development are described. The system, originally developed to measure braking deceleration, was subsequently adapted to measure lateral acceleration on curves. Applications to lateral acceleration measurements are discussed in Appendix C.

Measuring Longitudinal Acceleration

Average longitudinal acceleration can be determined by measuring time-rate-of-change of speed or, less directly, time-rate-of-change of position. Speed can be sensed directly by Doppler radar, but economically feasible, commercially available units (of the type used by the police) are not sufficiently accurate or selective. However, time-position data can be measured with considerable accuracy by several different methods. For this reason all of the methods that were seriously considered were based on the measurement of position and time.

To determine average acceleration, $\bar{a}$, over a given interval, a minimum of three time-position points is required. The smaller the interval defined by successive points, the more nearly the derived value of the acceleration approaches an instantaneous value. The fundamental problem in developing any event detection system is that as the distance (or time) interval over which $\bar{a}$ is determined decreases, the accuracy requirements for measuring the time intervals and placing the detectors increase.

A thorough error sensitivity analysis of the time/position system was performed to determine the effect of errors in time and position measurement on errors in computed acceleration values. The analysis, which is generalized to consider both three- and four-point detector systems,* is summarized in Figure 2. Figure 2 shows a plot of the error rate as a function of the time length of the station for three- and four-point systems. Error rate is expressed as $\Delta a/\Delta X$ in g's per inch (i.e., the error in computed acceleration per inch error in position measurement). An error in position measurement of X means that the first distance interval is actually X inches larger (or smaller) than measured and the last distance interval is X inches smaller (or larger) than measured respectively.

* A three-point system measures position and time of three points across an interval. A four-point system consists of two pairs of points in which each pair constitutes a velocity measuring station. The advantage of the four-point approach is that the distance between velocity stations need not be measured with fine accuracy.

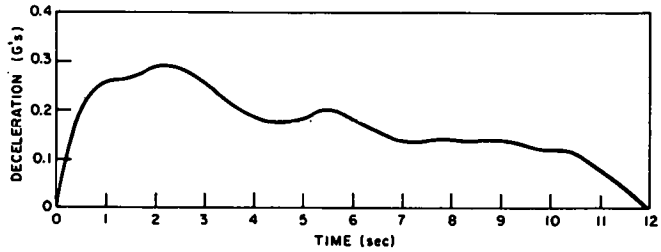

Figure 1. Typical braking deceleration trace.

Except at very short intervals, the three-point detector system is considerably less sensitive to position errors than the four-point detector system. At a 1-sec interval, the three-point detector system is four times as accurate as the four-point detector system when $V = 60$ mph. For a four-point system, the error rates are approximately 0.03, 0.06, and 0.09 g per inch at speeds of 20, 40, and 60 mph, respectively.

A similar analysis was performed for temporal errors. The analysis showed that acceptable accuracy in estimating

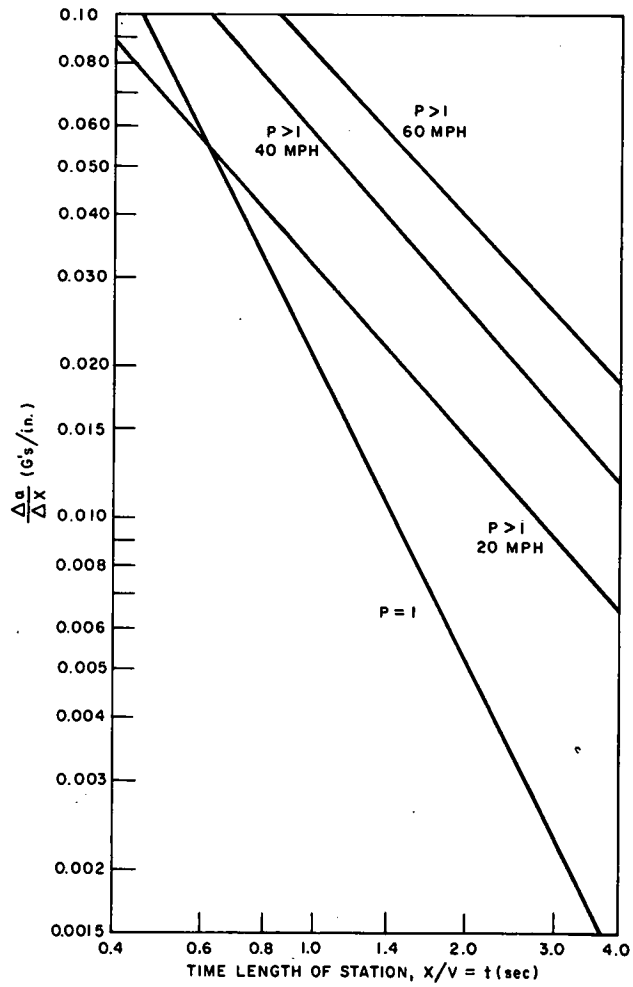

Figure 2. $\Delta a/\Delta X$ as a function of X/V for P=1 (three-point system) and P > 1 (four-point system).

the effect of temporal errors can be obtained by substituting $V_0\Delta t$ for ΔX in the above expression. Since 60 mph is very nearly equal to one inch per millisecond, the $P = 1$ and $P > 1$, 60-mph curves in Figure 2 can be used directly to estimate $\Delta a/\Delta t$ as a function of measurement interval time length for vehicles traveling at 60 mph. The relationship between the two detector configurations is basically the same for temporal as for spatial errors. Which approach is better depends on the nature of the measurement system. In general, the four-point detector system is feasible only in a system that provides extremely accurate measurement of time (i.e., $\Delta t << 0.001$ sec). For this reason, it was decided to concentrate on the three-point approach.

Over a time interval of 1.5 sec, the error rate for a three-point detector system is 0.01 g per inch. Thus to achieve ± 0.025-g accuracy in measuring acceleration over such an interval, the distances over which time is measured must be known to within 2½ in.

Instrumentation Approaches

FIRL originally proposed to use television as the basis of a system for measuring acceleration. The principle behind the application of TV to this problem is that TV raster lines can be made to serve as event detectors. Traffic at a site would be recorded on TV tape for subsequent laboratory analysis to determine the times at which each raster line was interrupted and thus obtain fine-grained time/position data for computer reduction. The advantages of this approach are that the data are amenable to automatic processing in the laboratory, and, in theory, fine time resolution is possible. However, further research on this approach revealed that uncertainty of the exact location of the raster lines and other distortion effects would result in position errors that would produce order-of-magnitude acceleration errors.

When it became evident that development of the TV system would be costly and the results unpredictable, a number of alternative approaches were evaluated. The most important of these were photography and discrete detectors. The final system developed was based on the use of discrete Tapeswitch detectors. However, it will be useful to consider the alternatives and to discuss the problems that resulted in their rejection.

Conventional time-lapse photography is sufficiently precise to meet the accuracy and time-resolution requirements. However, conventional photographic techniques were never seriously considered because the data reduction would be far too slow for the volume of data anticipated.

Photographic data in a form better suited to the requirements of the present program are obtainable by using a time-displacement (TD) camera, which is a shutterless camera with a narrow slit aperture the width of the film. The film is driven past the aperture at constant speed, and only that part of the image appearing through the aperture is recorded on the film. In the present application, the camera is mounted so that the 0.001-in. slit is parallel with the road and its field of view intercepts passing vehicles just below their cabs. The recorded image of a passing vehicle takes the form of a streak whose leading edge constitutes a continuous plot of longitudinal position versus time. The vertical dimension is time and the horizontal dimension is longitudinal position. A stationary car produces a vertical streak as does any stationary object. A vehicle traveling at infinite velocity would produce a horizontal streak. For any given camera setup (field of view, film speed), the slope of the streak represents velocity.

As with any photographic approach, the major drawback is that distortion, even in the highest quality lenses, and variations in the scale factor across the field of view of the lens make it difficult to achieve the accuracy required by determining distance from absolute measurements of intervals on the image. This problem can be eliminated simply by placing targets at measured intervals in the field of view. The targets produce an easily identifiable vertical streak on the film and function essentially as event detectors. Since the actual distance between targets is known, the problem is reduced to measuring the time required for a vehicle to cross intervals between successive targets.

A TD camera was procured and field-tested. The tests consisted of driving the instrumented vehicle through the TD camera's field of view at constant speeds and under various levels of braking and acceleration. During the test runs, vehicle speed and acceleration data were recorded from vehicle-mounted sensors. The film records were then reduced on a film reader to obtain a series of time/position points from each record. The time/position data were further processed by a computer to make the necessary geometric corrections for lens optics. Acceleration values were computed from the computer-corrected position data by two means. The first method was to fit 25 time/position points to a high-order (5th or 7th) polynomial, which was then differentiated twice to obtain the velocity and acceleration polynomials. The second method was to consider three successive time/position points at a time and compute the first and second differences to obtain velocity and acceleration values. The computed acceleration data were compared with the corresponding data obtained from the vehicle accelerometer.

The results of the tests were extremely disappointing. Neither method of computing acceleration produced acceptable results. The camera data were obviously grossly in error and bore little resemblance to the corresponding accelerometer data collected by the instrumented vehicle passing through the camera's field of view. In general, it was not possible to visually match corresponding camera and accelerometer records. In many instances, the computed acceleration values were in error by an order of magnitude. The computer program was refined to correct for optical lens distortion and the effects of the changing slant range between vehicle and camera. However, these changes did not result in a substantial change in the quality of the acceleration data. Figure 3 shows a typical plot of acceleration versus time in a constant velocity run. The true acceleration is always within ± 0.03 g of zero, while the values computed from camera data range between ± 0.25 g.

In analyzing the problem, it was concluded that the major sources of error were (1) the change in vehicle aspect as it passed through the camera's field of view, and (2) the uncertainty of a vehicle's lateral position in its lane. As the vehicle passes through the field of view, the part of the vehicle that the slit aperture sees as a leading edge is con-

stantly changing. This means that the leading (or trailing) edge of the streak on the film represents a different horizontal point on the vehicle at different points in the field of view. This disparity produces a positional uncertainty that can amount to more than 1 ft, and, because vehicle dimensions differ, a general solution is not possible. The second problem is that the vehicle's lateral position in the roadway is uncertain, and, because the slant range from the camera to the vehicle enters into the longitudinal position calculations, lateral uncertainty produces longitudinal uncertainty. The effects of both these problems are reduced as the camera is moved farther from the road and the lens is changed to maintain a constant length of roadway in the field of view. However, the camera-roadway distances required are so large (in excess of 200 ft) that, as a practical matter, very few sites would offer reasonable vantage points for the camera. On the basis of these findings, further work with the TD camera was abandoned.

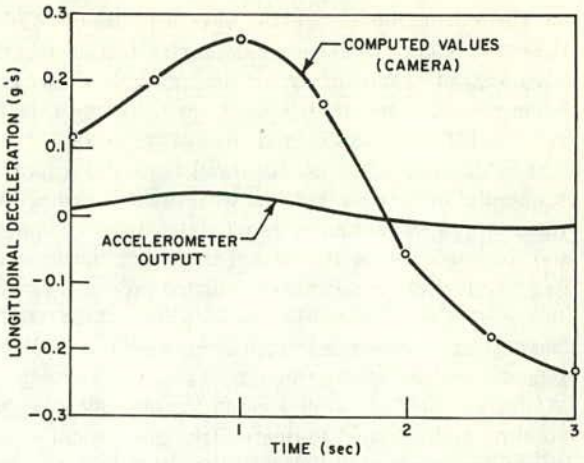

Figure 3. Comparison of accelerometer output and acceleration values computed from TD camera time-position data.

Development of the Tapeswitch System

The system finally developed by FIRL to obtain vehicle acceleration data is based on the use of Tapeswitch event detectors. Tapeswitch is the trade name for a vinyl-clad, flat, flexible, pressure-sensitive, electrical strip switch. It is ¾ in. wide, ⅜ in. thick, and can be cut to any length and fitted with a connecting lead. A series of such detectors, together with the appropriate electronics and recording equipment, can be used to determine the time-position signature of a vehicle over some distance from which data acceleration values can be computed.

The use of Tapeswitch as the basis for a system of discrete event detectors was considered early in the program but not pursued because at that time no quick and simple method for securing the material to the roads was known. Subsequently, it was found that double-coated industrial adhesive tape could be used for this purpose. Accordingly, experiments were conducted using double-coated tape to determine ease of application and to assess the durability of the bond and of the Tapeswitch itself in traffic. It was found that the Tapeswitch was easily applied with the double-coated tape and that the Tapeswitch and the bond would survive for several days on the highway, depending on the volume and nature of the traffic.

Although Tapeswitch detectors avoid the various sources of error typical of optical systems, there was still concern about the accuracy limitations of a system based on Tapeswitch. In particular, because it is the leading edge of a tire that activates the switch, it was believed that high-frequency variations in the length of a tire's footprint associated with vertical load fluctuations caused by surface irregularities might produce position errors amounting to several inches. To measure this effect, an experiment was conducted using a stroboscopic (strobe) camera to photograph the wheel of a car as it ran over a length of Tapeswitch, shown in Figure 4. Because the Tapeswitch triggered the strobe lamp, the photograph showed the position of the wheel relative to the Tapeswitch at the instant of switch closure. A series of such photographs was made with the vehicle traveling at different speeds and under various levels of braking. The experiment was conducted on a rough surface to obtain data under conditions worse than normally encountered on a major road. Measurements were made from the photographs to determine the trial-to-trial variations of the distance between a fixed point on the vehicle and the Tapeswitch edge. The standard deviation was found to be 0.31 in. In a second series of photographs, the standard deviation was 0.18 in. Because the only other source of position error in a Tapeswitch system would occur in the placement of the Tapeswitch detectors, it was concluded that position errors would generally be less than 1 in.

On the basis of these findings, it was decided to build and test a full system. The system, designed to accept up to

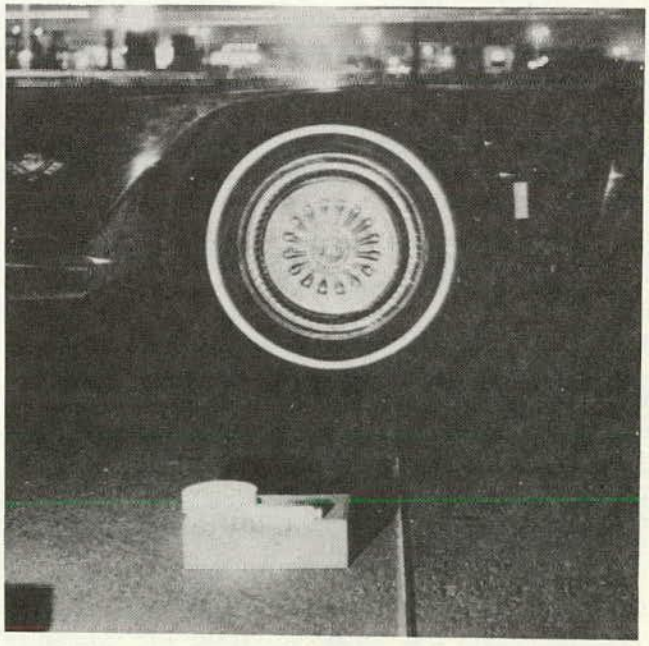

Figure 4. Example of strobe photograph of wheel activating Tapeswitch.

25 Tapeswitch inputs, consists of four parts: the Tapeswitch detectors having connectors and cables, the electronic package, a printer, and a power supply, which are shown in Figure 5. The electronics package consists of gating circuits, a 100-μ sec clock, and storage registers.

The gating circuits accept input from the Tapeswitch in sequential order only, statring with the first and ending with the last. In the system's initial state, only the input channel associated with the first Tapeswitch detector is open (i.e., activation of any other detector produces no response in the system). When the first detector is activated by the passage of a vehicle, its input channel closes and the input channel associated with the next Tapeswitch detector opens. Activation of the second detector causes its input channel to close and the next to open. This process continues until the system is manually reset or the last detector is activated, which automatically resets the system. The system thus tracks only one vehicle at a time through the installation, ignoring all others. In this manner, ambiguities are not caused by the presence of more than one vehicle in the system at a time.

The clock is initially set to zero. Activation of the first Tapeswitch detector starts the clock. The current clock time at each instant a detector is activated is stored in a buffer register and subsequently is transmitted to the printer. The printer, a Hewlett-Packard, high-speed, 12-channel digital printer (Model 5050B), prints the Tapeswitch sequence number and the current clock time to the nearest 100 μsec. Power is supplied by a 200-w Power Sources (Model 12140-A) charger-inverter using self-contained Nicad batteries.

The system includes controls for resetting and starting the system, for indicating good or bad data, and for entering and printing the clock time of some event, such as the onset of the amber traffic light. A series of switches is also included for turning on or off any input channel. This provision is used to accommodate the system to the number of detectors in actual use and to turn off any input channels associated with failed switches.

Figure 5. Tapeswitch system components.

Installation

For measuring longitudinal (braking) acceleration, the Tapeswitch detectors are laid parallel to each other, perpendicular to the direction of the lane. The detectors are 6 ft long in order to sense the traffic in one lane only, and each is fitted with a 10-ft-long lead terminating in a connector. Each detector is secured to the roadway by means of 3M Company double-coated neoprene industrial adhesive tape. The tape, which has a protective backing on one side, is applied to the detector prior to leaving the laboratories to give the adhesive time to set. In very cold weather, the pavement directly under the detector is first primed with Scotch Grip No. 77 spray adhesive, which becomes tacky in 15 sec.

The detectors are placed according to a variable spacing scheme in such a way that, for a vehicle decelerating to zero at the stop line at a constant 0.3 g, the time between successive detectors will be approximately 0.5 sec. The last detector (number 16) is placed 5 ft from the stop line. This scheme ensures acceptable accuracy and about 1-sec time resolution for vehicles decelerating at the 90th and 99th percentile g-levels.

To ensure accurate separation and parallel placement of the detectors, a measuring device is used which consists of two 6-ft-long masonite boards connected at both ends by steel measuring tapes, which arrangement is shown in Figure 6. The device is used as follows: Tapeswitch number 16 (closest to the intersection) is put down. The steel measuring tapes are set to the desired distance and clamped, and the leading edge of the trailing board is butted up against the Tapeswitch and the leading board pulled out until the measuring tapes are taut. With the tapes taut, the leading board is placed flat on the pavement and its leading edge is used as a guide for placing the next detector. This operation requires two workers and a policeman to control traffic.

Once the Tapeswitches are installed, only the necessary connections need be made. Each 6-ft length of Tapeswitch is prefitted with a 10-ft lead terminating in a connector that plugs into a corresponding numbered receptacle on the connecting cable. For easier handling, there are two connecting cables, each about 300 ft long, with appropriately spaced receptacles. The cables are then plugged into the electronics package and the system is ready to operate. In addition to the 16 lengths of Tapeswitch used in the system, one additional detector is installed and connected to a counter to provide a count of traffic in the instrumented lane. The entire operation takes about 45 min.

Data Collection

The system is controlled by one person from a parked car, which contains the components. The operator's tasks are to turn the system off when vehicles are approaching a green

signal, to turn the system on in anticipation of an amber signal, to reset the system after each record, to indicate by the activation of the appropriate marker whether the record was good or bad, and to maintain a log. Traffic count data are logged every half hour and weather conditions are logged whenever there is a change.

Should a Tapeswitch fail during data collection, the operator has the option of replacing it immediately or simply turning off its input channel. Normally one failed detector is not replaced.

Generally, less than 50 percent of the vehicles braking for a light stop at or beyond the last detector. This is because many vehicles come to a stop before the stop line and also because many of the vehicles observed were not first in a queue. Which vehicles in a queue are observed depends on the volume of traffic. When vehicle separations in the instrumented area are such that each vehicle comes to a stop before the next enters the system (10 to 12 sec), none are missed. However, separations of 5 or 6 sec are more typical and generally cause every other vehicle to be missed in moderately heavy traffic. The first vehicle and sometimes the first two vehicles to stop are missed when, after the system is reset in anticipation of an amber signal, the amber signal is ignored by the first vehicle to encounter it. It then becomes necessary to reset the system again, and vehicles already past the first detector are missed. Data were not collected on vehicles whose position in the queue was five or greater. This is because the speeds of braking vehicles well back in the queue are mismatched to the detector separations to such an extent that the time intervals over which acceleration is computed become too large (i.e., greater than 3 sec) for the acceleration data to be meaningful. Although queue position as such is not recorded, a vehicle's stopping position can be determined to within a few feet and queue position estimated on the basis of distance from the intersection. Although the data collection rate varies with traffic conditions, 30 vehicles per hour is a representative figure for signalized intersections.

Data Reduction

The output from the printer is key punched and computer processed to reduce the raw data to a series of individual records. Each record consists of the speed and acceleration of a single vehicle across 14 overlapping intervals in the approach to an intersection. These records are printed out for inspection and also stored on tape for further processing.

Acceleration values are obtained by successively computing the second difference on each set of three sequential time/position points. Figure 7 shows an example of this output. The records shown are for individual vehicles. Each record shows the clock time to 0.01 sec associated with each detector, the speed in miles per hour between each pair of detectors, and the braking deceleration across each triplet of adjacent detectors. Traffic count data are axle counts, not vehicle counts.

The second program performs summary operations on all of the records obtained at a given site. The output of the summary program is a frequency distribution of deceleration levels at each of the 14 intervals plus data on vehicle speeds.

Accuracy Tests

Once the Tapeswitch system was completed, a study was conducted to determine the accuracy of the G-values computed from the time/position data generated by the system. The instrumented vehicle made a series of runs over the installed Tapeswitch system and generated different and complex patterns of braking on successive runs. During the runs, vehicle acceleration was recorded from the vehicle accelerometer, and these data were compared with acceleration data computed from the Tapeswitch records. The results are shown in Figure 8. In each run, the acceleration points computed from the Tapeswitch data agree closely with accelerometer data. Over a range of from 0.03 to 0.48 g, the Tapeswitch data were within 0.02 g of the accelerometer data. The largest deviation occurred at the relatively unimportant lower end of the range (under 0.25 g). At the higher end of the range, most of the points are within 0.01 g of the accelerometer values. It was concluded that the Tapeswitch system would provide data of more than sufficient accuracy for the purposes of the program.

The Influence of Tapeswitch on Driver Behavior

Although the Tapeswitch installation is not obtrusive, it is visible, and there was some concern that drivers might react to the presence of the detectors by braking more conservatively. Accordingly, a study was undertaken to determine the effect on drivers of the presence of a full Tapeswitch installation. A problem in designing the experiment was that Tapeswitch detectors were (and are) the only method available for measuring acceleration in traffic. It was therefore decided to compare acceleration data obtained over one interval in the site having a disguised three-detector system with data obtained at the same point having an undisguised full Tapeswitch installation. The disguised system consisted of three 1-ft-long Tapeswitch detectors covered with dull black friction tape. The detectors were placed

Figure 6. Measuring boards used to position Tapeswitch detectors.

EXPERIMENT 3 12/13/70 CHURCH AND KING, NJ SITE TYPE 1

CONDITIONS

TIME	TRAFFIC COUNT	WEATHER	LIGHT C.C.E (S.) GREEN	AMBER	RED
1140A	0	ROAD DRY	55	5	35
1200P	478	ROAD DRY	55	5	35
1230P	344	ROAD DRY	55	5	35
100P	406	ROAD DRY	55	5	35
130P	520	ROAD DRY	55	5	35
200P	381	ROAD DRY	55	5	35
230P	368	ROAD DRY	55	5	35
300P	420	ROAD DRY	55	5	35
330P	400	ROAD DRY	55	5	35
400P	370	ROAD DRY	55	5	35

NOMINAL DISTANCE (FT.) BETWEEN SWITCH AND INTERSECTION

	385	340	300	260	225	190	160	135	110	85	65	50	35	20	10	5

TIME 1140A TRAFFIC COUNT 0 WEATHER ROAD DRY

R. 1	TIME (S.)	.00	.92	1.76	2.64	3.45	4.27	5.00	5.62	6.26	6.95	7.56	8.07	8.65	9.34	9.91	10.27
	VEL. (MPH.)	33.5	32.2	31.0	29.7	28.9	28.2	27.6	26.6	24.7	22.2	20.1	17.7	14.8	11.9	9.6	
	ACC. (G.)		.07	.07	.07	.05	.04	.04	.07	.13	.17	.17	.20	.21	.21	.23	
R. 2	TIME (S.)	.00	.95	1.87	2.85	3.79	4.80	5.78	6.71	7.79							
	VEL. (MPH.)	32.2	29.8	27.6	25.6	23.5	21.0	18.3	15.8								
	ACC. (G.)		.11	.10	.10	.10	.12	.13	.11								
R. 3	TIME (S.)	.00	.85	1.64	2.47	3.26	4.11	4.91	5.61	6.38	7.24	8.02	8.71	9.61	11.13		
	VEL. (MPH.)	35.9	34.7	32.7	30.4	27.9	25.8	24.1	22.2	19.9	17.4	14.7	11.4	6.7			
	ACC. (G.)		.06	.11	.13	.14	.12	.10	.12	.13	.14	.17	.19	.17			
R. 4	TIME (S.)	.00	.77	1.48	2.23	2.94	3.74	4.51	5.23	6.05	7.12	8.46					
	VEL. (MPH.)	39.9	38.2	36.4	33.7	29.9	26.4	23.8	20.8	15.9	10.1						
	ACC. (G.)		.10	.11	.17	.23	.20	.16	.18	.24	.22						
R. 5	TIME (S.)	.00	.76	1.45	2.15	2.78	3.45	4.06	4.62	5.23	5.92	6.60	7.24				
	VEL. (MPH.)	40.2	39.6	39.0	38.0	35.7	33.1	30.7	27.9	24.6	20.1	16.0					
	ACC. (G.)		.04	.04	.07	.16	.18	.19	.22	.23	.30	.29					

Figure 7. Example of computer output: vehicle speed and deceleration profiles.

back from the intersection at distances of 135, 110, and 85 ft, which correspond to the locations of Tapeswitches No. 8, 9, and 10 in the full system. The tests were conducted at two sites: (1) an intersection on the innermost southbound lane of Roosevelt Boulevard, a 12-lane urban boulevard with a 40-mph speed limit, and (2) a 600-ft-long single-lane exit ramp off I-78, in Philadelphia, which ends at a stop sign. The results of both studies are given in Table 1. Although in both studies the differences between the mean deceleration values were statistically significant, the differences are within 0.02 *g*, which is close to the limit of accuracy of the system and not of practical significance. Further, the differences are in different directions in the two studies. The 95th percentile acceleration values were identical at the Roosevelt Boulevard site and differed by only 0.01 *g* at the exit-ramp site. On the basis of these data, it was concluded that the presence of a full Tapeswitch installation has no important influence on driver braking behavior at an intersection.

Reliability

There were no reliability problems with the electronics, power supply, or printer. In general, the Tapeswitch detectors and/or the bond began to fail after from 2 to 5 days depending on the nature of the traffic. Detector reliability is poorer in cold than in warm weather. The effect of cold weather is to weaken the adhesive bond between the double-coated tape and the road surface. On road surfaces characterized by a coarse aggregate, the minimum operating (air) temperature without priming is about 40 deg F and on smooth surfaces about 30 deg F. Using Scotch Grip spray adhesive to prime the area directly under the Tapeswitch reduces the minimum operating temperature by about 10 deg. Even with the use of the primer on smooth roads, the bond failure rate in very cold weather is roughly twice as high as in warmer weather. The cold weather also decreases the reliability of the switch itself, partly because the material is more brittle in cold weather and partly because as soon as a bond begins to weaken, permitting part of the Tapeswitch to lift, it is much more susceptible to damage from traffic.

Tapeswitches cannot be installed with adhesive on a wet road but, once installed, will remain in place in the rain on smooth surfaces for several hours. Use of the primer improves the reliability of the bond in wet weather. To prevent the detectors from shorting in wet weather, the ends must be sealed with potting compound.

Although several detectors failed during data collection operations, this never presented a serious problem. Single switches can easily be replaced (the new switch is layed on the mark left by the old one) because even heavy traffic frequently allows 5- or 6-sec headways—more than the time required to change a detector. The best way to ensure reliability in operations is to use a detector for only 2 days.

RESEARCH ON DRIVER DEMAND

The first consideration in designing a data collection program was the selection of highway sites that, for the purpose of this program, can be divided into two classes: open sites and maneuver sites. Maneuver sites are those in which some aspect of the geometry or some control feature requires a specific maneuver (i.e., curves, intersections, ramps, etc.). Open sites are those which have no such factors and

in which all normal maneuvers occur as a consequence of driver choice or the influence of other traffic.

In normal driving, the greatest demand on friction (i.e., the highest levels of acceleration) is associated with geometric and control features. Although few data are available on open-section acceleration behavior of drivers, such data as do exist (*1, 12*) indicate that the distribution of braking and cornering forces on open sections is much lower (i.e., heavy demand occurs with much lower frequency) than at sites whose geometry requires a maneuver. Further, the frequency of accidents is substantially higher at maneuver sites than on tangent sections (*13*). While relatively little has been published on the topic, there does appear to be a strong relationship between the frequency of skidding accidents and geometric elements. Giles and Sabey (*14, 15*) report that, compared to tangent sections, the skidding accident rate is 80 times greater on traffic circles, 48 times greater on curves with a radius less than 500 ft, from 3.8 to 13 times greater on grades, and 7.3 times greater at intersections. Despite the fact that most of the highway system consists of tangent sections, only 2.3 percent of skidding accidents occurred on tangent sections. This does not mean that driver demand in tangent sections can be ignored. It does indicate, however, that the program emphasis should be on maneuver sites. Accordingly, most of the data were collected at maneuver sites.

The Tapeswitch system was used to collect data at a total of 12 different intersection sites, which are given in Table 2. The sites were in New Jersey and in the area of Philadelphia, Pennsylvania.

Almost all of the driver demand data were collected under dry conditions. Although wet-weather observations were made whenever possible for comparison purposes, it would not have been possible to collect sufficient data to meet the requirements of the program had data collection been limited to wet-weather conditions. It would, of course, have been possible to wet the pavement by other means, but the effect on drivers of the artificiality of an isolated wet section is unpredictable. However, the small volume of wet-weather data should not be regarded as a deficiency in the data. On the contrary, there are compelling reasons for basing pavement skid-resistance recommendations on the demand exhibited with dry pavement.

An implicit assumption is that drivers may be more conservative in wet conditions and demand less skid resistance than they do in dry conditions. To the extent that this is true, recommendations based on dry-pavement demand would result in unnecessarily high skid-resistance levels. However, although many drivers may adjust their driving habits when pavements are wet, this does not necessarily mean that all or even most drivers do. Thus, pavement skid-resistance recommendations based on wet-pavement behavior would accommodate only those motorists who drive, in fact, more conservatively when it rains.

Another important consideration is that it is not possible to measure maximum (and, therefore, controlling) levels of deceleration on a wet pavement. It is likely that many drivers attempting to brake at or near peak demand levels would skid. Thus, the highest deceleration values the system would record would be the maximum permitted by the wet pavement rather than what the driver demanded.

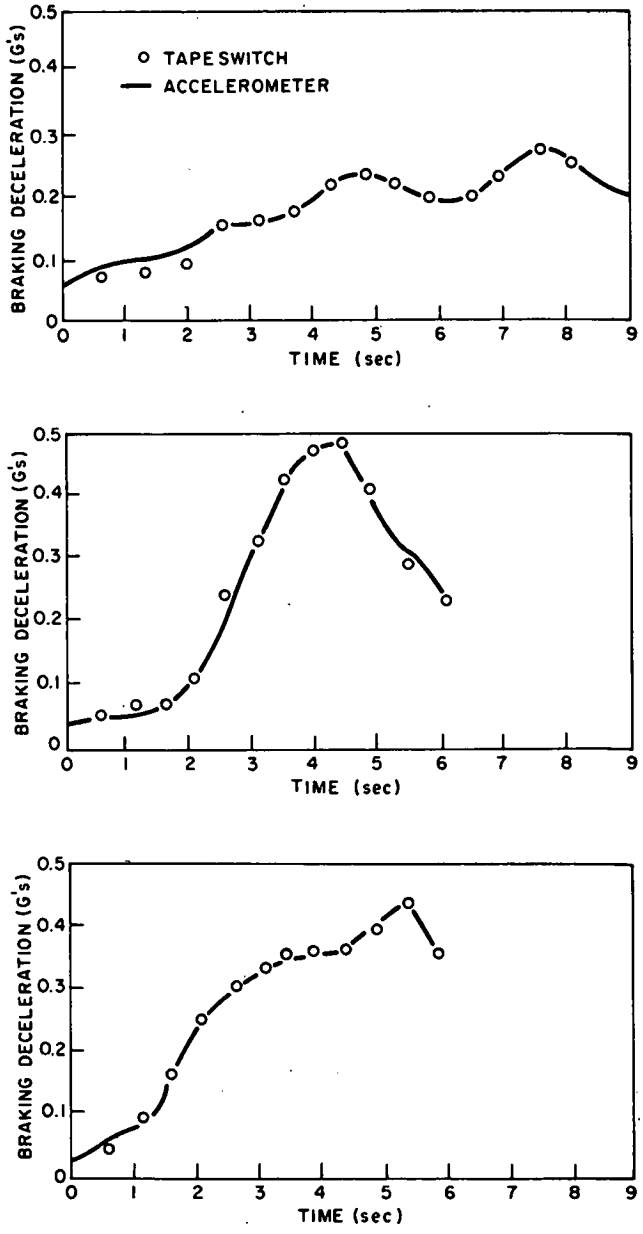

Figure 8. Comparisons of accelerometer output and deceleration data computed from Tapeswitch time-position points.

Furthermore, to the extent that demand does vary with pavement skid resistance (in the sense that demand increases as pavement skid resistance increases), it follows that elevating levels will produce a corresponding increase in demand. Under this assumption, the limiting level of demand that must be accommodated is dry-pavement demand. In any case, pavement skid-resistance recommendations based on dry-pavement demand are conservative.

Wet-pavement braking demand data were collected on 104 vehicles at three different intersection sites. Comparison of these data with the dry-pavement data collected at the same sites revealed no important differences. These data are presented more fully.

TABLE 1

COMPARISON OF SPEED AND DECELERATION DATA OBTAINED AT TWO LOCATIONS BY USING DISGUISED AND UNDISGUISED TAPESWITCH SYSTEMS

SYSTEM TYPE AND LOCATION	NO. OF OBSERVATIONS	AVG. HOURLY TEST-LANE TRAFFIC	SPEED		DECELERATION		
			MEAN	STANDARD DEVIATION	MEAN	STANDARD DEVIATION	95TH PERCENTILE
Disguised three-detector system:							
Freeway exit ramp	347	93	28.40	4.01	0.202	0.071	0.32
Urban boulevard	181	420	20.00	6.00	0.160	0.070	0.29
Undisguised full system:							
Freeway exit ramp	393	118	29.80	4.41	0.183	0.070	0.31
Urban boulevard	279	376	21.60	6.11	0.173	0.064	0.29

TABLE 2

SITE CHARACTERISTICS FOR INTERSECTIONS

INTERSECTION NO.	HIGHWAY TYPE *	AVERAGE HOURLY TRAFFIC	STOP SIGN OR LIGHT	AVERAGE SPEED AT DISTANCE OF 340–385 FT FROM STOP (MPH)	NO. VEHICLES OBSERVED	POSTED SPEED LIMIT (MPH)
1	4	450	Light	36.0	313	40
2	1	412	Light	36.2	296	45
3	5	426	Light	39.6	332	45
4	1	104	Sign	36.2	426	40
5	2	448	Light	37.5	327	40
6	4	116	Light	30.3	362	35
7	6	94	Sign	38.6	349	Not posted
8	6	112	Sign	40.3	329	Not posted
9	3	282	Light	41.2	423	40
10	2	406	Light	37.1	345	50
11	5	592	Light	39.6	341	50
12	3	370	Light	35.1	339	45

* Type 1: Two-lane rural—design speed, less than 50 mph, unpaved shoulders; width, including shoulders, less than 30 feet. Type 2: Two-lane rural—design speed, 60 mph or greater; paved shoulders; width, including shoulders, greater than 30 feet. Type 3: Four-lane divided rural or suburban highway—no access control; design speed 50 mph. Type 4: Multi-lane urban boulevard—design speed, 35-45 mph. Type 5: Multi-lane rural or suburban divided highway—partial access control; design speed, 60 mph or more. Type 6: Freeway exit ramp (intersection with through street).

Deceleration at Intersections—Data Collection

The Tapeswitch system was installed and operated and the raw data reduced to individual vehicle records as described in the previous section. Only one lane was instrumented. All data were collected during the day between the morning and evening rush hours. Rush-hour data collection was avoided because throughout most of a rush-hour period there was a stopped or slow-moving queue within the system at the onset of the amber signal. As described, the system was activated in anticipation of the amber signal in an attempt to record the first vehicle to stop. No vehicles further back than fifth in the queue were recorded. No distinction was made between classes of vehicles. Not all of the vehicles recorded came to a full stop. At stop-sign intersections, many vehicles slowed to 10 mph or less and continued, while some turned right or left. At both stop-sign and signal-light intersections, many vehicles stopped well beyond the last detector. Thus, the population from which the observed sample was drawn includes those vehicles from the first to the fifth in a queue braking at an intersection for a traffic signal or stop sign in the instrumented lane.

For each site, individual vehicle records were inspected

for anomalies before further analysis. Anomalies in the data can occur when the vehicle being tracked overtakes a slower lead vehicle. Occasionally, following distances are so close that the lead vehicle's front or rear wheels cross the next *active* detector before the following car, and track is transferred to the lead car. The resulting anomalies in the raw time/position data are easily identified since they produce typical patterns of meaninglessly large positive and negative acceleration values. Such data points were deleted before further analysis was undertaken.

Figures 9A and 9B show further refinement of the raw data. Figure 9A shows a number of representative deceleration notations that illustrate the variety of deceleration time histories observed. Each curve is for a single vehicle, and each point on the curve represents the *average* deceleration of the vehicle over the distance interval indicated on the abscissa. The distance interval for a point is given by the abscissa values immediately to the left and right of the abscissa value corresponding to the point. Thus, the interval associated with 160 ft is actually 190 to 135 ft.

Note that there is no single typical deceleration trace. Some drivers brake hardest early, some late, some in the middle of the maneuver, and some brake at a near constant level throughout. However, when the data are summarized, the trend shows braking to increase with decreasing distances from the intersection.

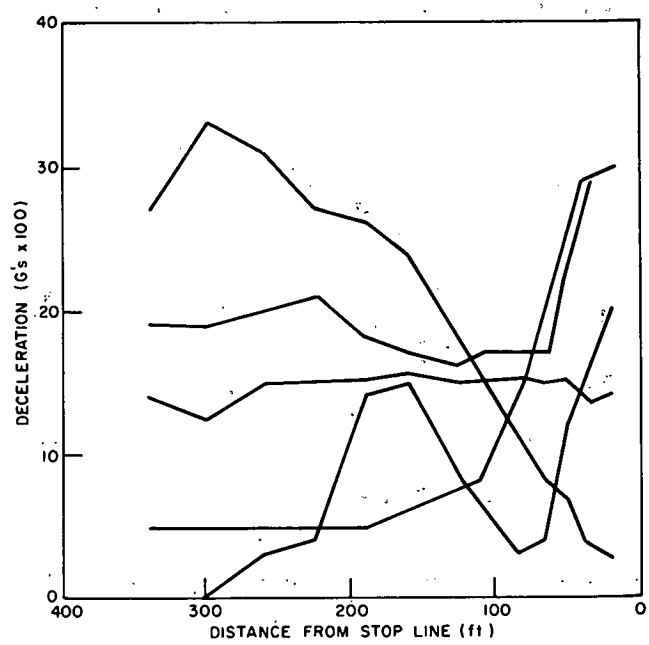

Figure 9A. Individual deceleration records.

SUMMARY OF TAPESWITCH EXPERIMENT STATISTICS

NOMINAL DISTANCE (FT.) OF CARS FROM INTERSECTION

	385-300	340-260	299-225	259-190	224-160	189-135	159-110	134-85	109-65	84-50	64-35	49-20	34-10	19-5
VMAX	50.6	49.5	47.6	46.6	45.8	45.9	46.3	47.1	47.8	48.4	48.8	29.2	26.0	15.2
V99	48.4	47.3	46.1	44.4	44.0	42.3	39.3	38.0	37.8	34.5	31.8	23.7	19.2	15.2
V95	44.4	43.4	42.8	41.5	39.2	36.7	35.0	32.1	29.6	27.1	24.0	21.8	18.5	14.4
V90	42.4	41.6	40.5	38.4	36.6	34.3	32.0	30.0	27.0	24.4	22.6	19.8	17.5	13.1
V85	40.7	39.7	38.2	36.4	34.7	32.2	29.8	27.8	25.9	23.1	20.9	19.4	16.2	12.9
V50	35.6	34.1	32.5	30.3	28.1	25.9	23.6	21.7	19.2	17.2	16.0	14.7	12.4	9.1
V15	31.0	29.7	27.7	25.2	22.8	19.8	16.8	14.5	13.9	12.1	11.6	10.8	9.4	6.7
VBAR	36.0	34.6	32.9	30.9	28.6	26.1	23.8	21.6	19.6	17.7	16.5	15.1	13.1	9.7
S(V)	4.90	5.02	5.30	5.60	5.86	6.15	6.20	6.27	5.95	5.70	5.45	3.95	3.51	2.75
AMAX	.28	.31	.26	.28	.29	.35	.39	.41	.41	.41	.42	.44	.44	.42
A99	.23	.24	.24	.25	.27	.30	.33	.33	.38	.39	.40	.43	.43	.42
A95	.16	.20	.20	.22	.23	.26	.27	.29	.32	.33	.39	.38	.37	.36
A90	.15	.17	.18	.20	.22	.24	.24	.25	.27	.28	.32	.36	.36	.35
A85	.13	.15	.17	.18	.20	.21	.22	.23	.24	.26	.29	.33	.35	.30
A50	.06	.10	.11	.12	.13	.15	.16	.17	.18	.19	.19	.21	.22	.23
A15	.02	.04	.05	.07	.09	.10	.11	.11	.11	.12	.13	.15	.14	.15
ABAR	.07	.10	.11	.12	.14	.15	.16	.17	.18	.19	.21	.22	.24	.23
S(A)	.054	.058	.055	.059	.055	.059	.061	.064	.069	.074	.083	.091	.091	.085

STATISTIC	STOPPING POINT (SP) (T.)	ATILDE1(225 - SP) (G.)	ATILDE2(225 - 50) (G.)	ATILDE3(50 - SP) (G.)
MAX	123.48	.32	.20	.46
99	105.24	.29	.13	.41
95	85.00	.26	.12	.36
90	73.97	.23	.11	.31
85	66.12	.22	.10	.29
50	31.17	.16	.07	.20
15	2.40	.12	.04	.12
MEAN	33.19	.17	.07	.21
S.D.	29.544	.048	.030	.082

PERCENTILE (P) OF DECELERATION	SPEED (MPH.) OF CAR HAVING PTH PERCENTILE DECELERATION (G.) AT DISTANCE (FT.) FROM INTERSECTION													
	340	300	260	225	190	160	135	110	85	65	50	35	20	10
99	46.3	34.2	42.8	39.6	44.0	38.3	35.0	36.0	31.2	27.8	23.9	23.7	19.2	14.4
95	34.5	35.8	42.1	42.0	24.1	32.1	18.4	24.7	30.2	23.1	25.2	19.8	17.5	13.1
90	35.0	36.4	35.6	35.1	24.3	33.3	25.7	29.4	21.9	23.3	22.1	22.0	14.9	14.9

Figure 9B. Example of summary data compiled for each test intersection.

Figure 9B * shows how the individual records were further reduced to provide summary data for each intersection. In each distance interval, the mean, median, and standard deviations and various empirical percentile levels of deceleration, A, and speed, V, were computed. Other summary data computed for each intersection included the mean, median, standard deviations, and empirical percentiles of vehicle stopping point, SP, relative to the stopping line, as well as average deceleration between key points near the intersection. The average deceleration variables (for which profile values were computed) were deceleration between 225 ft from the stopping line and the stopping point (ATILDE 1 (225-SP)), deceleration from 225 ft to 50 ft (ATILDE 2 (225-50)), and deceleration between 50 ft and the stopping point (ATILDE 3 (50-SP)). In addition, the speeds of cars having the 99th, 95th, and 90th deceleration percentile values in each distance interval were also obtained. Figure 10 is a plot of the median and 85th, 90th, 95th, and 99th percentile deceleration values for site No. 8. Similar plots for other sites are included in Appendix B. Figure 11 is a plot of the measured speed patterns associated with each of the decelerations for site No. 8.

Each deceleration curve shows the pth percentile level of deceleration as a function of distance from the intersection. Note that the curves are not traces of individual vehicles but simply connect the points representing the pth percentile at each distance interval. The curve marked MAX represents the *single* highest deceleration level observed in each interval (i.e., each point represents only one vehicle).

In general, higher initial deceleration levels are associated with higher average initial speeds (as recorded at 385 ft), and, although there are exceptions, the general trend is that acceleration increases monotonically as the intersection is approached. The major exception is site No. 3 where a maximum is reached between 100 and 200 ft. The ordering of the data from site to site is roughly preserved throughout most of the approach, but, in the last 50 ft, the data are highly variable. This is because many of the vehicles come to a stop well before the stop line; hence, the sample sizes for the last two intervals are small. These trends can be seen in Figure 12, which shows the 95th percentile deceleration profiles for each of the 12 sites.

Peak median deceleration levels tend to be quite low, generally less than 0.2 g. Peak 95th and 99th percentile values ranged roughly between 0.3 and 0.4 g and between 0.4 and 0.5 g, respectively. Peak maxima fall between 0.50 and 0.55 g at all intersections but one. At site No. 11 (a high-speed limited-access road), deceleration levels were higher than at the other sites, and maxima in excess of 0.6 g were observed. To help place these values in perspective, stopping distances from 35 and 60 mph at three g-levels are given in Table 3. The g-levels selected are those defined by drivers and passengers as comfortable, moderately severe, and severe and uncomfortable.

The ratings of Wilson's (*17*) subjects are consistent with the present study. Braking levels considered severe and uncomfortable would occur only about 1 percent of the time.

* Appendix E of the agency's final report includes the summary data for the 12 intersections under consideration.

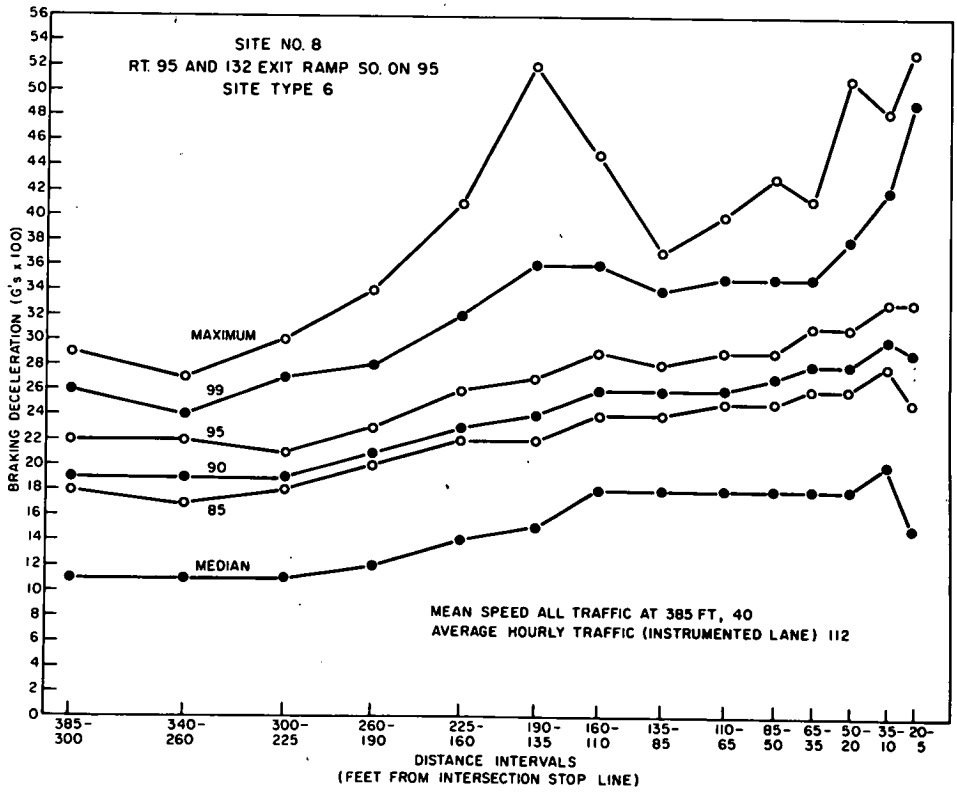

Figure 10. Site No. 8 deceleration profiles.

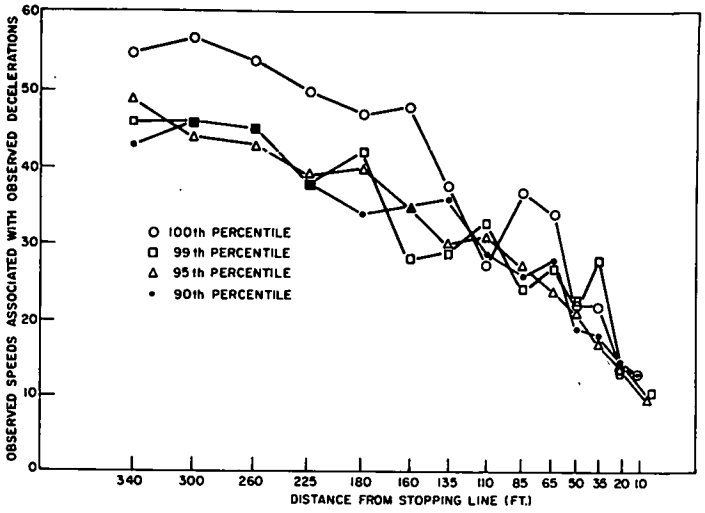

Figure 11. Observed speeds associated with decelerations versus distance from stop line, intersection site No. 8.

Rain Data

A total of 106 deceleration records were collected in the rain (moderate) at three different sites (No. 3, 10, and 12). Summary statistics were produced from these records as though they had all been obtained at one site.

Figure 13 shows the 99th percentile deceleration profile for the rain data and the weighted average of the corresponding points from sites No. 3, 10, and 12. The weighting was according to the relative contributions of the three sites to the rain sample. The curves were not plotted beyond 50 ft because of insufficient rain data at 35 and 20 ft. The maximum difference between the curves (0.045 *g*) occurs at 160 ft, at which point the 99th percentile rain deceleration is 0.370 *g* and the corresponding weighted average of the 99th percentile points is 0.325 *g*.

Table 4 gives the mean and 95th percentile speeds at 340 ft for each of the three sites, their weighted averages, and the corresponding wet-sample values. The values are very close although the rain 95th percentile speeds are slightly lower than the corresponding weighted averages.

Although the rain sample is small, it is large enough so that any substantial effect of rain on driver behavior would have been evident especially at the extreme deceleration levels. The data show no evidence of such an effect.

SKID STUDIES

This section summarizes the findings of the skid tests conducted by FIRL at the Texas Transportation Institute

TABLE 3

DECELERATION LEVELS AND THEIR RATINGS-

DECELERATION		STOPPING DISTANCE (FT)	
g	PASSENGER DEFINITION	35 MPH	60 MPH
0.27	Comfortable	152	456
0.34	Moderately severe	120	345
0.42	Severe and uncomfortable	97	286

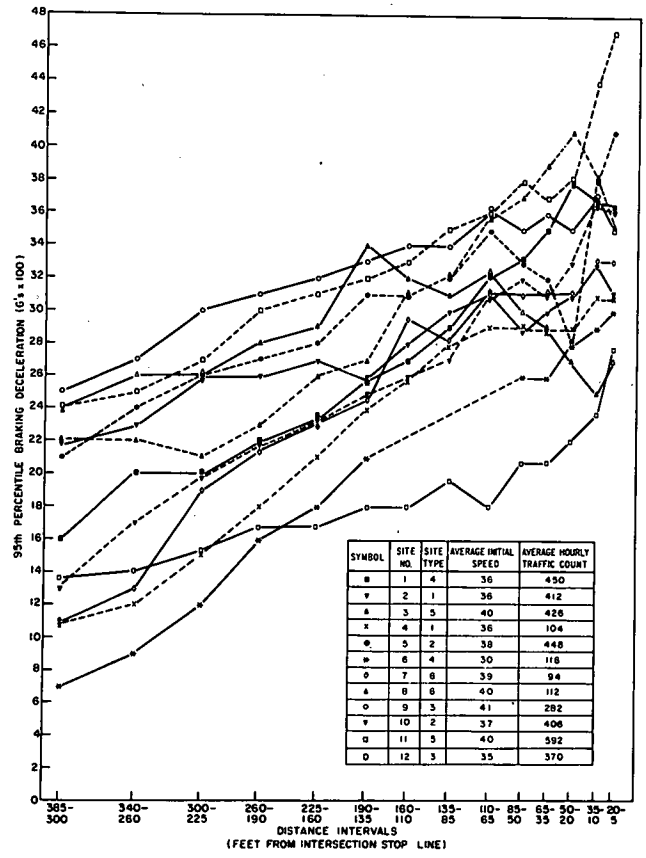

Figure 12. Ninety-fifth percentile profiles for 12 sites.

(TTI) skid pad facility. The objective of the tests was to determine empirically the relationship between the wet-pavement skid resistance and lateral and longitudinal vehicular acceleration, singly and in combination. The longitudinal acceleration tests resulted in reasonable accomplishment of the objective in terms of the vehicle, tire, and pavement combinations used during the study. The findings are reported in the remainder of this section. The lateral acceleration tests were less successful in that empirical relationships were not identified for the particular vehicle, tire, pavement, and curvature combinations studied. These findings are reported in Appendix C.

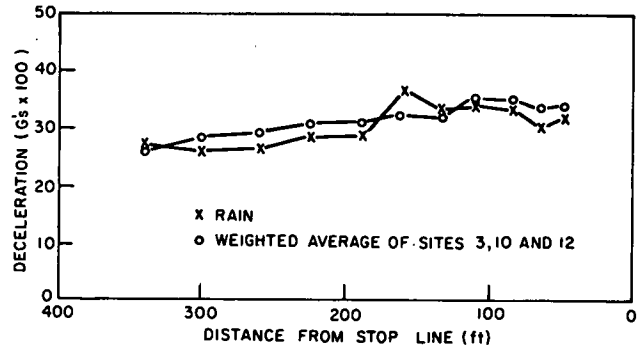

Figure 13. Ninety-ninth percentile deceleration in the rain and the weighted average of corresponding points from three sites.

TABLE 4

MEAN AND 95TH PERCENTILE SPEEDS AT 340 AND 225 FT FROM STOPPING POINT FOR SITES NO. 3, 10, AND 12; ALSO RAIN DATA AND THE WEIGHTED AVERAGES FOR THESE SITES

DISTANCE FROM STOPPING POINT	SITE NO. 3	10	12	WEIGHTED AVERAGE	RAIN DATA
V_{340}:					
Mean speed	39.6	37.1	35.1	36.4	36.7
95th percentile speed	50.7	47.5	44.0	48.5	46.5
V_{225}:					
Mean speed	32.9	31.0	30.6	30.7	31.3
95th percentile speed	43.8	41.5	37.7	41.4	40.2

The general method was to measure the maximum acceleration achievable in each mode on pavement surfaces having different measured skid resistance. These data, combined with the driver acceleration profiles previously discussed, were used to determine pavement skid resistance required to accommodate various levels of driver demand at intersections.

The skid-resistance/maximum-acceleration relationships were determined for a limited set of vehicles (*2*), tires (*3*), and surfaces (*6*). In the braking tests, the differences between vehicles and tires were not large relative to the differences between measured skid resistance of the pavements and other sources of uncertainty in the testing. The braking data can be considered generally applicable to American cars having tires in good condition.

Test Facilities

The TTI test facility consists of nine 24 by 600-ft skid pads and eight 12 by 400-ft 20-deg curves with a 100-ft tangent approach section. The curves and pads are situated such that there is ample room to accelerate to and stabilize at any speed of which a test vehicle is capable. The surfacing materials are illustrated in Figure 14. The numerical order designates both pads and curves:

1. Portland cement concrete (Fig. 14A).
2. Jennite flush seal.
3. Limestone hot mix, terrazzo finish.
4. Crushed gravel hot mix (Fig. 14B).
5. Rounded gravel hot mix.
6. Rounded gravel chip seal (Fig. 14C).
7. Lightweight aggregate chip seal (Fig. 14D).
8. Lightweight aggregate hot mix.
9. Painted portland cement concrete (Fig. 14E).

Pads 6 and 7 and curve 6 were not used at all because the aggregate was not properly bonded to the surface. Curve 1 was not used because depressions in the surface produced severe puddling.

Test Vehicles

Two test automobiles used in the study were a 1970 Plymouth Fury (full-sized) Sedan (Fig. 14F) and a 1971 Ford Mustang (Fig. 14G). During tests, the vehicles were fitted with an instrumentation package that provided pen recordings of the following parameters:

1. Time (1-sec time marks).
2. Distance (50-ft marks from fifth wheel).
3. Speed (from fifth wheel).
4. Longitudinal acceleration (accelerometer).
5. Lateral acceleration (accelerometer).
6. Throttle activation.
7. Brake-pedal activation.
8. Experimenter-activated event marks.

Both vehicles had three-speed automatic transmission, power disk (front) brakes, and power steering. The Plymouth had a 440 CID V8 engine and the Mustang a 351 CID V8 engine. Weights and weight distributions are given in Table 5.

The accelerometers were located approximately 15 in. behind the center of gravity (C.G.) in the Plymouth and approximately 8 in. behind the C.G. in the Mustang. In both vehicles, the accelerometers were mounted on the transmission tunnel at the center line of the vehicle.

Tires

The following three sets of tires were tested on the Plymouth:

1. B.F. Goodrich Silvertown Belted (fiber glass and polyester belted, bias-ply construction), H-78-15.
2. B.F. Goodrich Silvertown HT 4-ply Polyester (conventional bias ply), H-78-15.
3. B.F. Goodrich Silvertown Lifesaver Radial, H-78-15.

The Mustang was equipped with Uniroyal Fastrak belted (rayon) E78-14 tires. All tires were inflated to 26 lb.

TABLE 5

WEIGHTS AND WEIGHT DISTRIBUTIONS FOR TEST VEHICLES

	WEIGHT (LB)								
	FRONT				REAR				
VEHICLE	LEFT	RIGHT	TOTAL	(%)	LEFT	RIGHT	TOTAL	(%)	TOTAL
Plymouth	1240	1220	2460	52	1080	1180	2260	48	4720
Mustang	1080	1030	2110	56	810	840	1650	44	3760

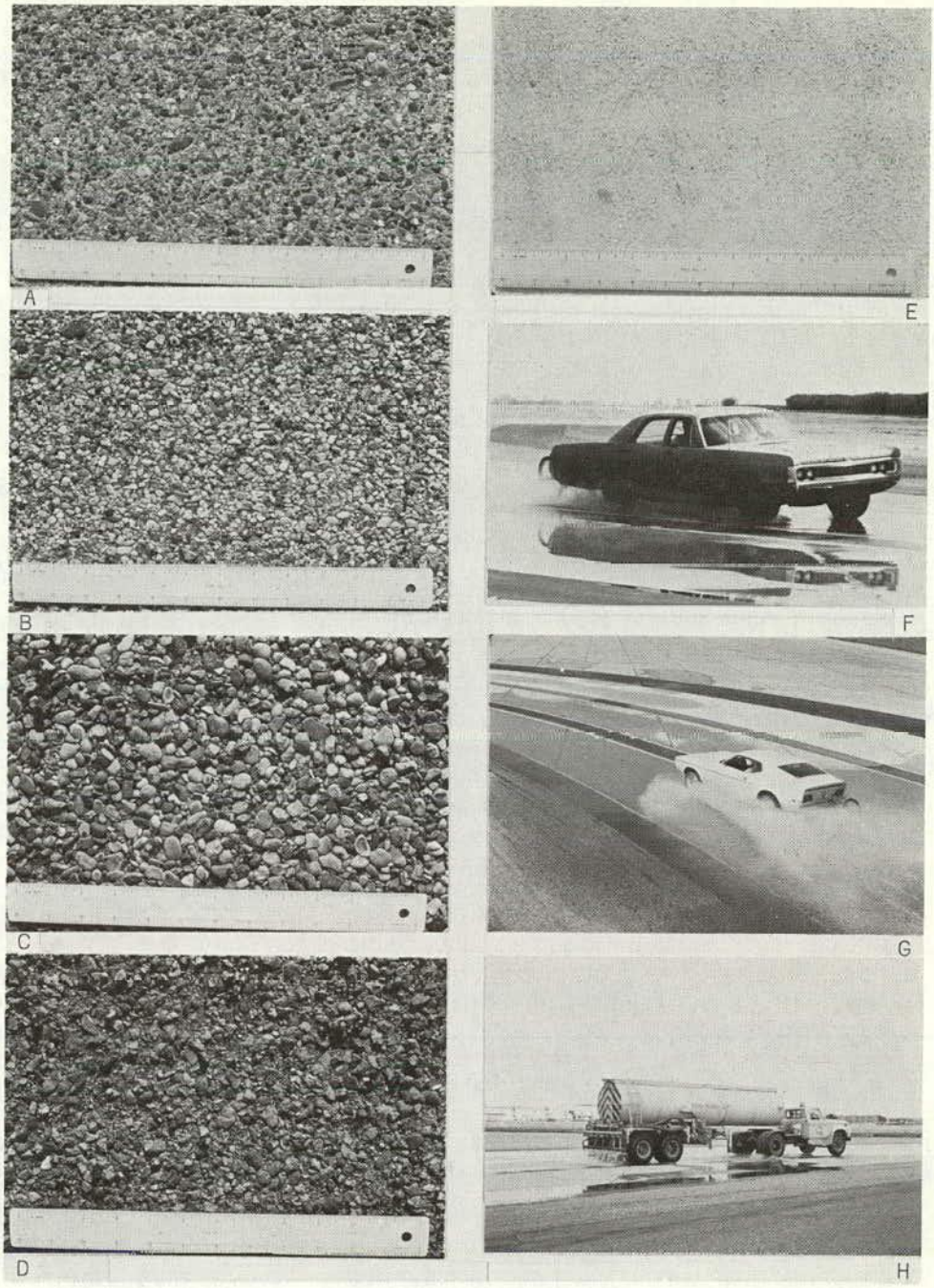

Figure 14. Random photos at the TTI test facility.

Skid Testing Procedures

Skid Trailer Tests

Three sets of skid-resistance measurements, expressed as skid numbers (SN), were obtained for the skid pads. One set was made with the National Bureau of Standards (NBS) skid trailer using internal watering; two sets were made with the Texas Highway Department (THD) skid trailer using internal watering and external watering. External water was applied by a watering truck (Fig. 14H). Each set of data was obtained at 20, 40, and 60 mph.

The same trailers were used to measure skid numbers for the curves. In addition, the University of Michigan Highway Safety Research Institute (HSRI) Mobile Tire Tester (MTT) was used to obtain cornering slip numbers (CSN) on the curves. In testing the curves, the trailers and the MTT passed over the curve at a tangent. The MTT tests were conducted with external watering.

Skid Pad Skid Numbers

Skid numbers were determined for the skid pads and are given in Table 6. Figure 15 shows the same data in graphic form for each of the seven pads showing skid numbers as a function of speed for the three trailers. In general, the skid number decreases with increasing speed. However, this generalization does not hold for all trailers and surfaces. The skid numbers obtained by the THD trailer using internal watering either do not change or actually increase between 40 and 60 mph on five of the seven surfaces tested. This is attributed to the fact that the rate of water deposition in the THD trailer is not proportional to speed. The THD trailer using external watering provided the best data in the sense that for all pads the skid numbers decrease monotonically with speed and exhibit the greatest slope. On two of the seven pads (No. 4 and 5), the NBS trailer skid numbers are not monotonic. However, because SN_{40} values conventionally characterize the surface, the behavior of the trailers at 60 and 20 mph, although interesting, is not critical. Further, since the NBS values were obtained through standard procedures, the NBS SN_{40} values are used as the characterizing values in the subsequent presentations.

Vehicle Skid Data

Five types of tests were performed: (1) braking, (2) cornering, (3) braking plus cornering, (4) forward acceleration, and (5) cornering plus (forward) acceleration. In all cases, the purpose of the test was to determine the maximum acceleration in the various modes and combinations that a given surface could sustain. The independent variables were (1) the surface, (2) the vehicle and tire combination, and (3) speeds (on the braking and forward acceleration tests). However, because of time limitations, not all possible combinations of all of the variables were tested. The braking test procedures are described here. Other tests are described in Appendix C.

Before the tests began, the watering truck made a number of passes over the pad to wet it thoroughly; thereafter, two watering passes were made prior to each run. This watering procedure was followed in all tests. In a braking run, the test vehicle was accelerated to and stabilized at a speed 2 to 5 mph greater than its assigned speed for that run. Upon reaching the pad, all four wheels were simultaneously locked by a sharp and hard application of the brakes. The brakes were kept locked until the vehicle had

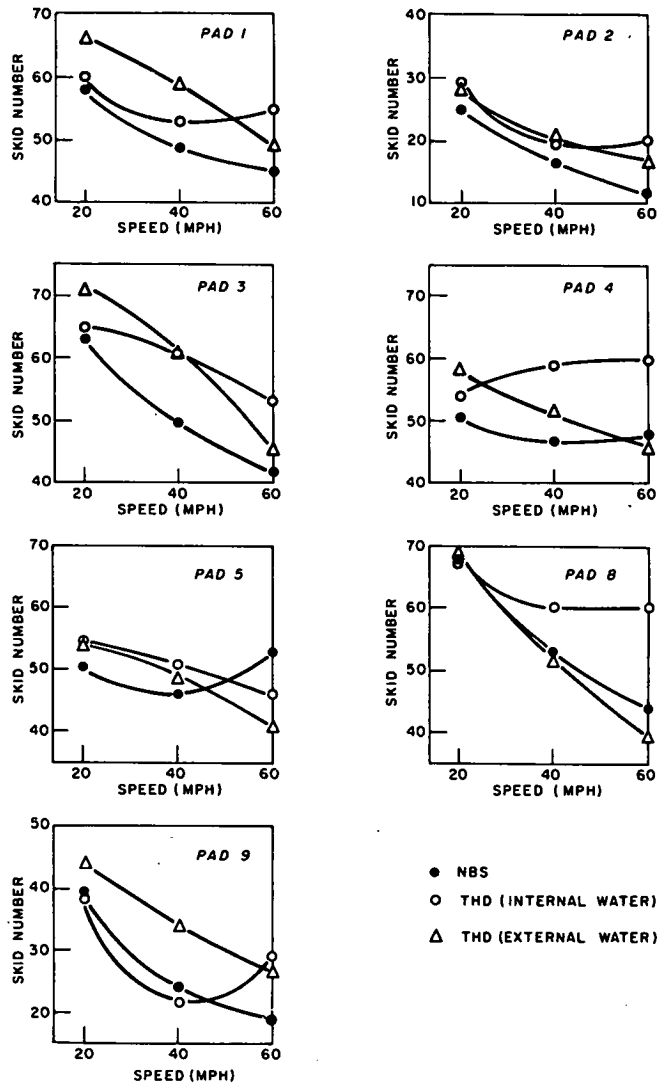

Figure 15. Skid number as a function of speed on seven skid pad surfaces.

TABLE 6

SKID NUMBERS AT 20, 40, AND 60 MPH FOR SEVEN SKID PAD SURFACES

SKID PAD	SKID NUMBER AT 20 MPH			SKID NUMBER AT 40 MPH			SKID NUMBER AT 60 MPH		
	NBS	THD [a]	THD [b]	NBS	THD [a]	THD [b]	NBS	THD [a]	THD [b]
1	58	60	67	48	53	59	45	55	48
2	25	29	28	17	19	20	12	20	17
3	63	65	72	50	61	61	42	53	45
4	51	54	58	47	59	52	48	60	46
5	51	54	54	42	51	48	53	46	41
8	69	68	59	53	60	52	44	60	39
9	39	38	44	24	22	34	19	29	27

[a] Internal. [b] External.

decelerated through its assigned speed. In any trial in which the vehicle began to spin or achieved any perceivable deviation from a straight-ahead orientation before the assigned speed was reached, the procedure was terminated and the data discarded. Subsequently, the data were reduced by reading off the longitudinal acceleration value corresponding in time to the assigned speed for the run. A sample recording is shown in Figure 16. The assigned speeds were 20, 40, and 60 mph.

Locked-wheel braking coefficients rather than rolling coefficients were obtained for the following reasons. A locked-wheel braking coefficient represents a single, definite, easily repeatable point, whereas a coefficient depends on percent wheel slip. Repeatable brake slip maxima for an automobile is difficult to obtain because of point-to-point and wheel-to-wheel variations in braking effectiveness associated with surface and braking system irregularities. Application of vehicle braking data to the determination of pavement skid-resistance requirements is likely to be more meaningful with locked than with rolling wheels because the SN_{40} values are obtained from locked-wheel measurements and, therefore, are more likely to correlate well with locked-wheel braking. Although rolling friction provides a closer representation of maximum braking capability, it is an ideal value that is rarely achieved in actual driving. According to prevailing opinion, most drivers in a panic situation on wet pavement are likely to lock their brakes. Sliding friction is, therefore, both a more realistic and more conservative representation of vehicle performance in the real world.

Skid Test Results

Figure 17 shows locked-wheel braking deceleration for the four tire/vehicle combinations as a function of speed on seven skid pads. With the exception of the Plymouth on pad 1, braking deceleration decreases with increasing speed. In most cases, the greatest change occurs between 20 and 40 mph. In this regard, the skid trailer whose data most closely resemble the automobile data is the THD trailer using external watering. The similarity of the data probably reflects the similarity of watering techniques. It is clear that there are complex interactions between surfaces, speeds, tires, and vehicles. Although no tire/vehicle combination was clearly worst or best, the Mustang with the belted, bias-ply tires was most frequently the worst combination and the Plymouth bias-ply tire combination most often the best. Also the Plymouth having belted, bias-ply tires was in the majority of instances a better combination than the Mustang with the same type of tire. This may be attributable to the more even front-rear weight distribution in the Plymouth.

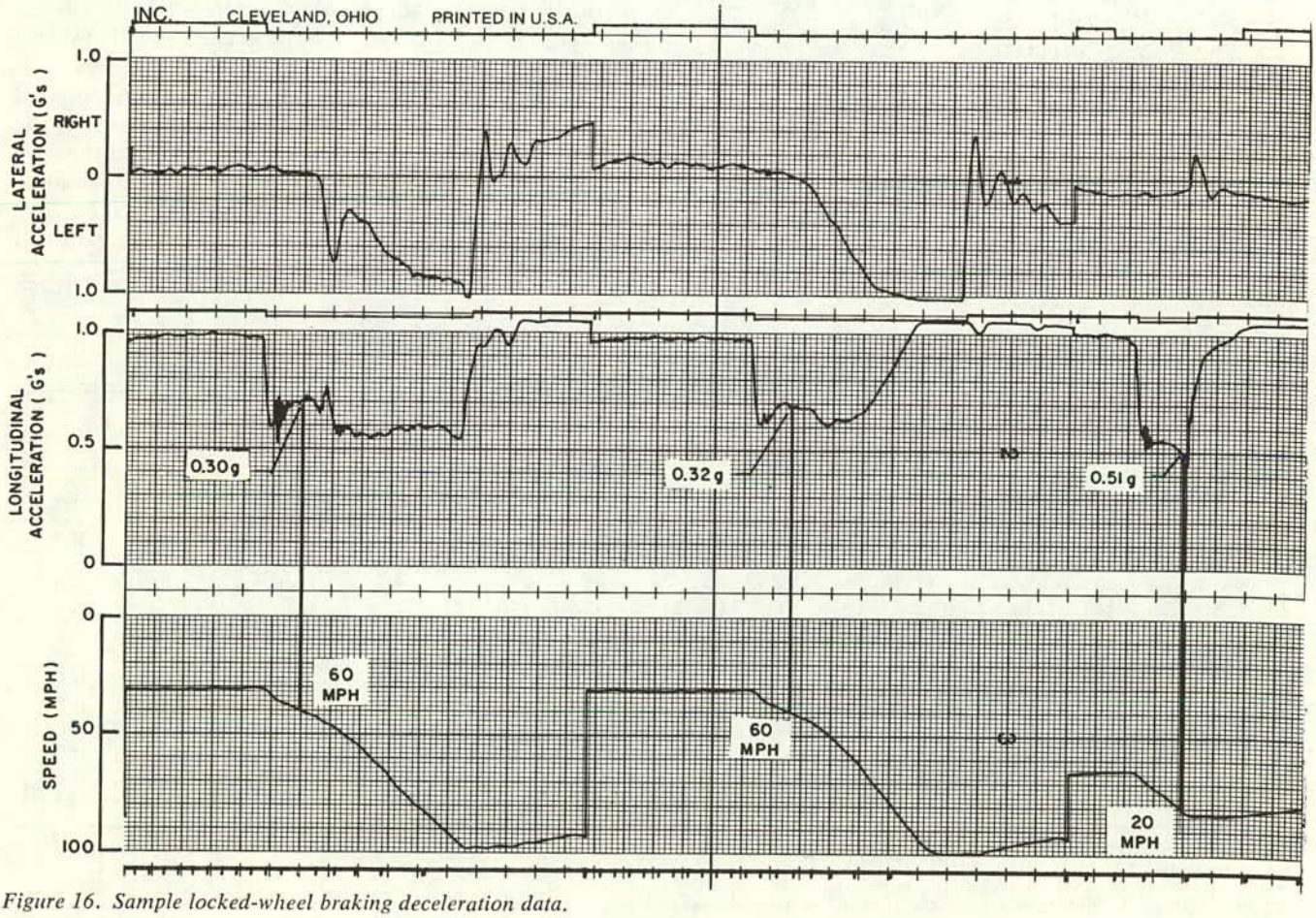

Figure 16. Sample locked-wheel braking deceleration data.

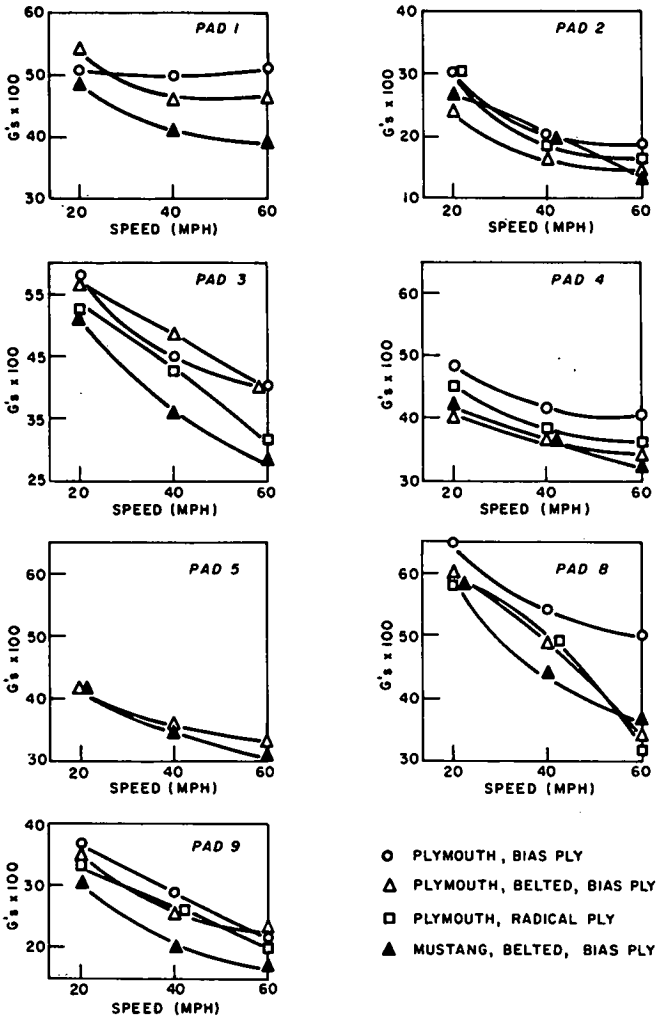

Figure 17. Locked-wheel braking deceleration as a function of speed on seven surfaces for four tire/vehicle combinations.

Figures 18 through 21 show locked-wheel braking deceleration as a function of the NBS SN_{40} values of the several pads. Each figure illustrates a different tire/vehicle combination. Regression lines have been fitted in each case and, in general, show a strong relationship exists between skid numbers and locked-wheel braking decelerations. Correlation coefficients are in excess of 0.90.

Because of the differences between the vehicle/tire combinations and the interactions between vehicle/tire combinations and the other variables, no one of these figures can be considered representative or even worst case. Accordingly, a deceleration versus skid number plot was made in which each point is the worst case from among the four vehicle/tire combinations at each of the three speeds. These data are shown in Figure 22 and are taken to represent a reasonable worst case for American cars on new, first-line tires. Figure 22 also shows worst-case deceleration at 10 mph. The lines were fitted to the data by means of linear regression.

SKID RESISTANCE REQUIRED TO ACCOMMODATE THE MEASURED DECELERATION PROFILES

To use deceleration level data to determine pavement friction requirements, it is necessary to specify the speed. For a given level of deceleration, the higher the speed, the greater the required skid number. Since the speed of braking vehicles is decreasing, the point of greatest deceleration is not necessarily the point of greatest demand. Hence, it is necessary to know the speeds associated with the various percentile levels of deceleration at each interval. Table 7 shows the empirical 95th and 99th percentile and maximum deceleration levels, the associated speeds, and the required skid resistances for all sites. The speeds shown are *not* the *p*th percentile speeds; they are the speeds in each interval of the vehicles braking at the *p*th percentile of deceleration. The skid-resistance requirements in terms of ASTM SN_{40} values were determined in each interval for the 95th and

TABLE 7

95TH PERCENTILES, 99TH PERCENTILES, AND MAXIMUM REQUIRED SKID RESISTANCE AND ASSOCIATED SPEEDS, DECELERATIONS, AND DISTANCES FOR 12 SITES

	SITE CHARACTERISTICS			95TH PERCENTILE				99TH PERCENTILE				MAXIMUM			
SITE NO.	HIGHWAY TYPE	$\bar{V}$ [a]	TC [b]	DECEL. (G)	SPEED	SN_{40} [c]	DIST. [d]	DECEL. (G)	SPEED	SN_{40} [c]	DIST. [d]	DECEL. (G)	SPEED	SN_{40} [c]	DIST. [d]
1	4	36	450	0.35	25	33	65	0.38	31	41	110	0.41	33	47	110
2	1	36	412	0.25	37	27	190	0.46	21	46	50	0.47	34	56	110
3	5	40	426	0.34	35	38	190	0.38	39	47	190	0.46	52	64	260
4	1	36	104	0.24	41	28	190	0.39	23	37	35	0.43	39	54	225
5	2	38	448	0.31	43	39	190	0.44	31	50	110	0.48	36	59	110
6	4	30	116	0.29	22	22	65	0.38	19	33	35	0.51	45	68	385
7	6	39	94	0.36	29	37	110	0.46	26	50	85	0.44	42	57	160
8	6	40	112	0.29	36	32	160	0.49	13	43	20	0.52	48	71	190
9	3	41	282	0.30	48	39	300	0.38	54	53	225	0.49	51	68	190
10	2	37	406	0.30	33	31	135	0.38	44	49	225	0.47	40	61	160
11	5	40	592	0.35	36	40	135	0.46	37	57	110	0.62	43	84	135
12	3	35	370	0.21	41	23	260	0.28	38	32	260	0.43	40	55	385

[a] Mean initial speed.
[b] Mean hourly traffic count.
[c] Required.
[d] From stop line. Each distance is the distance of the deceleration interval's first switch relative to the stop line.

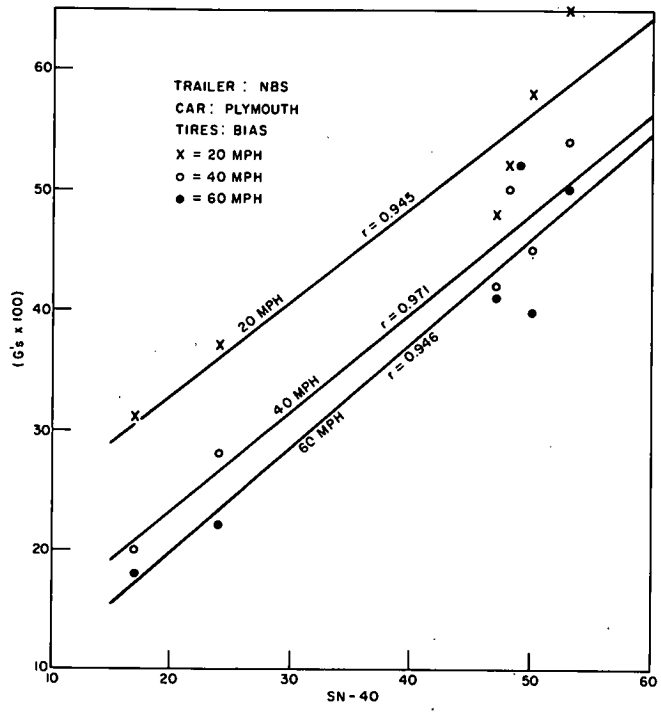

Figure 18. Locked-wheel braking deceleration as a function of skid number at three speeds, using bias-ply tires.

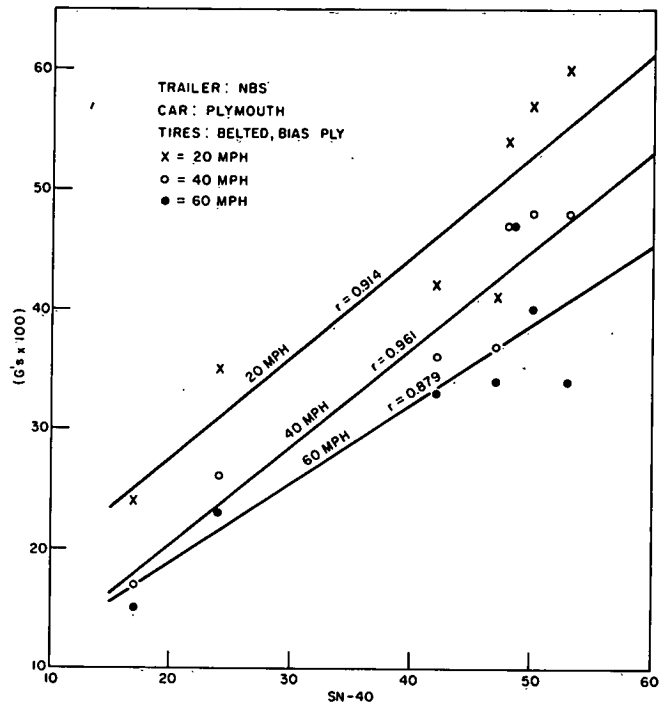

Figure 19. Locked-wheel braking deceleration as a function of skid number at three speeds, using belted, bias-ply tires.

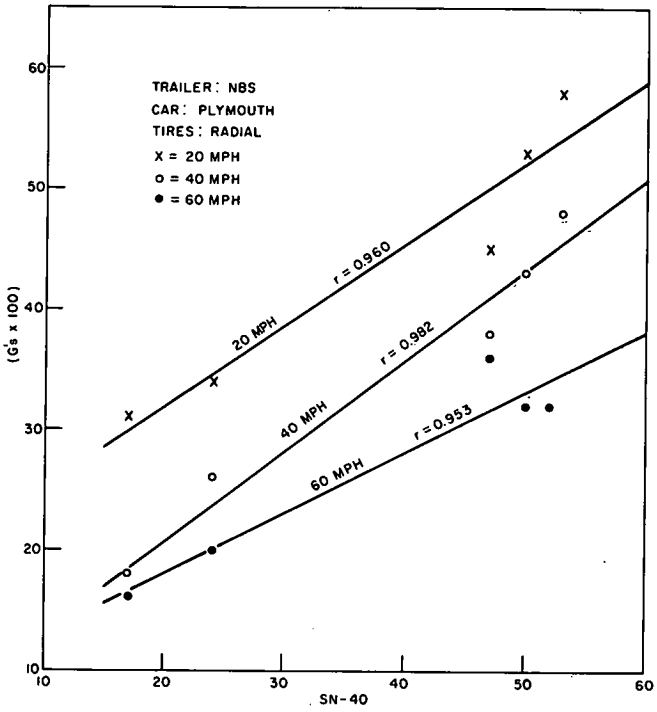

Figure 20. Locked-wheel braking deceleration as a function of skid number at three speeds, using radial tires.

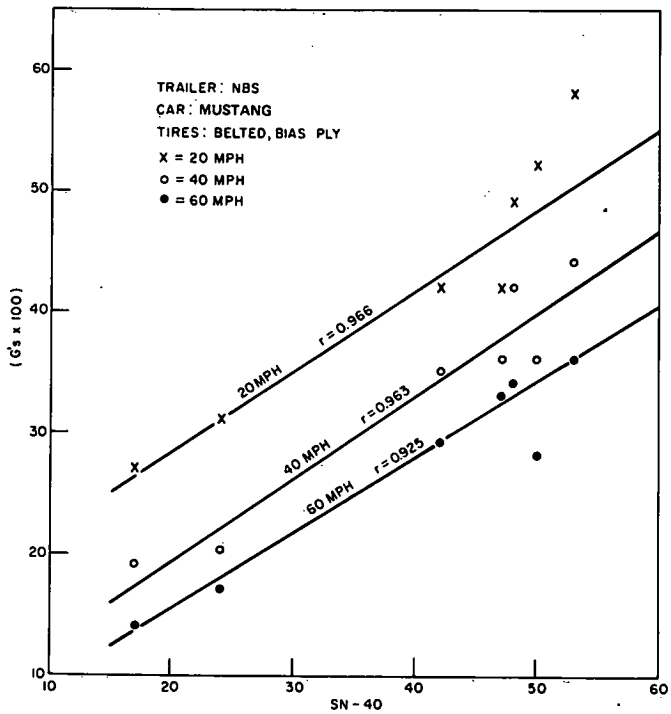

Figure 21. Locked-wheel braking deceleration as a function of skid number at three speeds, using belted, bias-ply tires in another test.

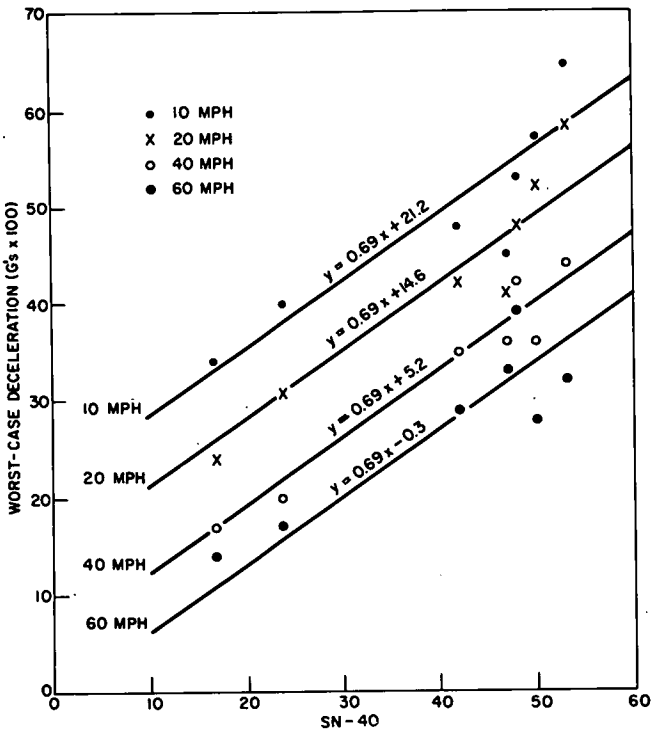

Figure 22. Minimum locked-wheel braking deceleration values as a function of NBS SN_{40}.

99th percentile and maximum deceleration levels using the relationships previously presented (see Fig. 22). Figure 23 shows the conversion of measured accelerations to skid resistance requirements for site No. 8. The full set of 36 figures showing 95th and 99th percentile and maximum deceleration levels and associated speed and required skid numbers for the 12 intersection sites are included in Appendix B (Fig. B-1 through B-12).

To facilitate conversions, Table 8 was produced from the relationships between deceleration, skid resistance, and speed shown in Figure 22. Table 9 lists the skid resistance requirements for the 12 intersection sites studied during the project as determined by the FIRL procedure. There is a considerable spread indicating a rather wide range of skid-resistance requirements for the sites studied. However, Table 10 shows that the skid resistance requirements follow a rather consistent pattern when the maximum or 100th percentile value is not considered. By listing the 12 sites in rank order on the basis of skid-resistance requirements (as given in Table 10), it is noted that the procedure can be

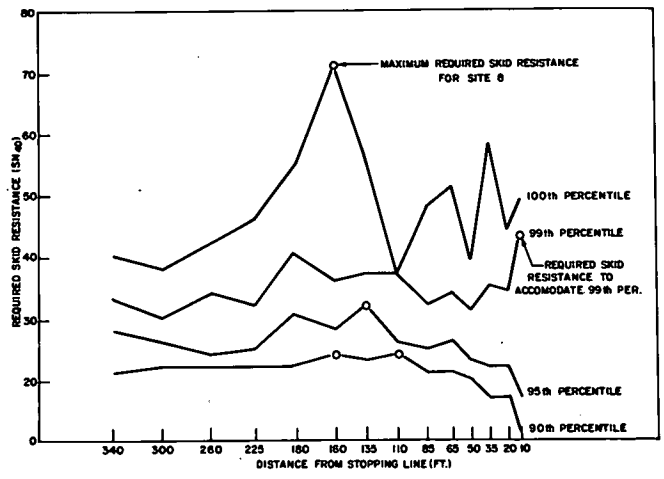

Figure 23. Required skid resistance predicted from observed decelerations and their associated speeds versus distance from stop line, intersection site No. 8.

TABLE 8

SN_{40} REQUIRED TO ACCOMMODATE VARIOUS COMBINATIONS OF SPEED AND ACCELERATION

BRAKING DECELERATION (g)	SPEED (MPH)						
	10	15	20	30	40	50	60
0.60	56.5						
0.58	53.0	58.2					
0.56	50.0	55.0	60.1				
0.54	47.4	52.3	57.5				
0.52	44.0	49.0	54.5				
0.50	41.4	46.1	51.3	58.0			
0.48	37.8	43.0	48.5	55.0			
0.46	35.0	40.0	45.2	52.3	58.6		
0.44	32.4	37.0	42.5	49.3	56.0		
0.42	28.5	34.0	39.5	46.5	52.5	57.5	
0.40	26.0	31.0	36.5	43.0	50.0	54.9	59.3
0.38	22.7	27.6	33.5	40.1	47.0	52.0	56.5
0.36	20.0	25.0	30.4	37.5	43.9	48.8	53.5
0.34	17.0	22.0	27.5	34.5	41.0	46.0	50.8
0.32	13.8	18.9	24.8	32.3	38.0	42.9	47.5
0.30	11.0	15.8	21.9	28.0	35.2	40.0	44.3
0.28		12.5	18.5	25.5	32.5	37.0	41.5
0.26		9.9	16.0	22.5	29.5	34.0	38.5
0.24			12.6	19.5	26.5	31.5	36.0
0.22			10.0	17.0	23.8	28.5	32.5
0.20				13.6	21.0	25.3	30.0

TABLE 9

MAXIMUM SKID NUMBER (SN_{40})* REQUIRED TO ACCOMMODATE pTH PERCENTILE DECELERATION

SITE NUMBER	100TH PERCENTILE	99TH PERCENTILE	95TH PERCENTILE	90TH PERCENTILE
1	47	41	33	27
2	56	46	27	23
3	64	47	38	29
4	54	37	28	23
5	59	50	39	28
6	68	33	22	19
7	57	50	37	33
8	71	43	32	24
9	68	53	39	36
10	61	49	31	26
11	84	57	40	32
12	55	32	23	19

* Computed using observed deceleration values and observed associated speeds.

useful in determining whether a particular site is in a category requiring normal, intermediate, or high pavement skid resistance to safely accommodate wet-pavement braking maneuvers of a vast majority of drivers using the site.

Table 8 also gives the distances from the intersection at which the peak skid resistance requirement occurred, the associated speed and deceleration, the mean approach speed, and average instrumented lane traffic count for each site. The SN_{40} required to accommodate the 99th percentile deceleration ranges from 32 to 57; to accommodate the maximum deceleration, the required values range from 47 to 84. The table also reveals that site type is not a reliable guide to skid-resistance requirements. For example, the 99th percentile requirements for the two type 3 sites are 32 and 53. There is some relationship between average approach speed and skid-resistance requirements as shown in Figure 24, but the relationship is obviously not very reliable. Part of the reason for this is that the approach speed was measured with the first two Tapeswitches at 385 and 340 ft. Many of the faster vehicles are already decelerating at this point so the range is compressed. Deeper analysis of the data, such as discussed in Chapter Three, was required to demonstrate a useful relationship between site characteristics and skid-resistance requirements.

TABLE 10

MAXIMUM SKID NUMBERS (SN_{40}) REQUIRED TO ACCOMMODATE 99TH PERCENTILE DECELERATION

SITE NO.	REQUIRED SKID NUMBER	SKID RESISTANCE REQUIREMENTS CATEGORY
11	57	High
9	53	
7	50	
5	50	
10	49	Intermediate
3	47	
2	46	
8	43	
1	41	
4	37	Normal
6	33	
12	32	

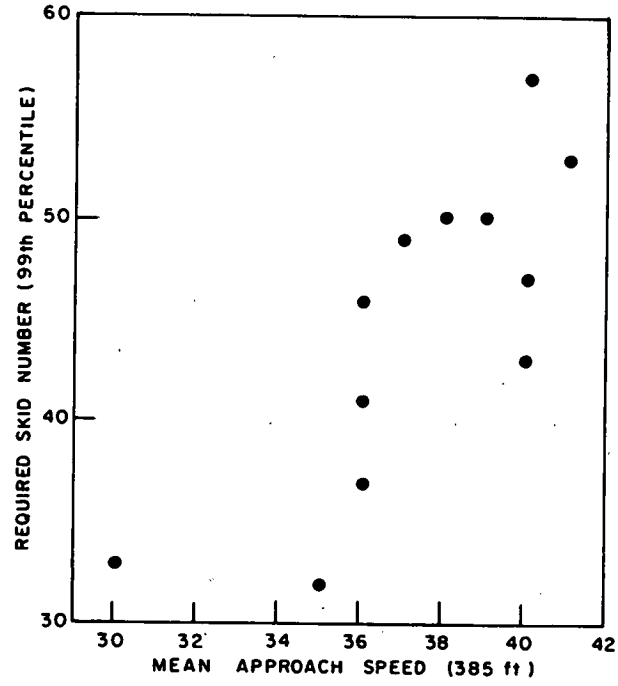

Figure 24. Required 99th percentile skid number and initial speed.

CHAPTER THREE

INTERPRETATION AND APPLICATIONS

INTRODUCTION

This chapter discusses the development and application of an intersection demand model (IDM) using data collected during the study. It also gives calculations of driver demand for skid resistance at each of the twelve intersection sites and presents tentative minimum skid-resistance requirements predicted from the model.

DEVELOPMENT OF THE INTERSECTION DEMAND MODEL

In developing an approach to the analysis of deceleration data, the primary goal was to relate intersection skid-resistance requirements to site parameters that could be measured easily. Obviously, an intersection site (or any braking site) can be instrumented with the vehicle acceleration measuring system described in Chapter Two. However,

it is realized that some highway agencies, for one reason or another, may not be in a position to use this technology. Accordingly, the analysis of the data was, in effect, a search for a set of site variables that could be measured with a simpler system than that used in this study. More specifically, a search was made for a set of parameters which, along with distance from the intersection, could be used to determine the skid resistance necessary to accommodate various percentile levels of demand. The intention is to introduce a model that can be refined and validated for general use as more data become available.

Two general modeling approaches were considered. In the first, percentile speed and deceleration data would be predicted from site characteristics. The deceleration/speed/required skid number relationships developed in Chapter Two would then be applied to the predicted values of speed and deceleration to determine the skid numbers. In the second approach, the required skid number would be determined for each speed/deceleration data point, and a model would be developed to predict required skid numbers directly from site characteristics. Although the second approach would yield a more direct and a simpler procedure, it was decided to follow the first approach.

The reason for this decision is that the skid numbers yielded by either approach would be highly dependent on the specific skid-resistance/deceleration relationships developed in the skid studies reported in Chapter Two. However, these relationships are based on a limited set of tires and vehicles and, hence, are very much subject to updating and revision. If and when such new data become available, a direct skid-resistance prediction model would be obsolete, and it would be difficult to incorporate the new data.

On the other hand, it would be easy to incorporate revised skid-number/deceleration relationships in a procedure in which these relationships are applied as an independent step. Accordingly, the development of a model to predict percentile speed and deceleration profiles as a function of site characteristics was undertaken.

Development Approach

The approach to the development of a skid-number prediction model was based on the apparent normality of the distribution of observed deceleration values in the various distance intervals. An analysis of the data indicated that the assumption of normality was statistically acceptable.

Because the data support the normality hypothesis, the best method of estimating deceleration percentiles is to calculate their values from the deceleration mean and standard deviation predicted for the particular interval. The percentile values are calculated using the relationship:

$$g_{p_d} = \bar{g}_d + z_p S_{g_d} \tag{7}$$

in which g_{p_d} is the pth deceleration percentile in the interval whose middle switch is at distance d from the stopping line; $\bar{g}_d$ and S_{g_d} are the deceleration mean and standard deviation predicted for the interval, and z_p is the standard normal deviate corresponding to the pth percentile.

The method of predicting the mean and standard deviation for the interval and then calculating percentiles based on the mean and standard deviation is superior to direct prediction of the percentiles from the values of other variables. In order to predict the percentiles directly, regression equations relating the percentiles to other variables would be required. The regression calculations would utilize empirical percentiles observed at the sites. However, the empirical percentiles of interest (the 95th and 99th) are extreme values representing as few as three cases and, as such, are unstable. It is more desirable to base the regression analysis upon the empirical means and standard deviations, which are more stable than extreme values. Since deceleration is normally distributed, the percentiles can then be estimated from the means and standard deviations predicted using the regression equations.

Accordingly, further analysis was undertaken to determine whether or not it would be possible to develop reliable prediction equations for (1) mean deceleration in each interval, (2) the standard deviation of the deceleration, and (3) the speeds associated with the 90th, 95th, and 99th percentile levels of deceleration in each interval. Three sets of predictor variables were chosen for evaluation in a series of stepwise linear-regression analyses. Each set includes a number of site characteristics variables and functions of these variables. The variables included in the different sets represent different levels of measurement complexity or difficulty. Set 1 includes the least complex variables; set 3, the most complex. The purpose of this procedure was to provide the traffic engineer with the opportunity to make a tradeoff between field measurement complexity and accuracy of prediction. As it developed, the set 2 and set 3 variables produced no improvement in prediction accuracy over set 1.

The variables in each of the three predictor sets are listed in Table 11. Except for the functions of distance (d, d^2, $\sqrt{d}$, and $1/d$), the variables are the means, standard deviations, and 95th percentile values of traffic parameters that must be measured at each site.

The distance variable, d, is the distance of the vehicle from the stop line at which deceleration is to be predicted.

The quantities V_{340} and V_{225} are the speeds at 340 and 225 ft, respectively. Although both of these variables are in sets 1 and 2, the regression analyses were conducted in such a way that only one of the two could be considered at a time. V_{225} was chosen as a variable because at 225 ft almost all vehicles are braking and, at the same time (as indicated by Table 7 with only one exception) peak demand (99th percentile) occurs at or within 225 ft.

Stopping point, SP, is the distance from the stop line at which a vehicle comes to a halt. Stopping point was estimated for the regression analysis as the position of the midpoint between the last Tapeswitch crossed and the next Tapeswitch. Although SP was included in the list of variables, its primary importance is that it is used to calculate the average deceleration of a vehicle between 225 ft and the SP, or ($\tilde{a}_1$), and 50 ft and the SP, or ($\tilde{a}_3$). The quantity $\tilde{a}_1$ is the average deceleration between 225 and 50 ft. The computation of $\tilde{a}_1$ is

$$\tilde{a}_1 = (1.467\, V_{225})^2/64.4\,(225 - SP) \tag{8}$$

This quantity was selected because it seemed reasonable to assume that peak values of deceleration are related to average values.

TABLE 11

PREDICTOR VARIABLES IN REGRESSION ANALYSES

VARIABLE NO.	IDENTIFICATION	SYMBOL	INCLUDED IN PREDICTOR SET 1	2	3
1	Distance	d	✓	✓	✓
2	Distance speed	d^2	✓	✓	✓
3	Square root of distance	$\sqrt{d}$	✓	✓	✓
4	Reciprocal of distance	$1/d$	✓	✓	✓
5	Mean average deceleration between 225 ft from stopping line and vehicle stopping point	$\bar{\bar{a}}_1$	✓	✓	✓
6	Standard deviation of $\tilde{a}_1$	$S_{\bar{a}}$	✓	✓	✓
7	95th percentile $\tilde{a}_1$ value	$\tilde{a}_{1_{95P}}$	✓	✓	✓
8	Average speed at 225 ft	$\bar{V}_{225}$	✓	✓	✓
9	Standard deviation of speed at 225 ft	$S_{V_{225}}$	✓	✓	✓
10	95th percentile speed at 225 ft	$V_{225_{95P}}$	✓	✓	✓
11	Average vehicle stopping point	$\overline{SP}$	✓	✓	✓
12	Standard deviation of vehicle stopping point	S_{SP}	✓	✓	✓
13	95th percentile stopping point	SP_{95P}	✓	✓	✓
14	Average hourly traffic count	$\overline{TC}_H$	✓	✓	✓
15	Maximum hourly traffic count	$TC_{H_{\max}}$	✓	✓	✓
16	Average speed at 340 ft	$\bar{V}_{340}$	✓	✓	✓
17	Standard deviation of speed at 340 ft	$S_{V_{340}}$	✓	✓	✓
18	95th percentile speed at 340 ft	$V_{340_{95P}}$	✓	✓	✓
19	Mean average deceleration between 225 ft and 50 ft from stopping line	$\bar{a}_2$		✓	
20	Standard deviation of $\bar{a}_2$	$S_{\bar{a}_2}$		✓	
21	95th percentile $\bar{a}_2$ value	$\bar{a}_{2_{95P}}$		✓	
22	Mean average deceleration between 50 ft from stopping line and vehicle stopping point	$\bar{a}_3$		✓	
23	Standard deviation of $\bar{a}_3$	$S_{\bar{a}_3}$		✓	
24	95th percentile $\bar{a}_3$ value	$\bar{a}_{3_{95P}}$		✓	
25	Average speed at 50 ft	$\bar{V}_{50}$		✓	
26	Standard deviation of speed at 50 ft	$S_{V_{50}}$		✓	
27	95th percentile speed at 50 ft	$V_{50_{95P}}$		✓	
28	Average deceleration at 225 ft	$\bar{g}_{225}$			✓
29	Standard deviation of deceleration at 225 ft	S_{g225}			✓
30	95th percentile deceleration at 225 ft	$g_{225_{95P}}$			✓
31	Mean deceleration observed at distance d	$\bar{P}g_d$	✓	✓	✓

The quantity g_{225} is the deceleration observed at 225 ft (i.e., between 260 and 190 ft).

Note that the distance variables and the mean deceleration at each distance $\bar{g}_d$ need not be measured. The mean deceleration values are used only in the prediction of the standard deviation of deceleration and are themselves predicted values.

For the engineer in the field, the minimum equipment requirements to measure the quantities appearing in Table 12 are as follows:

- Set 1: Two detectors (Tapeswitch or otherwise) and a 10-μs timer.
- Set 2: Two pairs of detectors and two 10-μs timers.
- Set 3: Three Tapeswitch detectors and two 1/10-μs timers or a recording system with equivalent accuracy.

Each set also requires the observation of stopping point for each stopping vehicle. Measurement procedures in the field are discussed in more detail under "Application of the Intersection Demand Model."

For the present analysis, values of the variables listed in Table 12 were computed from the same Tapeswitch data used to compute deceleration. Values of set 1 predictor variables used in the prediction equations are given in Table 12.

Predicting Deceleration and Speed

The objective of the initial regression analysis was to determine whether the mean deceleration could be predicted for each distance at a site. Three stepwise multiple-regression calculations (one for each set of predictor variables) were performed in this analysis. In each calculation, the values of the variable to be predicted were the deceleration means observed at the sites. The observed values of the variable to be predicted were weighted by the sample sizes in each regression analysis. In the first calculation, only

TABLE 12

VALUES OF PREDICTOR VARIABLES

SITE NO.	SITE VARIABLE $\bar{a}_1$	$S_{\bar{a}_1}$	$\bar{a}_{1_{95P}}$	V_{225}	$S_{V_{225}}$	$V_{225_{95P}}$	$\overline{SP}$	S_{SP}	SP_{95P}	$\overline{TC_H}$	$TC_{H_{max}}$	$\overline{V}_{340}$	$S_{V_{340}}$	$V_{340_{95P}}$
1	0.17	0.048	0.26	30.9	5.60	41.5	33.19	29.544	85.00	450	554	36.0	4.90	44.4
2	0.17	0.044	0.25	31.8	4.76	39.4	22.96	27.200	73.87	412	528	36.2	4.79	44.3
3	0.18	0.064	0.31	32.9	6.04	43.8	19.31	24.482	68.35	426	538	39.6	6.43	50.7
4	0.16	0.046	0.23	33.6	4.97	41.9	−24.73	21.108	2.56	104	156	36.2	5.61	45.4
5	0.17	0.059	0.28	31.8	5.86	42.1	22.61	23.470	58.91	448	518	37.5	5.83	47.1
6	0.16	0.043	0.22	30.0	4.83	38.5	0.20	9.232	15.91	116	180	30.3	5.68	42.0
7	0.20	0.052	0.28	36.1	4.92	43.5	1.24	11.316	17.13	94	152	38.6	7.60	48.0
8	0.18	0.051	0.26	34.6	5.04	42.3	−3.67	12.085	10.79	112	140	40.3	5.53	48.9
9	0.20	0.068	0.33	33.8	6.45	45.2	26.51	20.179	69.70	282	592	41.2	6.15	51.8
10	0.16	0.058	0.27	31.0	5.78	41.5	19.12	20.347	64.70	406	592	37.1	5.85	47.5
11	0.19	0.072	0.32	33.3	6.63	45.1	22.77	21.196	57.75	592	810	39.6	6.31	50.5
12	0.15	0.043	0.22	30.6	4.74	37.7	8.99	15.340	41.14	370	476	35.1	5.50	44.0

set 1 variables were considered as possible predictors (variables No. 1 to 18). Similarly, the second calculation considered only set 2 variables as predictors (variables No. 1 to 27), while the third calculation utilized only set 3 variables (variables No. 1 to 18 and 28 to 30).

The results of the calculations were analyzed and the three "best" prediction equations that could be obtained using the three sets of predictor variables were selected. The end result was that the equation containing the set 1 variables, which could be measured in a day using one pair of switches, was just as accurate as the equations requiring three and four switches.

A similar analysis was performed to determine whether the standard deviation of deceleration could be estimated for each distance at a site. The predicted mean deceleration at each distance (variable 31) was also considered as a possible predictor variable in this analysis. The results of the three calculations were analyzed as previously described. As in the case of the mean deceleration, it was concluded that the optimal prediction equation for the standard deviation was the best equation involving set 1 predictor variables.

Exactly analogous calculations were performed to estimate the speeds of cars having the 99th, 95th and 90th deceleration percentile values at each distance at a site. The results indicated that these variables could also be estimated accurately enough from the values of other variables. It was concluded that the optimal prediction equation for each associated speed was the best equation involving set 1 variables.

The equations selected are shown in Table 13. The standard error in the last column measures the equation's accuracy of prediction. (The standard error is expressed in the same unit of measurement as the variable predicted.) Since the standard error represents the dispersion of the observed values of the variable predicted about the values estimated using the equation, a minimal standard error is desirable. These standard errors were considered sufficiently small to warrant the prediction of the key variables using the predictor variables in question. Note that $\bar{g}_d$, the mean observed deceleration, is an independent variable in the equation predicting S_{g_d}. Although the prediction model was developed using the observed values, the user would employ the predicted values of $\bar{g}_d$ obtained from the first equation in Table 13.

Further analysis was performed to evaluate the accuracy of estimation of the deceleration percentiles using the normality assumption and the means and standard deviations obtained from the prediction equations. Deceleration means and standard deviations were calculated for each distance at each site by substituting the predictor variable values observed at the sites into the equations in Table 14. The calculated means and standard deviations were then used to estimate the 99th, 95th, and 90th deceleration percentiles for each distance at each site, employing the relationship based on the normality hypothesis [Eq. (7)]. The predicted deceleration percentiles were then compared to the corresponding percentiles observed at the sites. The comparison showed that the mean difference between the empirical and predicted 99th percentile deceleration levels was 0.02 g and that 32 percent of the estimated 99th percentiles were less than the corresponding observed 99th percentiles by more than 10 percent (of the value of the observed percentiles). The tendency to underestimate the 95th and 90th percentiles was much less pronounced, although great enough.

These results could indicate that the mean and/or the standard deviation of deceleration cannot be estimated accurately enough using the predictor variables considered in the study. However, it is more likely that some of the empirical deceleration distributions deviate from the normal distribution in such a way that their extreme-value percentiles are higher in value than those of an exactly normal distribution. It is also very possible that if more data could have been collected to define these distributions, the empirical 99th percentiles would actually have been lower in value. However, it was decided that the empirical percentiles should be accepted at face value.

The differences between corresponding predicted and empirical percentiles were computed so that three sets of differences were obtained (differences between 99th percentile estimates, 95th percentile estimates, etc.). Since the differences appeared normally distributed about their means in each set, difference percentiles were computed and tested

TABLE 13

PREDICTION EQUATIONS FOR KEY DECELERATION AND SPEED VARIABLES

VARIABLE PREDICTED	PREDICTOR VARIABLES	EQUATION	STANDARD ERROR OF PREDICTION
Mean deceleration at a site at distance d ($\bar{g}_d$)	Distance (d) Average deceleration between 225 ft and vehicle stopping point ($\bar{\bar{a}}_1$) Average hourly traffic count ($\overline{TC}_H$)	$\bar{g}_d = 0.021 - 0.000372\,d + 1.036\,a_1 + 0.0000410\,\overline{TC}_H$	0.0228
Standard deviation of deceleration at a site at distance d (S_{g_d})	Mean deceleration at distance d ($\bar{g}_d$) Reciprocal of distance ($1/d$) Square root of distance ($\sqrt{d}$) Standard deviation of speed at 225 ft ($S_{v_{225}}$) Standard deviation of $\bar{a}_1$ ($S_{\bar{a}_1}$)	$S_{g_d} = 0.00906 + 0.0831\,\bar{g}_d + 0.146(1/d) - 0.00102\,\sqrt{d} + 0.00616\,S_{v_{225}} + 0.404\,S_{\bar{a}_1}$	0.00515
Speed associated with 99th deceleration percentile at a site at distance d (Speed_{99P_d})	Square root of distance ($\sqrt{d}$) Average deceleration between 225 ft and vehicle stopping joint ($\bar{\bar{a}}_1$)	$\text{Speed}_{99P_d} = -5.063 + 1.896\,\sqrt{d} + 95.879\,\bar{\bar{a}}_1$	5.170
Speed associated with 95th deceleration percentile at a site at distance d Speed_{95P_d})	Square root of distance ($\sqrt{d}$) Average speed at 225 ft ($\overline{V}_{225}$)	$\text{Speed}_{95P_d} = -32.46 + 2.088\,\sqrt{d} + 1.203\,\overline{V}_{225}$	4.569
Speed associated with 90th deceleration percentile at a site at distance d (Speed_{90P_d})	Square root of distance ($\sqrt{d}$) Average speed at 225 ft ($\overline{V}_{225}$)	$\text{Speed}_{90P_d} = -23.72 + 1.983\,\sqrt{d} + 0.929\,\overline{V}_{225}$	3.724

for deviations from normality at the 5-percent level of significance using the Kolmogorov-Smirnov test. The results of the tests supported the normality hypothesis in each case. Because the underlying distributions of the differences had been identified, the 95th percentile difference (between predicted and empirical estimates), which could be expected to occur based on these data, could be estimated for each case. The mean and standard deviation of the differences and the 95th percentile difference estimated in each case (using the normal-distribution relationship $\bar{x}_p = x + z_p S_x$) are as shown in Table 14.

In order to ensure a more accurate prediction of the deceleration percentiles, the 95th percentile differences shown in Table 14 should be added to the percentile estimates based on the predicted means and standard deviations.

Predicting Required Skid Numbers

Accordingly, the deceleration percentiles estimated for the various distances at the 12 sites were each incremented by the appropriate 95th percentile difference as given in Table 14. The incremented deceleration percentiles and predicted associated speeds were then used to estimate skid numbers required at the various distances at each site. The skid number for a particular site and distance was obtained by entering the graph in Figure 22 with the deceleration percentile value and associated speed predicted for the site at that distance. The skid number that would be recommended for the site based on that deceleration percentile (and associated speed) is the maximum of the skid numbers estimated for the 14 distances. Accordingly, a single required skid number was obtained for each site based on each predicted deceleration percentile and associated speed.

For purposes of comparison, the same procedure was followed using the *observed* deceleration percentiles and associated speeds, and a required skid number was obtained for each site based on these values.

Table 15 gives the required skid numbers obtained using the predicted and observed values of the deceleration percentiles and associated speeds. As given in Table 15, the required skid numbers based on the predicted deceleration percentiles and associated speeds are generally greater and, hence, more conservative than the skid numbers estimated using the observed percentiles and associated speeds. For example, the ΔSN_{99P} column shows that the skid numbers corresponding to predicted 99th percentiles and associated speeds are greater than the values based on observed 99th percentiles and speeds in 9 of the 12 cases. Furthermore, the largest negative difference observed over the 12 pairs of skid numbers (corresponding to 99th percentiles) was four

TABLE 14

STATISTICS REPRESENTING DIFFERENCES BETWEEN PREDICTED AND EMPIRICAL PERCENTILES

DECELERATION PERCENTILE	MEAN DIFFERENCE ($\bar{x}$)	STANDARD DEVIATION OF DIFFERENCES (S_x)	95TH PERCENTILE DIFFERENCE (x_{95})
99	0.02	0.029	0.07
95	0.01	0.025	0.05
90	0.00	0.027	0.04

TABLE 15

REQUIRED SKID NUMBERS CORRESPONDING TO DECELERATION PERCENTILES (AND ASSOCIATED SPEEDS)

SITE NO.	REQUIRED SKID NUMBER (SN) CORRESPONDING TO PREDICTED (PRE) AND OBSERVED (OBS) VALUES OF pTH DECELERATION PERCENTILE								
	SN_{Pre99P}	SN_{Obs99P}	ΔSN_{99P}	SN_{Pre95P}	SN_{Obs95P}	ΔSN_{95P}	SN_{Pre90P}	SN_{Obs90P}	ΔSN_{90P}
1	46	41	5	32	33	−1	27	27	0
2	44	46	−2	32	27	5	27	23	4
3	51	47	4	38	38	0	32	29	3
4	40	37	3	30	28	2	24	23	1
5	47	50	−3	35	39	−4	29	28	1
6	35	33	2	24	22	2	18	19	−1
7	52	50	2	39	37	2	33	33	0
8	46	43	3	34	32	2	29	24	5
9	56	53	3	42	39	3	35	36	−1
10	45	49	−4	31	31	0	26	26	0
11	58	57	1	42	40	2	35	32	3
12	39	32	7	27	23	4	22	19	3
		Mean (ΔSN):	1.8			1.4			1.5

skid-number units (site No. 10). This amount of underestimation (i.e., amount of risk) was considered reasonable. The mean difference between the required skid-number values was about two skid-number units in this case—the mean (ΔSN) was 1.8 skid numbers—so that, on the average, the required skid numbers based on the predicted values were two skid number units higher (and more conservative) than those based on the observed values.

As mentioned above, each predicted deceleration percentile was incremented by the appropriate 95th percentile difference expected to occur between future predicted and empirical percentiles (based on the present data). If the 99th percentile difference had been added instead, the skid numbers corresponding to the predicted percentiles would have been about one unit higher (for a given associated speed). However, this gain was not considered high enough to necessitate a change to a 99th percentile difference increment.

APPLICATION OF THE INTERSECTION DEMAND MODEL

The intersection demand model (IDM) estimates skid-resistance requirements. To use the model to determine a required skid number for a particular intersection, a certain amount of data must be collected at the site. The advantage of the model is that the data required and the necessary instrumentation are far less complex and more easily obtained than deceleration data using the entire Tapeswitch system.

All of the necessary data can be obtained in one day with relatively simple equipment and a single observer. The required measurements are:

1. The speed of each vehicle at a point 225 ft from the stop line (V_{225}).
2. The average deceleration of each vehicle between 225 ft and the stop line ($\tilde{a}$).
3. The average hourly traffic count in the lane(s) of interest ($\overline{TC}_H$).

There are any number of ways of measuring V_{225}. Perhaps the simplest is to use two Tapeswitches evenly bracketing 225 ft and an interval timer. With a 30-ft separation of the detectors, a 0.01-sec interval timer will provide sufficient accuracy. To determine average deceleration, either the stopping point (SP) or the time required to stop from 225 ft (T_{225}) must be known. Since many vehicles will coast the last few feet to a stop at a walking pace, time to stop will not always provide a meaningful basis for computing $\tilde{a}$.

Stopping point can be estimated with sufficient accuracy for the model by selecting a series of landmarks (trees, building features, light or utility poles, etc.) that, from a fixed vantage point, are in line-of-sight with 20-ft distance intervals in the instrumented lane. Determination of the SP (front of the vehicle) to within 10 ft is sufficient. Average deceleration for a given vehicle is then given by.

$$\tilde{a} = V_{225}^2/30(225 - SP) \qquad (9)$$

Since these parameters are normally distributed and exhibit stable standard deviations, accurate estimates of percentile skid-number requirements can be made on the basis of a sample size of 200.

The axle count can be obtained by attaching an electrically operated counter to one of the Tapeswitch detectors.

The necessary statistics for input to the IDM are:

1. $\bar{\tilde{a}}$, the mean average deceleration (in g's).
2. $\overline{TC}_H$, mean hourly single-lane axle count in lane of interest.
3. S_{V225}, the standard deviation of the speed at 225 ft (in mph).
4. $S_{\tilde{a}}$, the standard deviation of $\tilde{a}$ (in g's).
5. $\overline{V}_{225}$, the mean speed at 225 ft (in mph).

The IDM consists of five equations to predict g_d, the mean deceleration at any point between 385 ft and the stop line; S_{g_d}, the standard deviation of deceleration at the point; and the speed associated with 90th, 95th, and 99th percentile deceleration at the point ($V90_d$, $V95_d$, and $V99_d$).

To determine the skid number required to accommodate a given percentile demand, only three equations are used, that is, Eq. (10) and (11) plus either Eq. (12), (13), or (14), whichever one is the appropriate speed equation. In addition to the five statistics listed, two other parameters enter into the equations. These are d_i, the distance from the intersection of the point at which demand is to be determined, and $\bar{g}_d$, mean deceleration at the same point. The equations are as follows:

$$\bar{g}_d = \frac{1}{1000}(1036\,\bar{a} + 0.041\,\overline{TC}_H - 0.372d + 21) \tag{10}$$

Units: g's
Standard error of prediction = 0.023 g

$$S_{g_d} = \frac{1}{1000}(83.1 + 146/d - 1.02\sqrt{d} + 6.16\,S_{V225} + 404 S_{\bar{a}} + 9.06) \tag{11}$$

Units: g's
Standard error of prediction = 0.0052 g

$$V99_d = 95.88\,\bar{a} + 1.896\sqrt{d} - 5.063 \tag{12}$$

Units: mph
Standard error of prediction = 5.17 mph

$$V95_d = 1.203\,\overline{V}_{225} + 2.088\sqrt{d} - 32.46 \tag{13}$$

Units: mph
Standard of error of prediction = 4.57 mph

$$V90_d = 0.929\,\overline{V}_{225} + 1.983\sqrt{d} - 23.72 \tag{14}$$

Units: mph
Standard error of prediction = 3.72 mph

Raw data for the model (V_{225} and SP) should be collected during periods of freely flowing traffic. Data should not be collected during periods when there is nearly always a slowly moving or stopped queue of vehicles at the intersection. Further, data collection should be limited to the first five vehicles in a queue that come to a stop at the intersection. At stop-sign-controlled intersections, many vehicles never come to a complete halt. At such sites, data collection should be limited to vehicles that actually stop or slow to a crawl. In the latter instance, it will be necessary to estimate the "stopping point."

An alternative at stop-sign-controlled intersections is to employ a second pair of detectors (or some other method of determining speed) at a point near the stop line, for example at 20 ft, to provide an approximation of $\bar{a}$. The same equations would be used with the same inputs except that average deceleration ($\bar{a}$) would be defined by:

$$\bar{a} = \frac{(V_{225} - V_{20})^2}{(30)(205)} \tag{15}$$

Using the measurement techniques outlined above, it should be possible for one observer, manually operating the equipment and recording the data, to obtain an adequate sample (150 to 200 vehicles) in 4 to 6 hr.

To determine the controlling demand at a site, it is necessary to compute demand at each of several points in the approach to the intersection. Because the only parameter in the equations that changes with distance is distance, the computations for a particular site are relatively simple. It is recommended that, for a start, estimated demand be computed at distances of 20, 40, 80, 120, 160, and 320 ft. This will indicate the shape of the demand curve and the location of the demand peak. Once this is done, one or two additional interpolated points may be computed, if desired, to firmly establish the peak. The procedures for determining demand at a given distance, d, are:

1. Compute the required input parameters from the raw data ($\bar{a}$, $S_{\bar{a}}$, $\overline{V}_{225}$, S_{V225}, $\overline{TC}_H$).
2. Solve Eqs. (10) and (11) for the appropriate distance to determine g_d and S_{g_d}.
3. Compute the estimated pth percentile deceleration. The computations for the 90th, 95th, and 99th percentile deceleration are:

$$g_{90P} = \bar{g}_d + 1.28\,S_{g_d} + 0.04$$

$$g_{95P} = \bar{g}_d + 1.64\,S_{g_d} + 0.05$$

$$g_{99P} = \bar{g}_d + 1.96\,S_{g_d} + 0.07$$

4. Use the appropriate speed equation [Eq. (12), (13), or (14)] to determine the speed associated with the pth percentile deceleration level, VP_d.
5. Enter Table 8 to determine the SN_{40} required to accommodate $\bar{g}_d$ at VP_d. Table 9 was computed from the equations plotted in Figure 22 in Chapter Two.

This series of calculations should be repeated to obtain seven required SN_{40} values for 20, 40, 80, 120, 160, 240, and 320 ft. The maximum value (i.e., the highest required SN_{40} of the seven) will be a close estimate of the SN_{40} required to accommodate the pth percentile demand.

The value yielded by the model for a particular site incorporates a factor to allow for possible errors of underestimation. Users should refrain from adding an additional safety margin (except as noted below) because, if anything, the predicted values are likely to be slightly higher than required.

TENTATIVE SKID-RESISTANCE REQUIREMENTS FOR INTERSECTIONS

When it is not feasible to use either the Tapeswitch system or the IDM to determine pavement skid-resistance requirements, the information in Table 16 can provide general guidelines for minimum requirements. It must be recognized that these guidelines are very tentative because they are based on extremely limited field data (12 intersections in the eastern Pennsylvania and New Jersey areas). They cannot be applied universally but should be evaluated and modified by further field studies. They are based on the generally increasing demand with traffic speed, an SN_{40} value of 40 as a desirable minimum for any condition, and the recognition that an SN_{40} value of 55 accommodates substantially all of the 99th percentile demand of the 12 sites studied. It is emphasized that these tentative skid-resistance requirements apply only to the short distance (the

TABLE 16

TENTATIVE GENERAL MINIMUM SKID RESISTANCE REQUIREMENTS AT INTERSECTIONS

DESIGN OR TRAFFIC SPEED (MPH)	L POINT * (FT)	MINIMUM SKID RESISTANCE (SN_{40})
Below 40	330	40
40–55	415	45
Above 55	480	55

* The L point is the distance from the stop point at which skid-resistance requirements apply.

L point to the stop point) at intersection sites where braking is a frequent maneuver and the required skid resistance under wet-pavement conditions is higher than on mainline sections of roadway. The traffic speed is defined as the 85th percentile speed of freely moving traffic at a sufficient distance from the intersection so that traffic speeds are not influenced by the intersection. The recommended minimum distance from the intersection at which traffic speed measurements are to be made are 1200, 800, and 500 ft, respectively, for fast, intermediate, and slow traffic.

CHAPTER FOUR

CONCLUSIONS AND RECOMMENDATIONS

The major conclusions of the study are discussed, and the recommendations that arise from these conclusions are presented in this chapter. Recommendations for further research are also offered.

CONCLUSIONS

1. External observation of driver demand at traffic maneuver sites is a rational and practical basis for establishing pavement skid-resistance requirements for such sites. Driver demand is defined as lateral or longitudinal acceleration. The required skid resistance at a site is that which will accommodate the vast majority of drivers (e.g., the 99th percentile demand). The required skid resistance is determined from empirical relationships between various levels of pavement skid resistance and the maximum acceleration levels they will accommodate.

2. A system of discrete Tapeswitch event detectors can be used to measure the positions of a vehicle maneuvering in traffic at different instants of time to accurately determine peak lateral and longitudinal acceleration demand.

3. Use of Tapeswitch detectors to measure longitudinal acceleration is a practical method for highway agencies to determine driver demand at intersections and other braking sites. Use of the detectors to measure lateral acceleration is not considered practical for routine application.

4. Reliable relationships exist between peak longitudinal accelerations and easily measured traffic parameters, and it was possible to develop useful regression models based on these relationships to predict demand.

5. Usefully reliable relationships exist between pavement skid resistance, as measured by an ASTM skid trailer, and longitudinal accelerations (braking deceleration). However, there is evidence of interactions between tires, vehicle types, and pavement surfaces that introduce some unexplained variability into the relationships.

6. Reliable relationships do not exist between pavement skid resistance and maximum lateral acceleration when tire and vehicle-type factors are not considered.

7. Demonstrations at 12 intersection sites indicate that the empirical and analytical techniques developed in this study can be employed to determine skid-resistance requirements for intersections and braking sites.

RECOMMENDATIONS

It is recommended that agencies requiring a high degree of certainty in determining skid-resistance requirements associated with braking or those wishing to perform additional research on driver demand at intersections should avail themselves of the entire Tapeswitch system described in Chapter Two (and Appendix B * of the agency's final report). The entire Tapeswitch system yields spot acceleration and speed values for individual vehicles across 14 overlapping distance intervals ranging from 385 ft to the stop line in the approach to an intersection. It is recommended that the pth percentile (e.g., 95th or 99th) acceleration and the associated speed be measured in each interval, and that the highest corresponding skid number from Table 9 be considered the required skid resistance.

For agencies desiring a simpler approach to estimating pavement skid-resistance requirements at intersections, it is recommended that the IDM be used for determining acceleration and speed and Table 9 used for conversion to skid-resistance requirements. Although the model is based upon measurements at only 12 intersections, the approach appears valid for interim applications. It requires far simpler equipment and methodology than is involved when the entire Tapeswitch system is used.

* Not published in this report. Copies of the agency's final report are available on request to the Program Director, NCHRP.

When it is not feasible to use either the Tapeswitch system or the IDM, Table 16 can provide general guidelines for determining minimum skid-resistance requirements at intersections.

The Tapeswitch system configuration is recommended for agencies desiring to perform additional research on driver cornering behavior. It is *not* recommended at this time that highway agencies use the Tapeswitch system as a practical method for determining skid-resistance requirements on curves. In its application to the measurement of lateral acceleration, the Tapeswitch system is far more complex and difficult to use and less accurate than its application to the measurement of longitudinal acceleration. Furthermore, the relationship between skid-resistance requirements and lateral acceleration is so ill-defined that application to curves will provide no certainty of accuracy.

RECOMMENDATIONS FOR FURTHER RESEARCH

1. The data collected in this program should be subjected to further treatment to:
   a. Reduce and analyze the data on freeway exit lanes.
   b. Determine whether or not the intersection demand model applies to freeway exit-lane behavior.
   c. Establish with more precision the relationship between average acceleration and peak demand in braking and cornering maneuvers.
   d. Study the relationships between curve geometry, vehicle path, and lateral acceleration.
   e. Determine whether or not the Tapeswitch procedures and intersection demand and lateral acceleration models can be simplified or refined.

2. Additional driver demand data should be collected with the Tapeswitch system on both curves and intersections to (1) extend the statistical base of the study, (2) further validate and refine the models, and (3) collect data on a broader range of site types. In addition, research should be conducted to determine:
   a. Driver braking behavior at intersections located on horizontal curves.
   b. The effect of grade on braking and cornering behavior.
   c. The effect of rain on braking and cornering behavior.
   d. The effect of curve geometric variables—in particular, length, degree of curvature, superelevation, lane width, and spiral design—on cornering behavior.

3. The Tapeswitch system should be used to measure driver demand required:
   a. While passing on two-lane highways.
   b. In unstable freeway traffic.

4. Additional skid studies should be conducted to refine the relationships between acceleration and pavement skid resistance established in the present study. In particular, further studies should be conducted to determine the relationship between skid resistance and maximum acceleration in cornering, braking, and driving modes, singly and in combination, as mediated by tire type, size, and condition, vehicle type and surface materials. This work is especially needed with regard to lateral acceleration.

5. Efforts should be made to develop a simpler alternative to the Tapeswitch system for measuring lateral acceleration on curves.

REFERENCES

1. KUMMER, W. H., and MEYER, W. E., "Tentative Skid-Resistance Requirements for Main Rural Highways," *NCHRP Report 37* (1967) 80 pp.
2. JURKAT, M. P., "Analysis of Pavement Skid Numbers for Selected Locations on the New Jersey State Highway System," Bur. of Public Roads, HPR-PR-1/31 (1969) 7710.
3. GILES, C. G., and SABEY, B. E., "A Note on the Problem of Seasonal Variation in Skidding Resistance," *Proc. 1st Internat. Skid Prev. Conf.*, Virginia Highway Research Council, Part 2 (1959).
4. AUTOMOTIVE SAFETY FOUNDATION, *Traffic Control and Roadway Elements* (1963).
5. BEATON, J. L., et al., "Reduction of Accidents by Pavement Grooving," *HRB Spec. Rep. 101* (1969) pp. 110-125.
6. HATHERLY, L. W., et al., "The Skid Resistance of City Streets and Road Safety," *Inst. Hwy. Engrs. J.*, London, Vol. 16, No. 4 (1969).
7. AASHO, "Highway Design and Operational Practices Related to Highway Safety." A report of the Special AASHO Traffic Safety Committee (1967) 71 pp.
8. NICHOLAS, J. H., SABEY, B. E., and KIRKHAM, R. J., "Skid Resistance of Pad Surfaces: Recent Research," *Municipal Engineering*, Vol 139 (1962) p. 3802.
9. ELLIS, J. R., "The Dynamics of Vehicles During Braking," *Inst. of Mechanical Engineers Symposium on the Control of Vehicles* (1963).
10. HOLMES, K. E., and STONE, R. D., "Tire Forces as Functions of Cornering and Braking Slip on Wet Road Surfaces," *RL Rep. LR 254*, Road Research Laboratory (1969).

11. AMERICAN SOCIETY FOR TESTING AND MATERIALS, "Highway Skid Resistance," *ASTM STP 456* (1968).
12. SMITH, J. G., and SMITH, J. E., "Lateral Forces on Vehicles During Driving," *Automobile Engineer* (Dec. 1967).
13. KIHLBERG, J. K., and THARP, K. J., "Accident Rates as Related to Design Elements of Rural Highways," *NCHRP Report 47* (1968) 173 pp.
14. GILES, C. G., and SABEY, B. E., "Accident Reports and Skidding Accident Sites," The Public Works and Municipal Services Congress, The Institute of Municipal Engineers and the Road Research Laboratory, *Report No. 13* (Nov. 1956).
15. GILES, C. G., and SABEY, B. E., "Skidding as a Factor in Accidents on the Roads in Great Britain," *Proc. International Skid Prevention Conf.* (1958).
16. AMERICAN ASSOCIATION OF STATE HIGHWAY OFFICIALS, "A Policy on the Geometric Design of Rural Highways" (1965) 650 pp.
17. WILSON, E. E., "Deceleration Distances for High Speed Vehicles." *HRB Proc.*, Vol. 20 (1940) pp. 393-397.
18 TARAGIN, A., "Driver Performance on Horizontal Curves." *HRB Proc.*, Vol. 33 (1954) pp. 446-466.
19. SPURR, R. T., "Subjective Assessment of Brake Performance." *Automobile Engineer,* Vol. 55, No. 10 (Sept. 1965) pp. 393-395.
20. SPURR, R. T., "Subjective Aspects of Braking." *Automobile Engineer,* Vol. 59, No. 2 (Feb. 1969) pp. 58-61.
21. TIGNOR, S., "Car Deceleration Performance Changes Little From 1955 to 1968." *SAE Journal* (Apr. 1965) p. 65.
22. BEAKEY, J., "Acceleration and Deceleration Characteristics of Private Passenger Vehicles." *HRB Proc.*, Vol. 18(1) (1938) pp. 81-89.
23. CRAWFORD, A., and TAYLOR, D. H., "Driver Behavior at Traffic Lights; Critical Amber Period." *Traffic Engineering and Control* (Dec. 1961) pp. 473-478, 482.
24. CRAWFORD, A., "Driver Judgement and Error During the Critical Amber Period at Traffic Lights." *Ergonomics,* Vol. 5, No. 4 (1962) pp. 513-532.
25. MAY, A. D., "Clearance Interval at Traffic Signals." *Highway Research Record,* No. 221 (1968) pp. 41-71.
26. HERMAN, R., et al., "Problem of the Amber Signal Light." *Traffic Engineering and Control* (1963) p. 5.
27. GAZIS, D., et al., "The Problem of the Amber Light in Traffic Flow." *Operations Research,* Vol. 8, No. 1 (1960).
28 RITCHIE, M., et al., "A Study of the Relationship Between Forward Velocity and Lateral Acceleration in Curves During Normal Driving." Ritchie, Inc., Dayton, Ohio (June 1968).
29. GRAY, P. H., and KAUK, W. H., "Driver Operations Characteristics on Circular and Elongated Freeway Exit Loop Ramps." M.S. Thesis, Dept. of Civil Engineering, Northwestern Univ. (1966).
30. WILLIAMS, K., and DAVIS, M. M., "Vehicle Operating Characteristics on Outer Loop Deceleration Lanes of Interchanges." Dept. of Civil Engineering, Toronto University, *Rept. 43* (Mar. 1968) pp. 78.
31. FARBER, E., et al., *Conceptualization of Overtaking and Passing on Two-Lane Rural Roads,* The Franklin Institute Research Laboratories, TR-1-193 Final Report to Bureau of Public Roads, Contract No CPR-11-2770 (1967).
32. FARBER, E., et al., *Overtaking and Passing Under Adverse Visibility Conditions,* The Franklin Institute Research Laboratories, TR-1-218, Final Report to Bureau of Public Roads, Contract No. FH-11-6145 (1969).
33. JOHANSSON, G., and RUMAR, K., "Visible Distances and Safe Approach Speeds for Night Driving," *Ergonomics,* Vol. 11, No. 3 (May 1968) pp. 275-282.

APPENDIX A

LITERATURE REVIEW

INTRODUCTION

In normal driving, it is likely that the greatest demand on friction (i.e., the highest levels of acceleration) is associated with geometric features. Although little data are available on the acceleration behavior of drivers on tangent sections, such data as do exist (*1, 12*) indicate that the distribution of braking and cornering forces on open sections is much lower (i.e., heavy demand occurs with much lower frequency) than at sites whose geometry requires a maneuver. Further, the frequency of accidents is substantially higher at maneuver sites than on tangent sections (*13*). Relatively little data have been published on the topic of the frequency of skidding accidents and geometric elements, but there does appear to be a strong relationship between them. Giles and Sabey (*14, 15*) report that relative to tangent sections the skidding accident rate is 80 times greater on traffic circles, 48 times greater on curves with a radius less than 500 ft, from 3.8 to 13 times greater on grades, and 7.3 times greater at intersections. Despite the fact that most of the

highway system consists of tangent sections, only 2.3 percent of skidding accidents occurred on tangent sections. This does not mean that driver demand in tangent sections can be ignored. It does indicate, however, that the program should emphasize maneuver sites.

A number of studies in the highway literature report data on driver braking, forward acceleration, and cornering behavior at curves, ramps, and intersections. Few of these present acceleration data, but in many instances it was possible to compute acceleration values from reported time, speed, and distance data. The more important of these studies are discussed further. It should be noted that all of the data were obtained on dry pavement.

BRAKING

Spurr (*19*) reports the results of a study that assessed the ability of drivers to judge deceleration in an automobile. Spurr's subjects were able to make surprisingly accurate and consistent judgments of deceleration. The judgments were apparently associated with proprioceptive cues as drivers were able to make accurate judgments while blindfolded and were able to accurately reproduce deceleration levels experienced in one car in another car. In a later study (*20*), conducted by the same author to determine the patterns of deceleration in braking, a recording decelerometer mounted in an automobile was used to trace deceleration patterns from various initial speeds to rest. The average level of deceleration increased with increasing velocity. However, despite the apparent ability of drivers to produce consistent levels of deceleration, there were considerable differences between individuals. Further, deceleration levels were not constant during a given stop. For a typical driver, deceleration increased throughout the stop, frequently with a fairly sharp peak just before rest. While average decelerations over the full period did not exceed 0.4 *g* for any driver, peak levels were as much as 2.5 times the average. In general, the ratio of peak to average deceleration diminished with increasing average acceleration. The highest frequency of the *G*-level fluctuations was roughly 0.5 to 1.0 cycle per second.

Wilson (*17*) performed a study in 1940 to determine maximum deceleration rates for a passenger vehicle and also the maximum deceleration rates considered comfortable by drivers and passengers and, hence, acceptable for normal driving. Maximum average deceleration from 70 mph computed on the basis of stopping distance was found to be approximately 0.7 *g*. This is comparable to the maximum achievable by contemporary vehicles on dry pavement (*21*). The series of stopping tests conducted to determine acceptable levels of deceleration produced the following classifications:

Comfortable to passenger—preferred by driver—0.27 *g*.

Undesirable but not alarming to passengers—the driver would rather not use—0.34 *g*.

Severe and uncomfortable to passengers—driver classes as an emergency stop—0.43 *g*.

This range of values is comparable to that observed by Spurr.

A convenient way of categorizing driving situations requiring deceleration is to consider whether or not the driver is free to choose the points at which he commences and terminates braking. A driver who simply wishes to slow his vehicle with no sense of urgency or to stop his vehicle to pull off the highway at a nonspecific point is completely free in his choice of deceleration level (i.e., when he commences and when he terminates braking). In approaching a stop sign or a signal light, that has turned red while the driver is far from the intersection, the driver is free to choose the point at which he begins to brake, but must terminate braking (bring his vehicle to a stop) at a specific point. However, he is still free to choose a level of deceleration.

Situations in which the driver is not free to choose either the starting or stopping point of braking occur most frequently at signalized intersections when the signal turns from green to amber when the driver is within the distance at which he would normally begin to brake. In such situations, the rate of deceleration required to stop at the intersection is determined by the driver's approach speed and his distance from the intersection when the light turns amber. If the driver chooses to stop for the light, the average rate of deceleration is determined. However, the driver is free to choose whether to accept that level of deceleration or to proceed through the intersection.

The classic study of braking at stop-sign-controlled intersections was performed by Beakey (*22*) whose data are reported in the AASHTO Policy on Geometric Design (*16*). Beakey observed the acceleration and deceleration behavior of traffic approaching and departing a stop-sign-controlled intersection. The roads on which the observations took place were suburban boulevards on which traffic speeds were comparable to those on rural highways. The deceleration levels reported by Beakey were computed by observing the changes in the average speed of braking vehicles across 50-ft intervals in the approach to the intersection. The values thus represent deceleration averaged across both vehicles and distance intervals. Beakey's deceleration data are at best crude averages when one considers the observation accuracy required to determine acceleration and his observation methods (stopwatch).

Beakey's data indicate that the higher the initial speed, the greater the distance from the intersection at which drivers began to brake and the greater the rate of deceleration. At every vehicle speed, the average deceleration increased as the distance to the intersection diminished, the greatest deceleration occurring during the last few feet before the stop. Average decelerations at this point ranged from about 0.3 to 0.5 *g*. However, those vehicles that achieved a deceleration rate of 0.5 *g* at or near the stop were decelerating at an average rate of only 0.16 *g* as they passed through 40 mph.

An analysis of Beakey's data reveals that the relationship between initial approach velocity and the distance from the intersection at which drivers begin to brake is approximated by the expression:

$$D = 3.98V^{1.22} \qquad \text{(A-1)}$$

The equivalent expression in g's is:

$$G = V^{0.78}/119.1 \qquad \text{(A-2)}$$

where D is the distance in feet and V is speed in miles per hour. The value of the exponent of V in the above expressions reflects the manner in which drivers varied average braking force with approach speed. At a given level of deceleration, the distance required to stop increases with the square of the velocity. If the average level of deceleration adopted by a given driver were independent of speed, then the value of the exponents in the expressions for D and G would have been 2 and 0, respectively. However, Beakey's curves were based on the average time required for the vehicles observed to traverse various distance intervals in the test section. For this reason, there was no way of knowing whether the expressions for braking distance and deceleration represent the performance of consistent individual drivers or merely conglomerates of more varied individual performances and, therefore, not representative of any individual driver. The curves suggest that the drivers increased braking forces throughout the braking maneuver. The same results would be obtained, however, by averaging the performance of many drivers each of whom brake at a different constant level of deceleration.

Crawford and Taylor (*23, 24*) report the results of controlled experiments of drivers' stop/continue decision-making at a signalized intersection. As a subject approached the intersection at some constant speed, the traffic signal was turned from green to amber. The approach speed and the distance separating the vehicle and the intersection at which the amber light was activated were varied from trial to trial. The range of separation distances at each speed included distances so short that no subject attempted to stop and distances so long that all subjects stopped. The study was conducted on an airport runway and the conditions made it apparent to subjects that no possibility of collision with another vehicle existed. The duration of the amber light was 3 sec.

Crawford's data are plotted in Figure A-1A. The figure shows the percent of the occasion for which drivers stopped as a function of the deceleration required to stop expressed in G at various approach speeds. The deceleration values

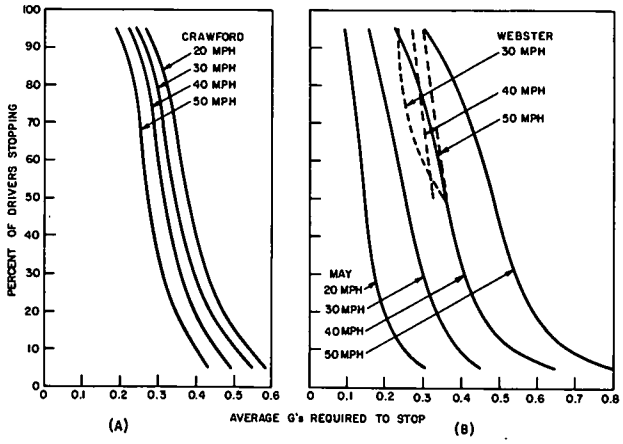

Figure A-1. Percentage of drivers stopping as a function of G's required to stop.

were computed from the equivalent percentile distances by the equation:

$$G = \frac{V^2}{64.4D} \qquad \text{(A-3)}$$

where V is the velocity in feet per second and D is the distance in feet from the intersection once the amber signal was activated. Crawford found the relationship between the distance from the intersection at which various percentages of drivers stopped and the approach speed to be given by:

$$D = KV^n \qquad \text{(A-4)}$$

where K is an empirically determined constant that varies with the percentage of stops, V is approach speed at miles per hour, and n has the value 1.63. Values of K for different percentages of stops are shown in Table A-1. Using the relationship between deceleration, distance, and velocity, Crawford's expression can be rewritten as

$$G = CV^m \qquad \text{(A-5)}$$

where $C = 1.80/K$ and $m = 2 - n = 0.37$. The plotted points in Figure A-1A were obtained from this expression.

Figure A-1A shows, in effect, the percentage of drivers who were willing to employ a given level of deceleration at the various approach speeds. For example, at an approach speed of 30 mph, only 5 percent of the drivers were willing to attempt a stop at a distance that would have required 0.5 g.

The value of the exponents in Crawford's expressions reflect the manner in which the drivers who decided to stop varied braking force with approach speed. At a given level of deceleration, the distance required to stop increases with the square of the velocity. Had the deceleration level associated with a given percentage of stops been constant, then n and m would have taken on the values 2 and 0, respectively, and there would have been no separation between the curves in Figure A-1A. On the other hand, had the distances at which drivers were willing to stop varied directly with the velocity, the values of both n and m would be equal to 1, and the curves in Figure A-1A would have exhibited even more separation.

An opportunity to apply Crawford's formulations to data obtained under actual traffic conditions is provided by May's study (*25*). May observed traffic approaching signalized intersections and determined whether or not drivers stopped for the amber light as a function of their speed and distance from the intersection when the amber light ap-

TABLE A-1

VALUES OF K FOR DIFFERENT PERCENTAGES OF DRIVERS STOPPING

PERCENTAGE OF DRIVERS STOPPING	VALUES OF K	
	CRAWFORD (*24*)	MAY (*25*)
0.95	0.542	16.2
0.80	0.440	12.9
0.50	0.360	10.2
0.20	0.292	7.9
0.05	0.239	5.6

peared. From May's published data, it was possible to determine the percentage of drivers stopping as a function of distance and velocity. These data were subjected to a visual curve-fitting process that yielded the relationship given in Eq. (A-4), which was a reasonably good fit for approach speeds between 20 to 50 mph. Values of K are shown in Table A-1 and n took on the value 0.729.

In the equivalent expression for deceleration, Eq. (5), m equals 1.27 and C is as previously defined. Values computed from this expression are shown in Figure A-1B. The curves in Figure A-1B exhibit considerably more spread than Crawford's data (Figure A-1A) and, in fact, bracket Crawford's data. The spread of the curves is reflected in the value of m, which is greater than 1, indicating that the rate of deceleration increased exponentially with approach speed.

Also plotted on Figure A-1B are data from Webster as reported in Herman, et al. (*26*). Webster's data are different from Crawford's and May's in that they show little variation in deceleration with approach velocity (i.e., the value of n is approximately 2).

Because it was necessary to pool data across many conditions to obtain these data and because the curve-fitting process was crude, the percentage acceptance of the various levels of acceleration required to stop, as shown in Figure A-1B, should be viewed with caution. Nevertheless, it is apparent from May's data that a sizable percentage of drivers employed what can only be termed emergency-level braking to stop at the intersection. Further, it should be recognized that the g values plotted in the figure represent average levels of deceleration required to stop in a given distance at a given speed and do not take into account the delay in onset of braking associated with reaction time nor the fact that peak values of deceleration may be twice the average.

The substantial increase in level of deceleration with approach speed, as revealed by the spread of the curve in Figure A-1B, is probably at least in part associated with the nature of the decision that a driver must make. Depending on the width of the intersection and the duration of the amber signal, certain ranges of distance and approach velocity can produce a dilemma in which a driver must choose between emergency-level braking to stop or acceleration to clear the intersection before termination of the amber signal. This problem has been treated in detail (*26, 27*). For present purposes it is sufficient to point out that the seriousness of the dilemma, as well as the range of approach distances over which it occurs, increases with increasing approach speed and intersection width and decreases rapidly with increasing amber duration. In particular, at a given intersection, at those combinations of approach speed and distance associated with a given level of deceleration required to stop, the forward acceleration required to clear the intersection increases with increasing approach speed. For example, at a 70-ft intersection with a 3-sec amber duration, a vehicle that is traveling 60 mph and is 300 ft from the intersection at the onset of the amber must decelerate at 0.4 g or accelerate at 0.7 g (well beyond the capabilities of any vehicle short of a drag racer). The same level of deceleration, 0.4 g, is required to stop at a speed of 35 mph at a distance of 100 ft. However, the associated required clearance acceleration is only 0.1 g at this speed and distance combination. Thus, a driver is much more likely to stop at 60 mph and 300 ft than at 35 mph and 100 ft because the associated required clearance acceleration is impossible in the former case but within vehicle capability in the latter. The influence of this effect is obvious in Figure A-1B. A driver was much more likely to stop with a deceleration of 0.4 at 50 mph than at lesser speed. While it was not possible on the basis of May's data to show the explicit effect of either amber duration or intersection width on deceleration, there was evidence that amber duration and pavement warning markings influenced driver behavior.

Kummer and Meyer (*1*) conducted a pilot study of driver braking behavior in business-section traffic and on the open highway. Plotted in Figure A-2 are the cumulative frequencies of peak deceleration observed during brake applications under three conditions: (a) a 276-mile trip on rural highways, which included stops at intersections; (2) a random course in business-section traffic; and (c) stops at stop signs. In all conditions, very few of the brake applications resulted in decelerations exceeding 0.35 g. However, considering that the values plotted represent peak readings rather than average deceleration over some interval, they are substantially lower than would be expected on the basis of the average values observed by Beakey or those computed from May's data.

ACCELERATION AT INTERSECTIONS

For vehicles accelerating to traffic speeds from rest at a stop sign, Beakey found that the level of acceleration throughout the maneuver is greater for cars that achieve

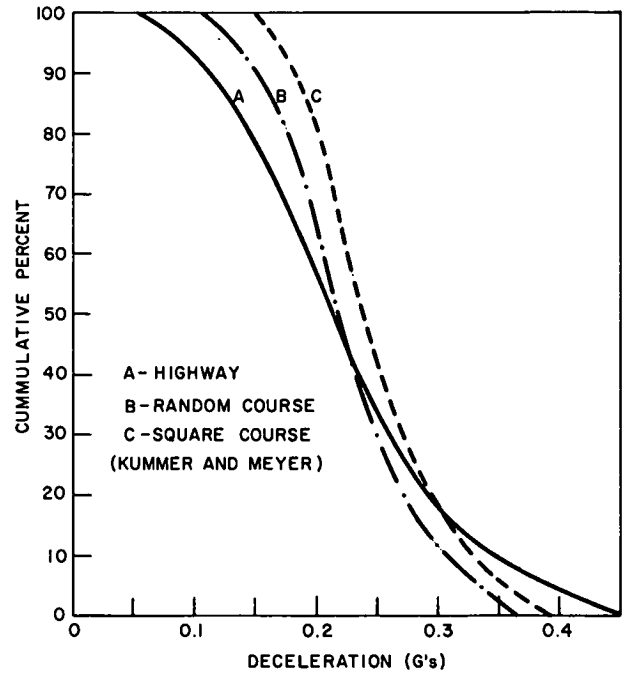

Figure A-2. Cumulative distribution of braking deceleration levels in three driving situations.

higher terminal speeds. Peak levels of acceleration occurred at the start with typical values ranging from 0.20 to 0.25 *g*. Levels of acceleration decreased monotonically with distance from the intersection, and, at 200 ft from the intersection, average values were under 0.10 *g*. The comments made earlier about Beakey's measurement techniques and the accuracy of the deceleration data also apply to the acceleration data. At best, the values reported are crude averages across both vehicles and intervals.

According to the authors' analysis of May's data, less than 1 percent of the drivers who elected to pass through the intersection exceeded 0.2 *g*. Apparently most drivers chose to accept fairly high levels of braking deceleration rather than accelerate through the intersection even when the required acceleration is low.

CORNERING

In cornering, the variables that define lateral acceleration are the radius of curvature, vehicle speed, and superelevation. These are related by the expression

$$G = \frac{V^2}{15R} - e \qquad \text{(A-6)}$$

where G is lateral acceleration expressed as a fraction of the gravitational constant; V is vehicle speed, in miles per hour; R is the radius of the curve, in feet; and e is superelevation, in feet per feet. An alternative form is

$$G = \frac{V^2 D}{85{,}900} - e, D = \frac{5730}{R} \qquad \text{(A-7)}$$

where D is degree of curvature.

A number of studies of side friction factors in cornering were performed in the 1930's and 40's. These led to the design recommendations contained in the AASHTO Policy on Geometric Design (*16*). In general, the findings were that drivers make less of a demand on the lateral friction coefficient on mild, rather than sharp, curves and at high, rather than low, speeds.

The most comprehensive study of driver cornering behavior was conducted by Taragin (*18*) who observed the speed of thousands of vehicles on horizontal curves on two-lane rural roads with degrees of curvature ranging from 3° to 29°. Taragin found a linear relationship with a high correlation (0.81) between speed and degree of curvature. Using the relationships above, Taragin's equations relating speed and degree of curvature can be transformed to show the relationship between curvature and cornering force expressed in G. These are given for the 50th, 90th, and 95th percentile vehicle:

$$G_{50} = \frac{D(46.3 - 0.75D)^2}{85{,}900} - e \qquad \text{(A-8)}$$

$$G_{90} = \frac{D(55.2 - 0.91D)^2}{85{,}900} - e \qquad \text{(A-9)}$$

$$G_{95} = \frac{D(58.5 - D)^2}{85{,}900} - e \qquad \text{(A-10)}$$

These curves are plotted in Figure A-3. Note that the form is cubic and that the curves have maxima at $D \approx 20°$ at which point the 95 percentile lateral acceleration was 0.35. Taragin found that drivers were unaffected by superelevation. For this reason, the lateral acceleration values plotted in Figure A-3 are not corrected for superelevation.

The high correlation between speed and degree of curvature noted by Taragin suggests that drivers are quite accurate in judging degree of curvature. Since degree of curvature and sight distance are closely related, the possibility arises that drivers adjust their speeds on the basis of sight distance. Taragin's analysis showed degree of curvature and sight distance to have independent effects; however, the effect of the former on speed was three times that of the later. While he did not measure braking deceleration on the approaches to curves, Taragin reported that drivers completed braking before entering the turn.

In Ritchie's (*28*) more recent study, 50 men and women subjects drove a vehicle having a lateral accelerometer to assess cornering forces on horizontal curves. Ritchie's data for the 95th, 85th, and 50th percentile maneuver are shown in Figure A-4. Although no curves were fitted, the relationship is apparently a cubic one because maxima occur at speeds between 20 and 25 mph. For the 95th-percentile driver, the maximum lateral acceleration was 0.38 *g*. Because Ritchie did not record degree of curvature, his data cannot be directly related to Taragin's. However, Ritchie's data are not inconsistent with Taragin's (i.e., the relationship between lateral acceleration and speed reported by Ritchie is consistent with the relationship between lateral acceleration and degree of curvature noted by Taragin).

In two separate studies, Gray and Kauk (*29*) and Williams and Davis (*30*) observed the speeds of vehicles on freeway exit-ramp curves. These data were transformed to express the 50th, 90th, and 95-percentile lateral acceleration as a function of degree of curvature and are plotted in that form in Figure A-5. The Williams and Davis' data are roughly similar to Taragin's data and show a maxima at $D = 20°$; however, Gray and Kauk's data suggest that lateral acceleration continues to increase with increasing degree of curvature beyond the apparent maximum of 20° in the Williams and Davis' data.

With the exception of Ritchie's data, the lateral acceleration values plotted in Figures A-3 through A-5 were com-

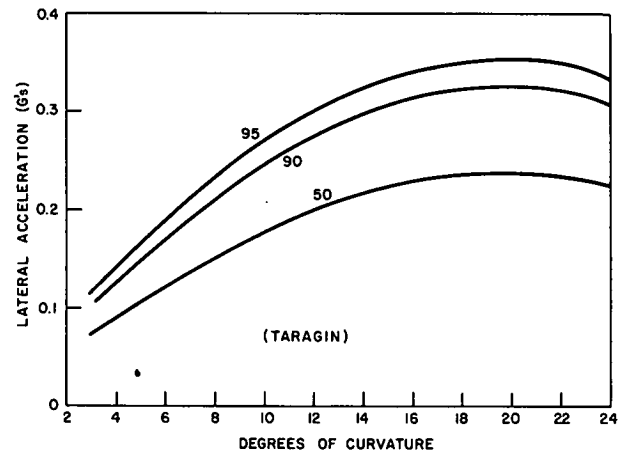

Figure A-3. Lateral acceleration of the 50th, 90th, and 95th percentile vehicle as a function of degree of curvature on rural, two-lane highway curves.

puted from the relationship between lateral acceleration, speed, and degree of curvature as noted. This computation assumes that a driver is describing a perfect arc whose radius is equal to the given radius of curvature. However, in actual driving practice, the driver may deviate from this ideal in several ways. The degree of curvature given for a curve is usually measured at the center line and the driver may be following a parallel arc with a greater or lesser radius. However, on all but the sharpest curves, simple lateral displacement has a very small effect. Even on a 40° curve, the difference in lateral acceleration between the extreme inside and outside of a curve on a 24-ft-wide roadway is less than 3 percent.

If the path followed by the driver is not a parallel arc, then the resulting acceleration can be substantially affected, especially on sharp curves.

Drivers tend to "flatten" a curve by using the width of the lane to describe an arc that takes the vehicle from the outside of the curve toward the inside on the entrance and from the inside toward the outside on the exit. Depending on the total change of central angle, the radius of the turn, and the lane width, the radius of the arc described by the vehicle can be considerably greater than the arc of the curve center line. The radius R of the inscribed arc is given by

$$R = \tfrac{1}{2}\,\frac{2r(r+w)\cos\theta/2 - (r+w)^2 - r^2}{(r+w)\cos\theta/2 - r} \qquad \text{(A-11)}$$

where r is the radius of the curve measured at the center line, w is the lane width, and θ is the total change in central angle. As an example, for a curve whose $r = 600$ ft, $w = 12$ ft, and $\theta = 30°$, its $R = 1422$. If the driver followed the center-line arc, at 50 mph the lateral acceleration would be 0.27 g. If the driver followed the ideal arc using the full lane width, the lateral acceleration would be only 0.12 g. Further, when steering around a turn, a driver does not hold the steering wheel stationary but makes continuous corrections resulting in continuous, if small, fluctuations in lateral acceleration.

A number of studies have been performed to determine the path followed by drivers in rounding a curve, but none of these present sufficient data to permit meaningful calculations of acceleration. Nevertheless, such geometric factors as lane width, shoulder treatment, and transition geometry are likely to have an influence on the path followed by drivers in rounding a turn and, hence, on peak lateral acceleration.

A rough estimate of the importance of these deviations is provided by Ritchie's data, which were obtained by a vehicle-mounted accelerometer and which, therefore, reflect

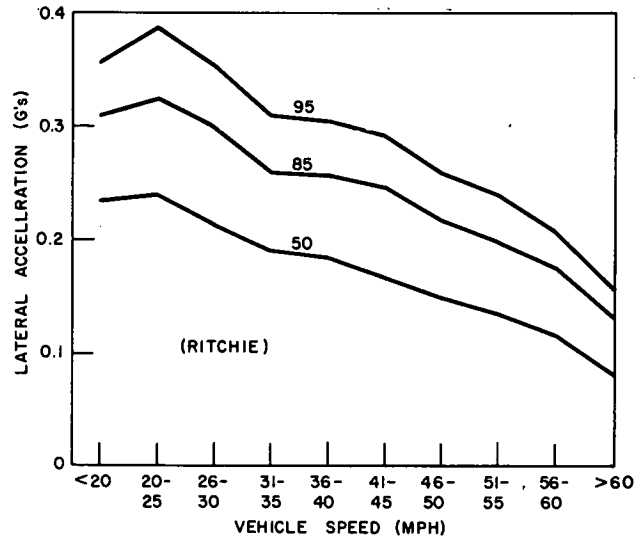

Figure A-4. Lateral acceleration on highway curves as a function of vehicle speed for the 95th, 85th, and 50th percentile vehicle.

all lateral factors. The maxima recorded by Ritchie are in very close accord with the maxima computed from Taragin's data. On this basis, it does not appear that path deviations are responsible for a substantial additional lateral force (i.e., a good estimate of the lateral acceleration on a curve can be computed from speed and radius of curvature).

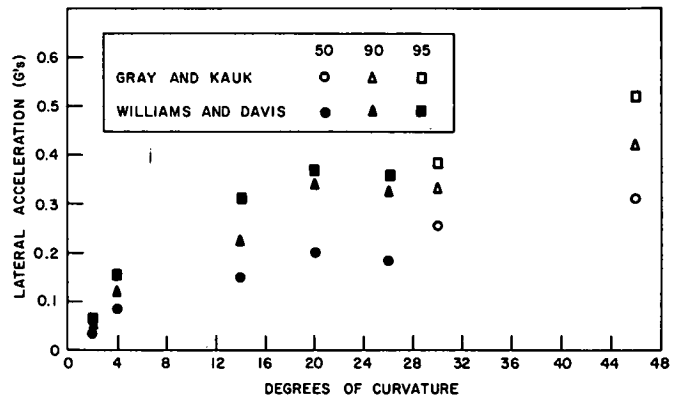

Figure A-5. Lateral acceleration of the 50th, 90th, and 95th percentile vehicles on freeway exit ramp curves as a function of degree of curvature.

APPENDIX B

REQUIRED SKID NUMBER, DECELERATION, AND SPEED PROFILE PLOTS FOR STUDY INTERSECTIONS

This appendix contains plots of summary data as collected and computed for each of the 12 intersection sites. The plots show the several levels of speed and deceleration values plus computed skid-resistance requirements at various distances from a stopping point.

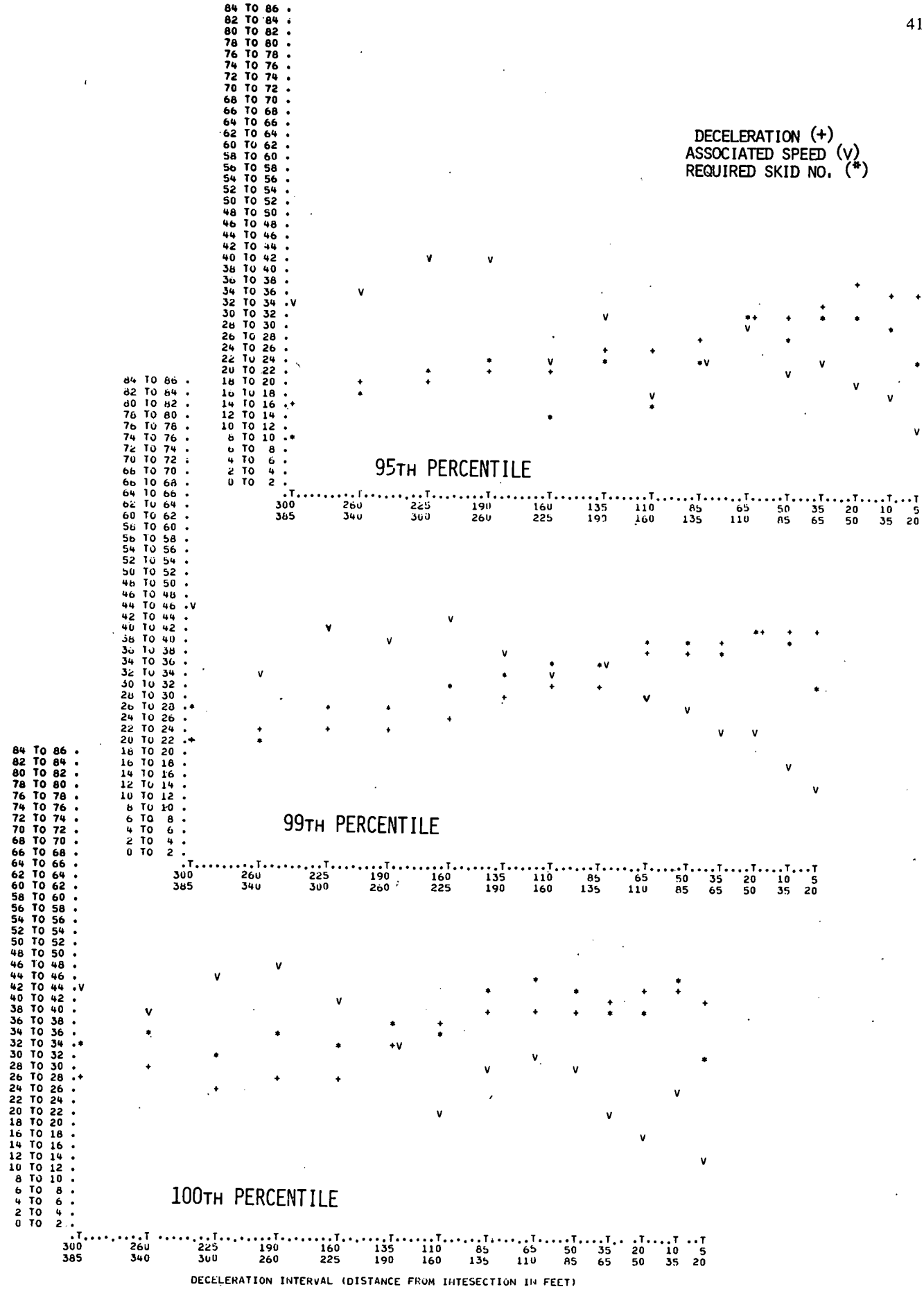

Figure B-1. Summary data for site No. 1, type 4, at mean initial speed of 36 mph with mean lane traffic of 444 vph.

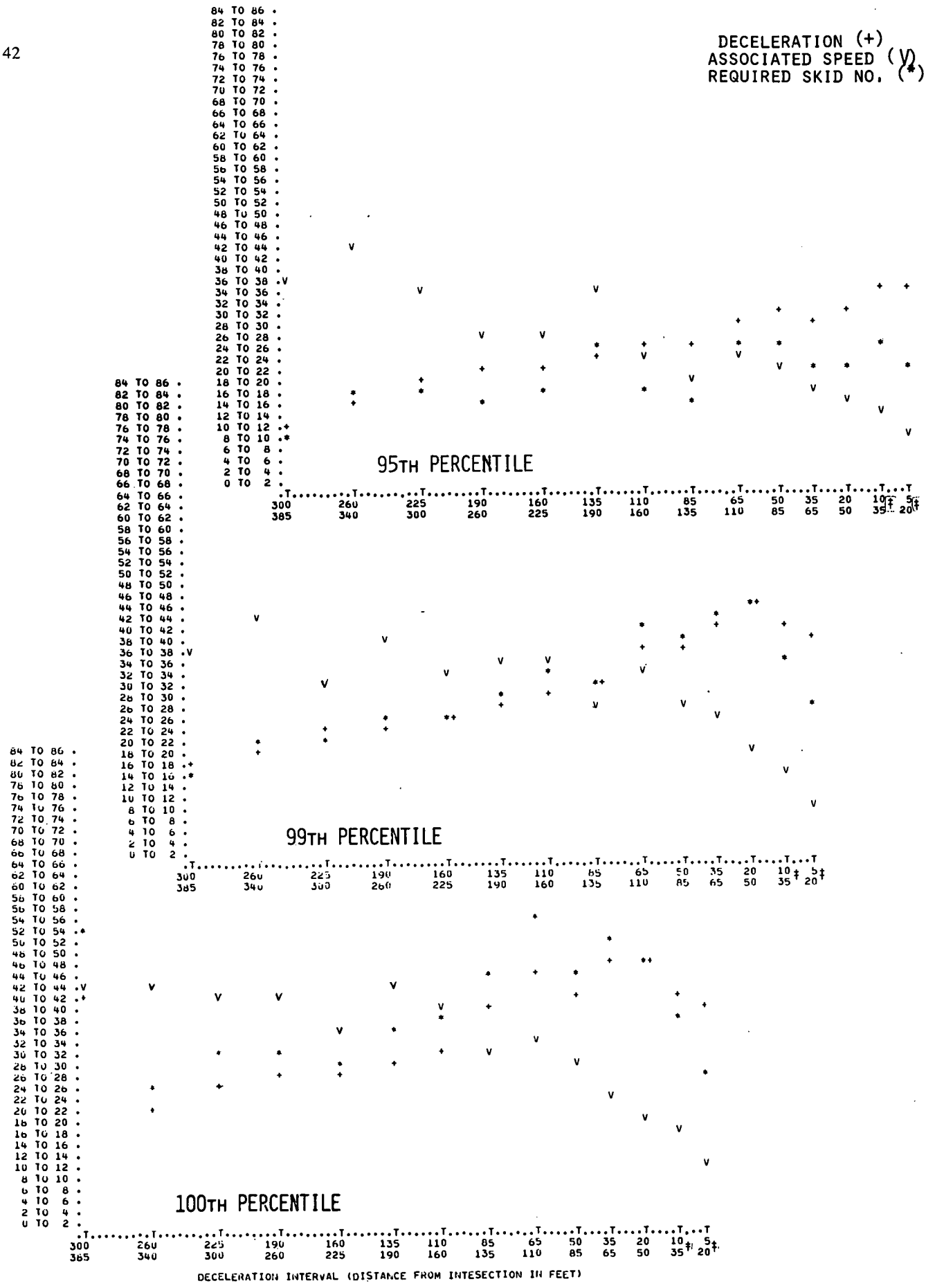

†The skid numbers estimated for these intervals were disregarded because the percentile values were not based on a sufficiently large sample.

Figure B-2. Summary data for site No. 2, type 1, at mean initial speed of 36 mph with mean lane traffic of 412 vph.

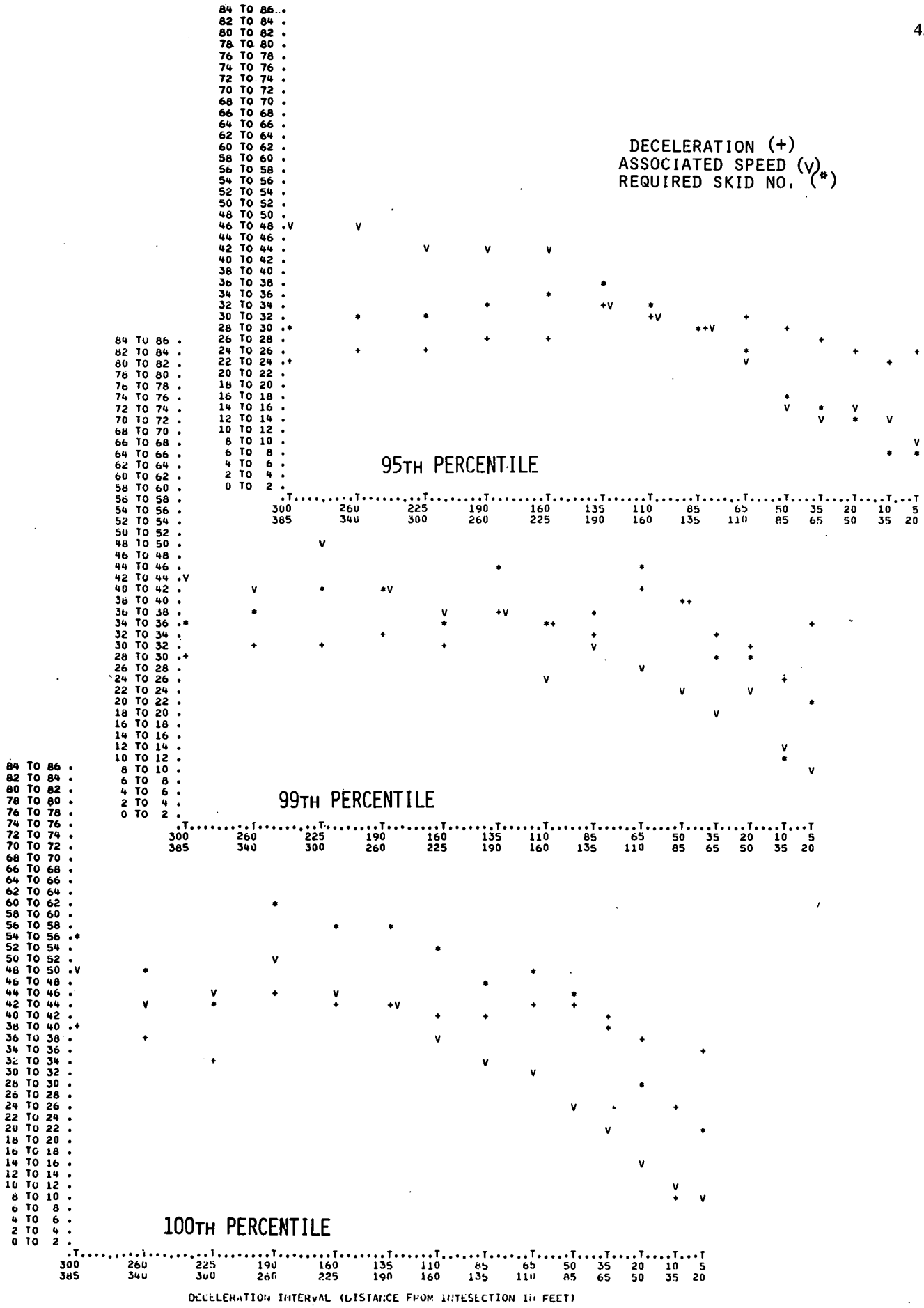

Figure B-3. Summary data for site No. 3, type 5, at mean initial speed of 40 mph with mean lane traffic at 435 vph.

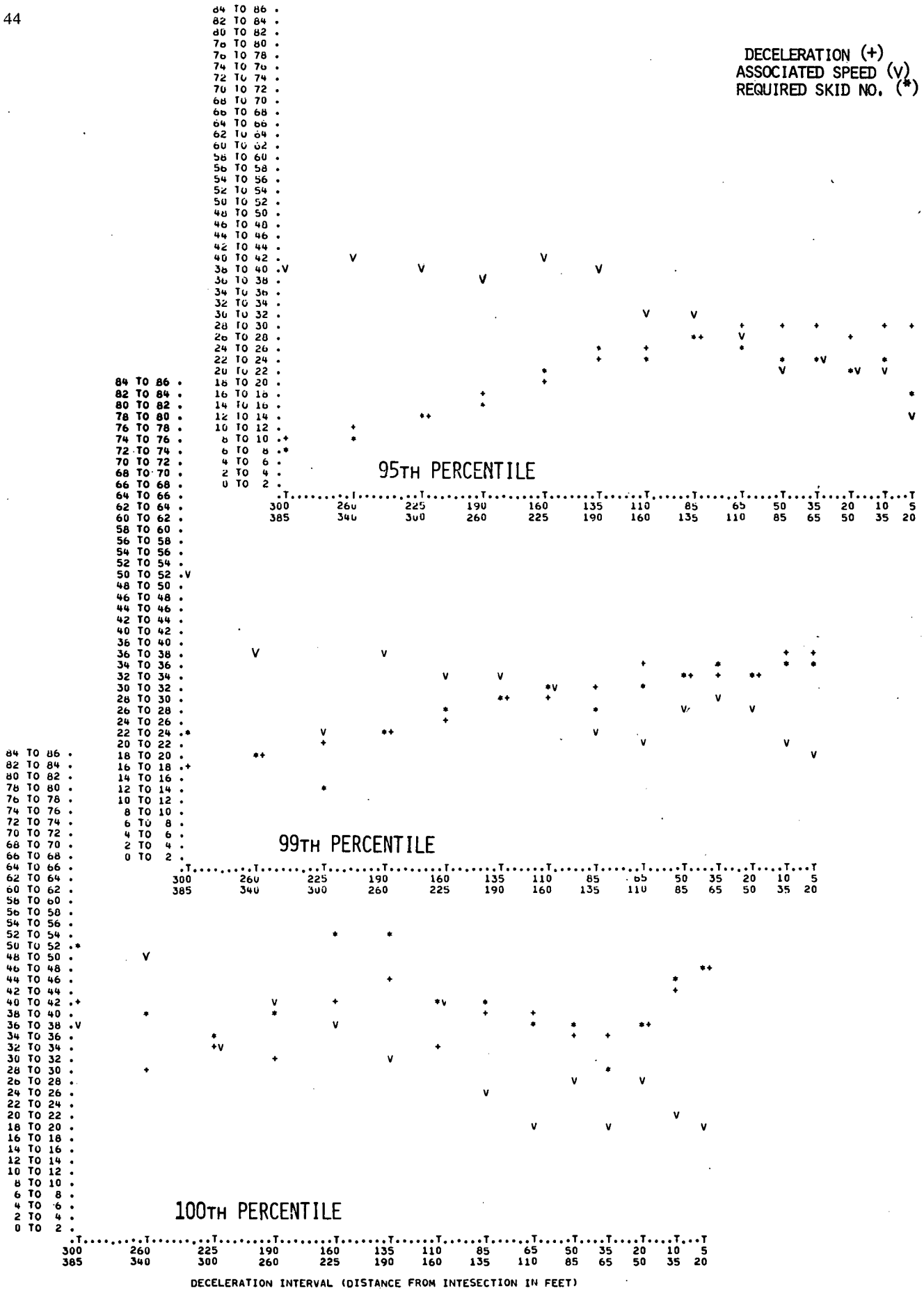

Figure B-4. Summary data for site No. 4, type 1, at mean initial speed of 36 mph with mean lane traffic of 109 vph.

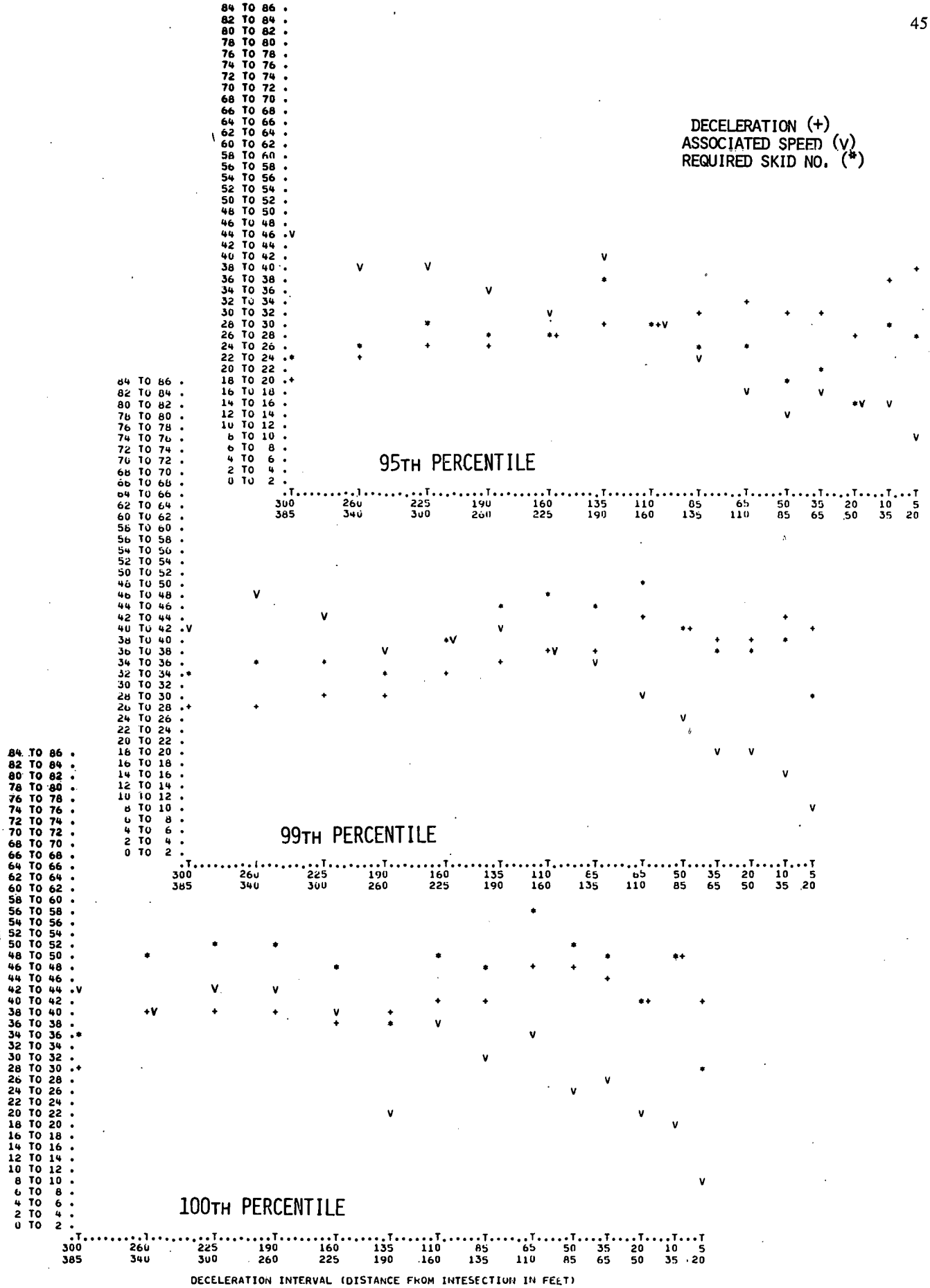

Figure B-5. Summary data for site No. 5, type 2, at mean initial speed of 38 mph with mean lane traffic of 453 vph.

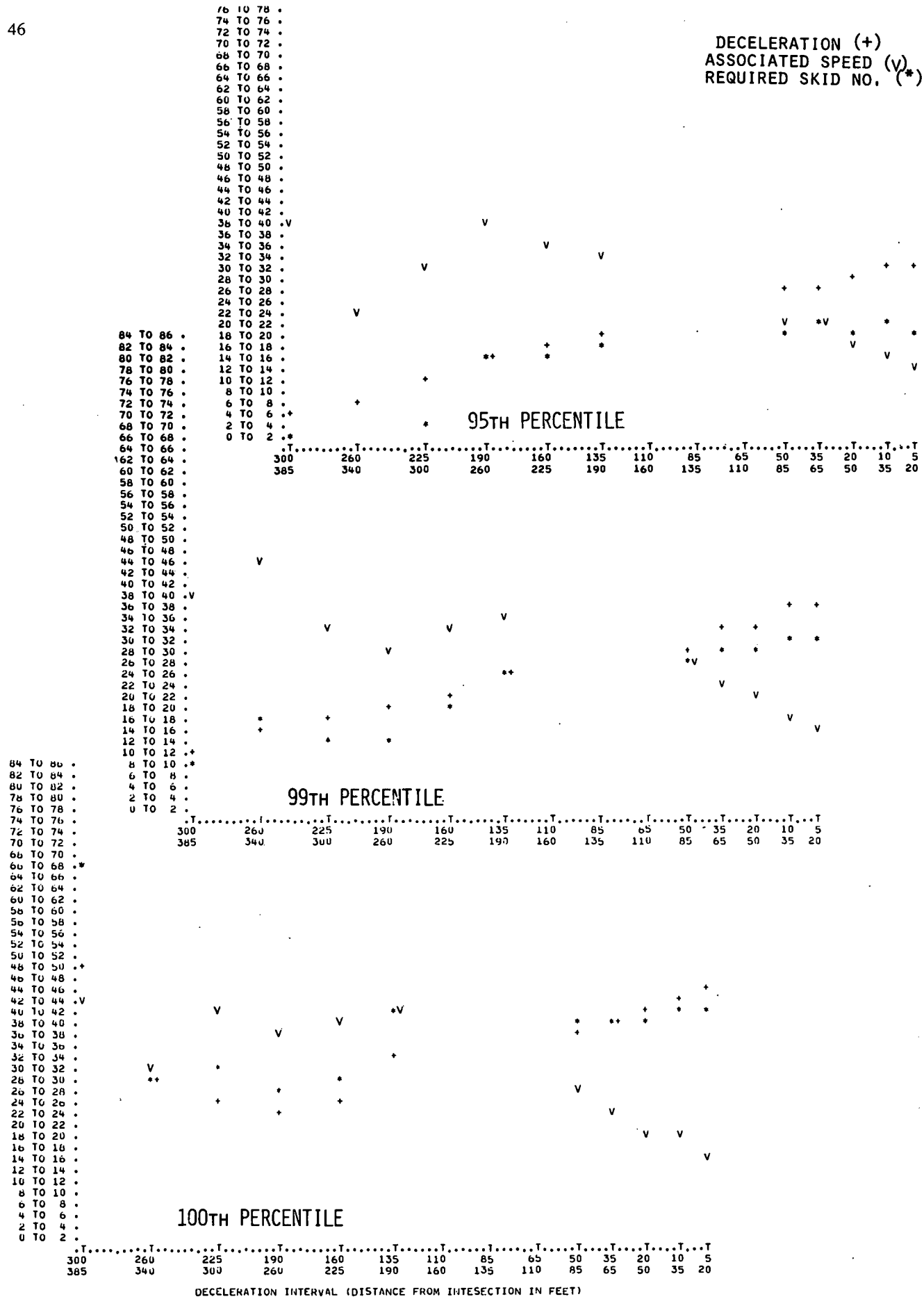

Figure B-6. Summary data for site No. 6, type 4, at mean initial speed of 30 mph with mean lane traffic of 115 vph.

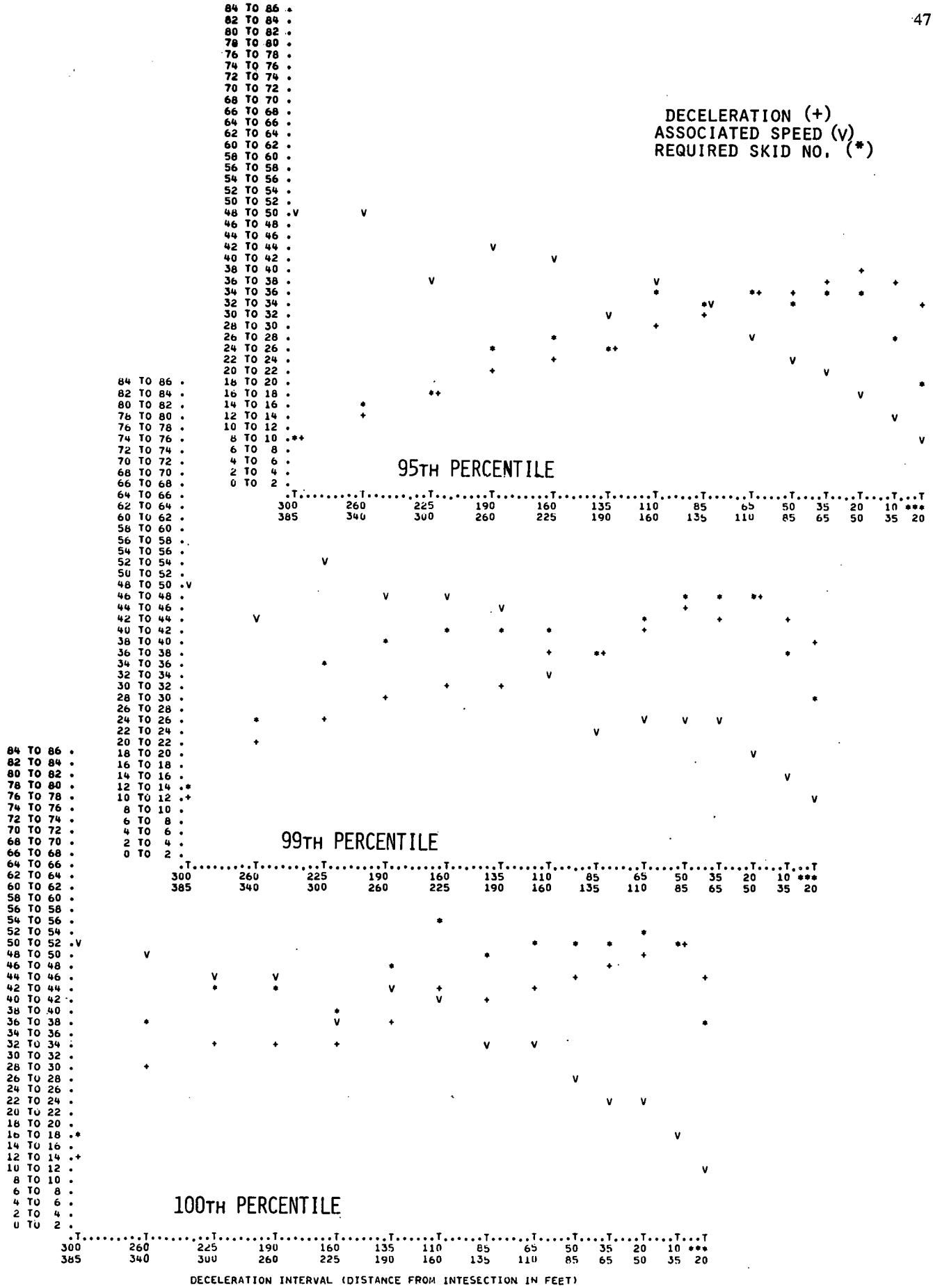

Figure B-7. Summary data for site No. 7, type 6, at mean initial speed of 39 mph with mean lane traffic of 93 vph.

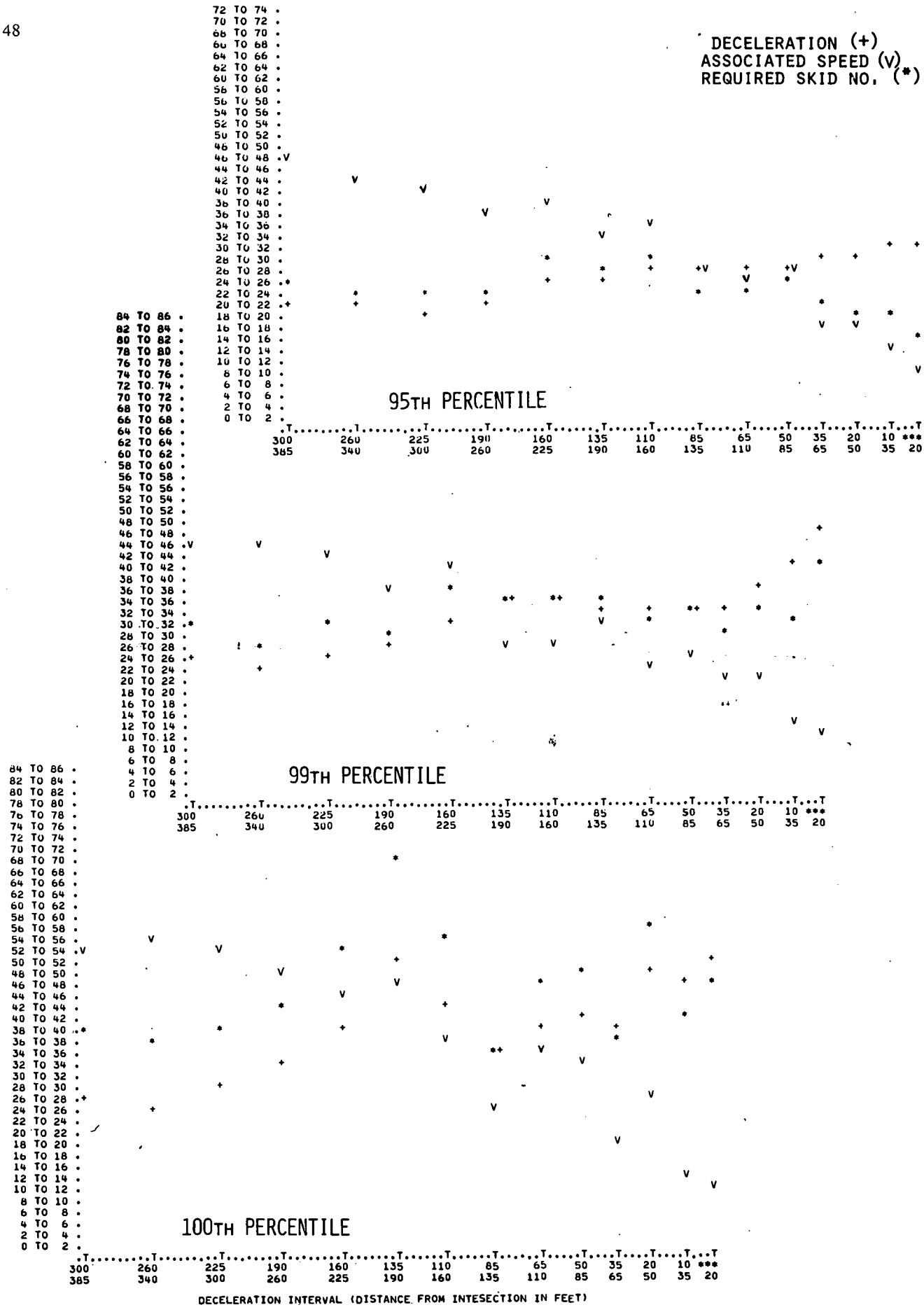

Figure B-8. Summary data for site No. 8, type 6, at mean initial speed of 40 mph with mean lane traffic of 113 vph.

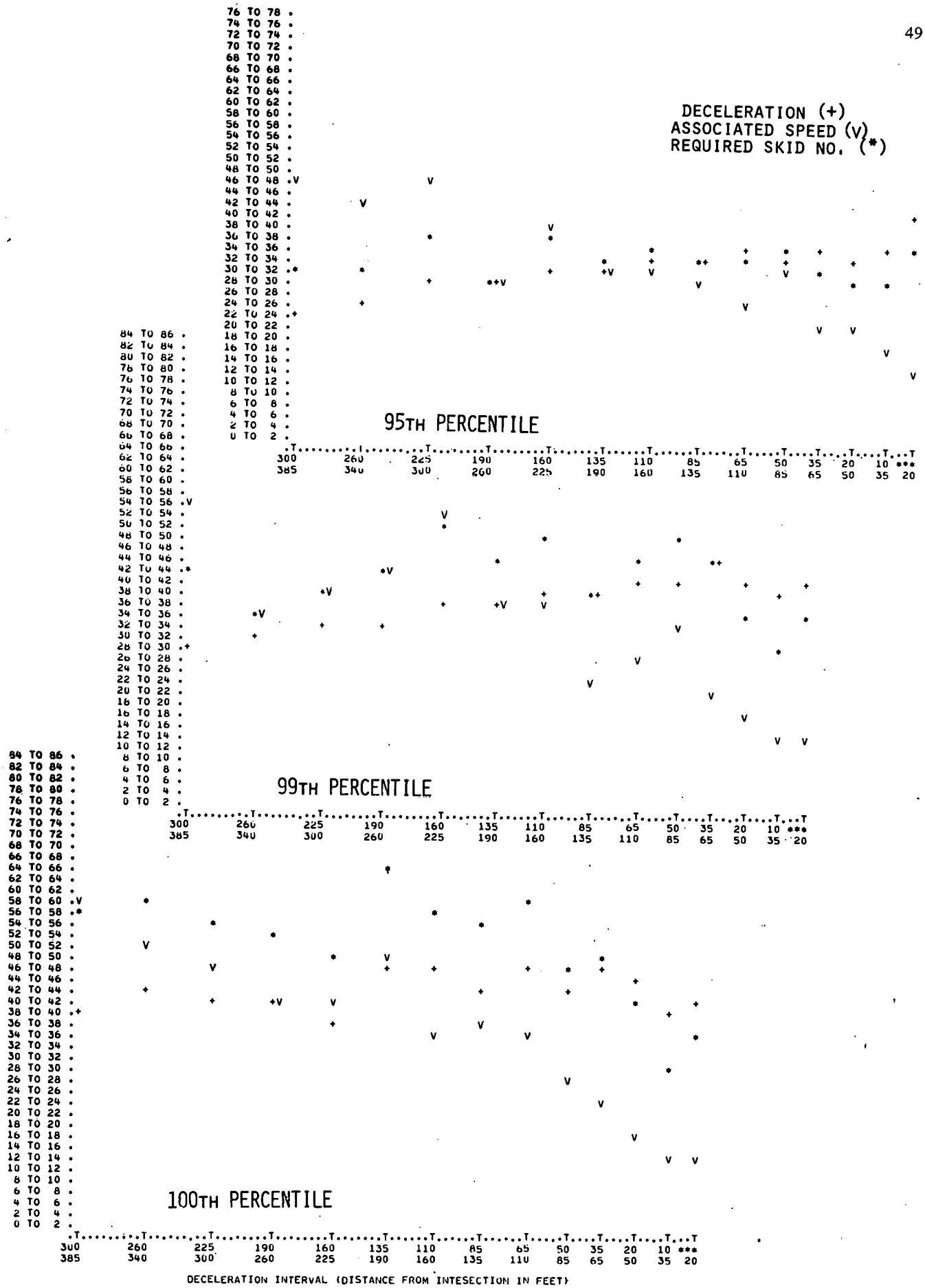

Figure B-9. Summary data for site No. 9, type 3, at mean initial speed of 41 mph with mean lane traffic of 286 vph.

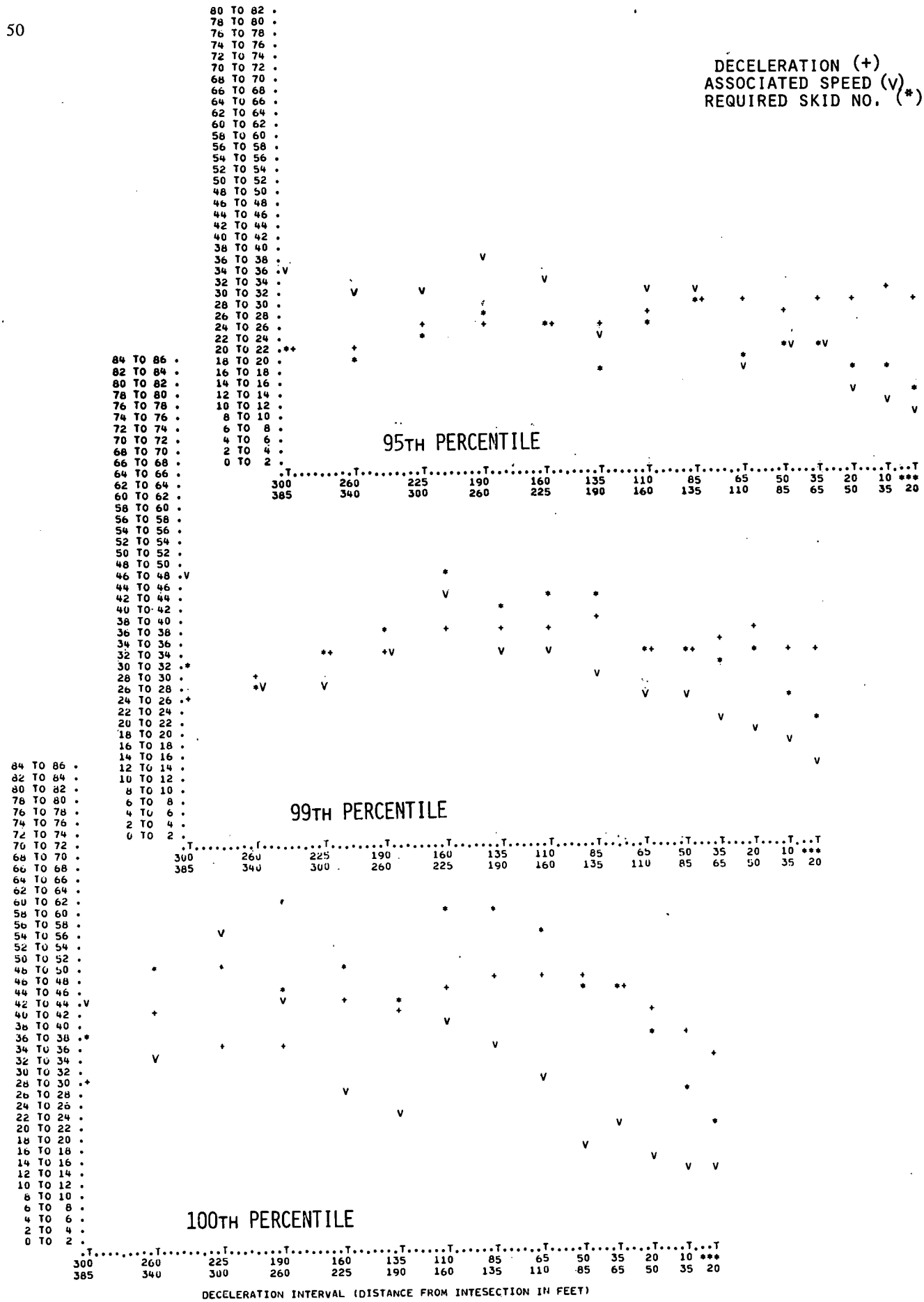

Figure B-10. Summary data for site No. 10, type 2, at mean initial speed of 37 mph with mean lane traffic of 409 vph.

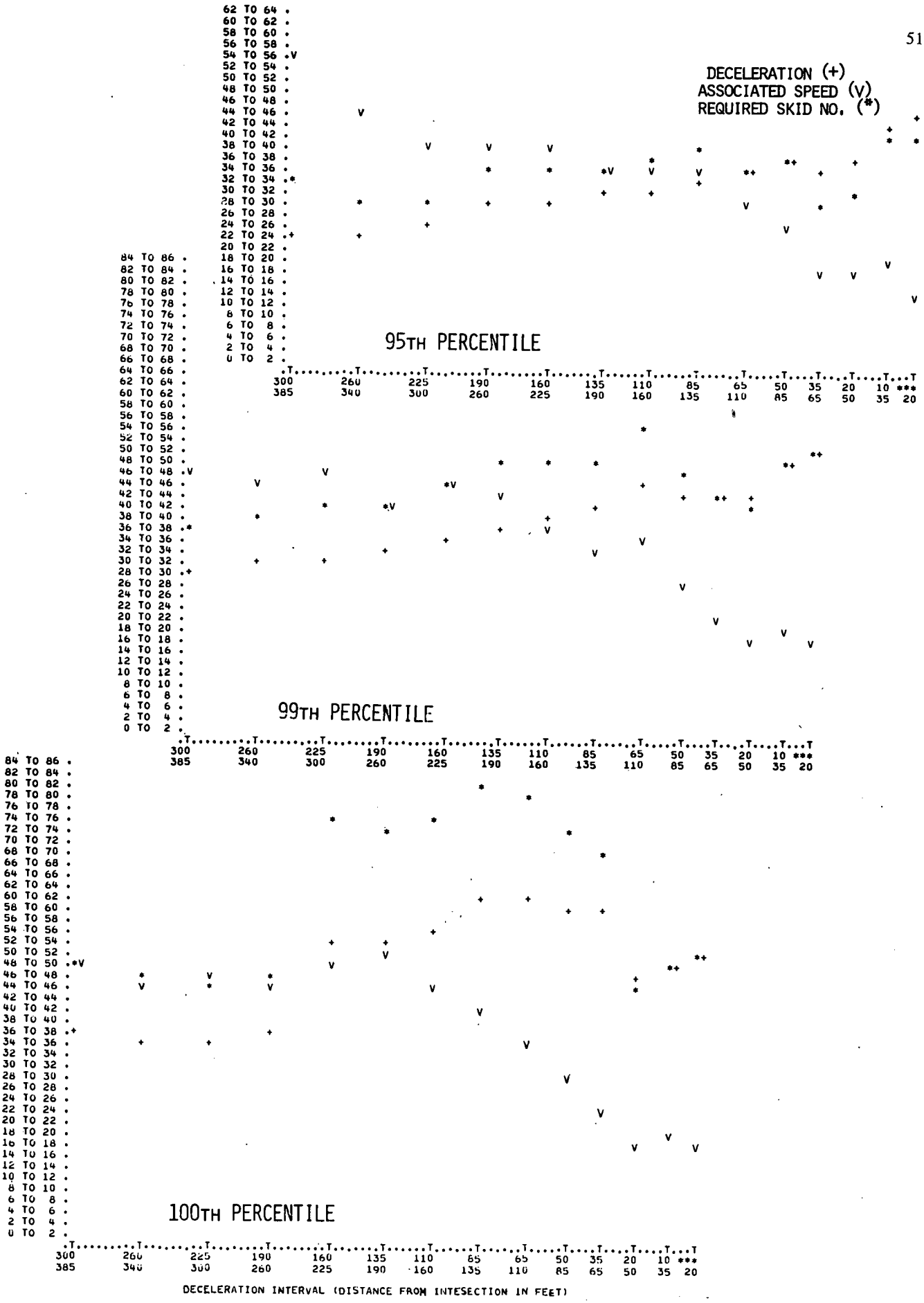

Figure B-11. Summary data for site No. 11, type 5, at mean initial speed of 40 mph with mean lane traffic of 553 vph.

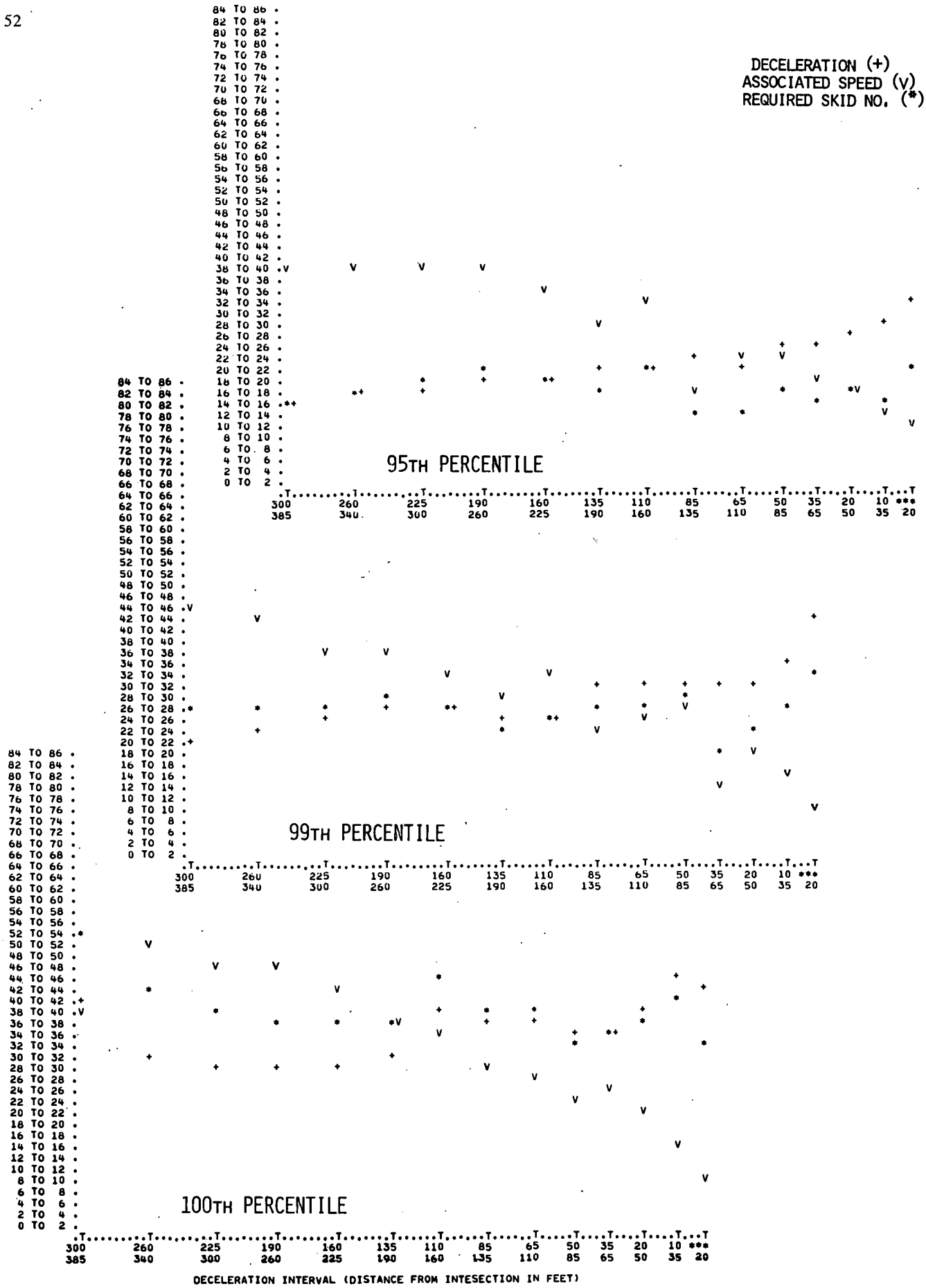

Figure B-12. Summary data for site No. 12, type 3, at mean initial speed of 35 mph with mean lane traffic of 367 vph.

APPENDIX C

MEASURING LATERAL ACCELERATION PROFILES ON CURVES

INTRODUCTION

It was not possible to develop procedures for determining pavement skid-resistance requirements for curves because a systematic relationship between skid resistance and maximum achievable lateral acceleration did not emerge from the TTI skid tests. Nevertheless, the research resulted in the successful design of a system for measuring driver acceleration profiles on curves, and this system is described here. It utilizes the basic Tapeswitch system described in Chapter Two but a different installation configuration.

APPLICATION OF THE TAPESWITCH SYSTEM TO CURVES

Measurement Configuration

The lateral or radial acceleration of a vehicle describing a curved path is given by

$$G_R = V^2/15R \qquad \text{(C-1)}$$

where G_R is radial acceleration, V is vehicle speed in mph, and R is the radius of the curve in feet. If the speed and radius of curvature are known, the expression can be used to compute an estimate of the lateral acceleration. This assumes that the vehicle is following a constant arc parallel to the center line of the roadway. However, drivers do not necessarily follow a constant radius in cornering, and in order to obtain values closer to the true instantaneous lateral acceleration values, it is desirable to measure the true radius of curvature of the vehicle's path over relatively short intervals.

Vehicle path can be determined by fitting an arc to three points representing the vehicle's position at three different times under the assumption that if the points are close together a circular arc will be a reasonable approximation of the path. Extensive analysis was required to develop a Tapeswitch detector configuration and a mathematical treatment of the data that would provide the data and ensure acceptably accurate results. The problem is that, over intervals of 0.5 to 2.0 sec, the distance traveled by a vehicle is very short compared with the total diameter of the circle whose radius defines the local path. A number of alternative approaches were studied, and it was determined that the best solution is to treat the vehicle's path as a deviation from the curve of the road edge. The lateral distance of the vehicle from the road edge can be determined at a number of points by appropriately configured detectors. Consider the configuration of perpendicular (or radial) and diagonal detectors shown in Figure C-1. This configuration measures the traverse times of a vehicle's right front wheel between successive detectors. Assuming the speed across the three detectors to be constant, the times between the switches

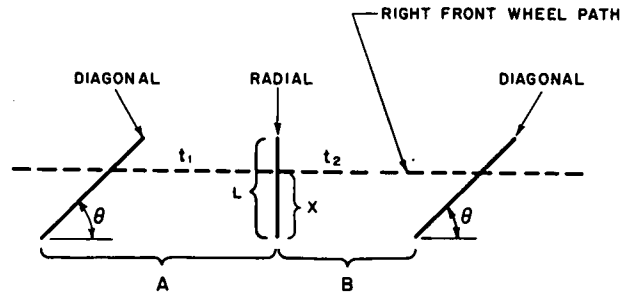

Figure C-1. Computing X, the distance of the right front wheel from the road edge.

will be proportional to the distances, or,

$$P = t_1/t_2 = d_1/d_2 \qquad \text{(C-2)}$$

Solving for d_1 and d_2

$$d_1 = A - X/\tan\theta \qquad \text{(C-3)}$$

$$d_2 = B + X/\tan\theta \qquad \text{(C-4)}$$

then

$$X = \frac{(A + PB)\tan\theta}{P + 1} \qquad \text{(C-5)}$$

where X is the distance of the vehicle's right front wheel from the reference line established by the road-edge ends of the detectors (nominally a reference line parallel to the road edge), and A, B, and θ are as shown in Figure C-1. Thus, three detectors are required to obtain lateral position at one point. By alternating radial and diagonal detectors, each diagonal detector can be used with both the preceding and the following radial detector. Four alternative diagonals and three radials will thus yield three independent values of X from which the radius of the vehicle's trajectory over that interval can be determined. Similarly, a system of 13 alternating diagonal and 12 radial detectors will provide estimates of the radius of the vehicle's trajectory in ten overlapping intervals. Such a system is shown in Figure C-2. Analysis has revealed that for any path a vehicle can follow and still remain on the road, the computation of X is not sensitive to the fact that the path is an arc or that the path chord is not parallel to the road edge chord.

Three values of X measured at three successive radials are sufficient to determine the radius of curvature of the right- and front-wheel path if the local radius of curvature of road edge over that interval is known. The expressions are (see Fig. C-3):

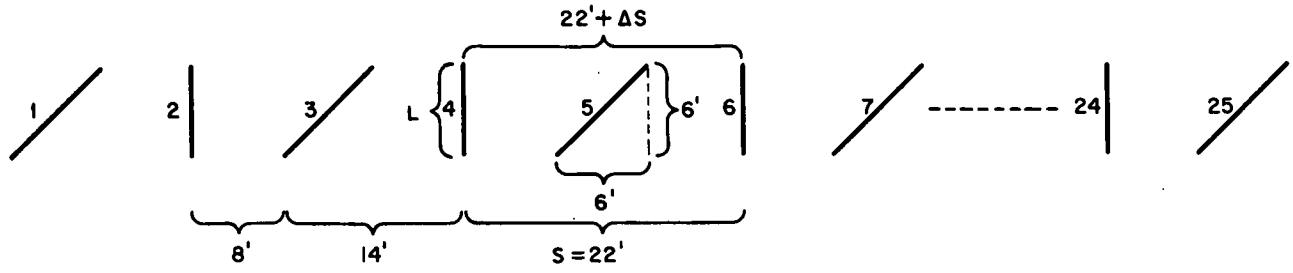

ΔS = 132/R̄, where R̄ is the average radius of the curve in the instrumented section.

Figure C-2. Detector layout and dimensions.

$$L_1^2 = (X_1 + R)^2 + (X_2 + R)^2 - 2(X_1 + R)(X_2 + R)\cos\beta \quad \text{(C-6)}$$

$$L_2^2 = (X_2 + R)^2 + (X_3 + R)^2 - 2(X_2 + R)(X_3 + R)\cos\beta \quad \text{(C-7)}$$

$$L_3^2 = (X_1 + R)^2 + (X_3 + R)^2 - 2(X_1 + R)(X_3 + R)\cos(2\beta) \quad \text{(C-8)}$$

where

$$R = S^2/2M \quad \text{(C-9)}$$

the local radius of curvature, and

$$\sin\beta/2 = 11/R \quad \text{(C-10)}$$

Then the radius of the vehicle path is given by

$$r^2 = \frac{L_1^2 L_2^2 L_3^2}{4L_1^2 L_2^2 - (L_1^2 + L_2^2 - L_3^2)^2} \quad \text{(C-11)}$$

Thus, three successive values of X are used to determine a local path radius, r. With FIRL's configuration, ten values of r across ten overlapping intervals are computed for each vehicle. To use the above expression, it is necessary to determine R, the radius of curvature of the road for each interval. Although an attempt is made to place the detectors a constant distance from the road edge, the edge is often poorly defined, and it is actually the placement of the detectors that defines the "road edge" for the purposes of computation. Since there can be no certainty that the ends of the manually placed detectors actually define a constant radius curve, the true local radius defined by each trio of radial detectors must be determined. By Eq. (C-9), R is given by M and S and S is fixed for any installation. It was concluded that R could be determined for each trio of radials by measuring M, the perpendicular distance from the road end of radial "I" to the line connecting the curb ends of radials $I-1$ and $I+1$.

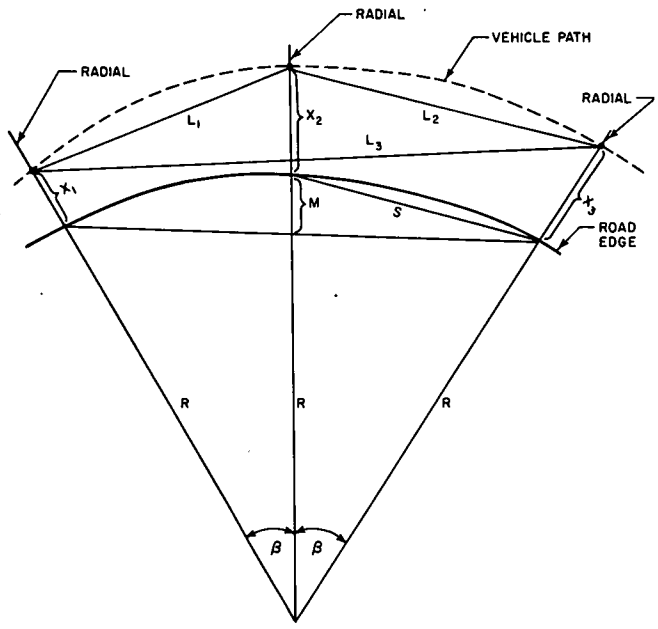

Figure C-3. Computing r, the radius of the vehicle path.

Speed is easily determined from the travel times between radials, which are spaced at known distances. For each value of r, lateral acceleration is computed from the expression

$$G_R = V^2/15r \quad \text{(C-1a)}$$

where V is the average speed of the vehicle in the interval over which the local radius r was determined. In principle, the system provides the data required to compute lateral acceleration, based on the measurement of the radius of curvature of the vehicle's local path, in ten overlapping intervals.

An important design problem was to determine the optimal dimensions for the configuration shown in Figure C-2. As shown in the following discussion, error sensitivity increases as the distance between detectors decreases. However, the computations for lateral position (X) assume constant speed across a trio of detectors, an assumption that is feasible only if the detectors are close together. The minimum spacing is given by the printer's cycling rate of 50 ms. The distance a vehicle moving at 80 mph can travel in 50 ms is 6 ft. However, 8 ft was used as a minimum to provide a safety factor for the printer. Although a systematic analysis of speed variation effects was not performed, it was apparent that this was the single most important consideration. Hence, it was decided to configure

the system with a separation of 8 ft between a radial and the closest end point of the adjacent diagonals. In the initial configuration to collect data on the first two curve sites, the dimensions were (see Fig. C-2):

$S = 22$ ft
$L = 6$ ft (radial detector length)
$K = 8$ ft (diagonal detector length)
$\theta = 45°$

Experience with the system led to changes in detector lengths and the diagonal angle as:

$L = 8$ ft
$K = 10$ ft
$\theta = 57°$

In both configurations the length of the base of the triangle formed by the diagonal and the road edge was 6 ft, and the distance from the end points of the diagonal to the near radial was 8 ft.

The detectors were lengthened to minimize loss of data due to vehicles drifting left or right out of the system. Drivers in the outside lane tend to encroach on the shoulder on outside turns and on the opposing lane in inside turns. Each time the track is transferred in this manner, considerable time errors are introduced and obvious anomalies appear in the data. For this reason, on outside turns, the detectors were placed to overlap the hard shoulder by 1 ft.

Accuracy and Calibration

Eq. (C-11) for computing r is cumbersome and requires doubly precise arithmetic in the computer for acceptable accuracy. It is also not readily amenable to error sensitivity analysis. An excellent approximation formula, accurate to within about 1 percent, is

$$r = \frac{S^2 + h^2 + 2hM}{2(M + h)} \qquad \text{(C-12)}$$

where

$$h = X_2 \frac{X_1 + X_3}{2} \qquad \text{(C-13)}$$

and S and M are as shown in Figure C-3. This expression has been used to estimate the sensitivity of the computations to errors in the dimensions that enter into the computations. In G's per inch, the rates are approximately as follows:

$$\Delta G/\Delta S \approx V^2 (h + M)/45S^3 \qquad \text{(C-14)}$$

$$\Delta G/\Delta M = \Delta G/\Delta X_2 \approx V^2/90S^2 \qquad \text{(C-15)}$$

$$\Delta G/\Delta X_1 = \Delta G/\Delta X_3 \approx -V^2/180S^2 \qquad \text{(C-16)}$$

The effect of errors in S is negligible except at high speed and for large values of $h + M$. At $h + M = 3$ (a maximum value) and at $V = 60$ mph, the error rate is $G/S = 0.23$ g per inch. The effect of errors in M and X is much greater. Note that

$$\Delta G/\Delta M = \Delta G/\Delta X_2 = 2\Delta G/X_{1,3} \qquad \text{(C-17)}$$

Since X_1 is an X_2 at some point, G/X_2 is the controlling error rate. Figure C-4 is a plot of $\Delta G/\Delta M$ $(= \Delta G/\Delta X_2)$ as a function of velocity. At 60 mph, the error rate is 0.08 g per inch. This is not serious for errors in M, since M is less than 1 ft for radii exceeding 250 ft and can be measured easily to within ⅛ in. Errors in X_2 are likely to be on the order of ½ in. so that at 60 mph, lateral acceleration errors of 0.04 or 0.05 g can be anticipated.

On the basis of these findings, it was decided to check the measurement accuracy of the configuration shown in Figure C-2. Before the system was used in traffic, it was tested on a 320-ft-radius curve on a closed road with the instrumented vehicle. A series of runs at various speeds was made with the instrumented vehicle, and the Tapeswitch system and vehicle accelerometer outputs were compared. Three such comparisons are shown in Figure C-5. These data are typical of the results. In general, errors were less than 0.04 g, and the system is able to reproduce the lateral acceleration trace produced by sharp maneuvers.

However, in later data, pronounced errors (as much as 0.08 g) were found in the lateral acceleration values computed from Tapeswitch data. Because the errors were systematic in size and direction at each measurement interval in a given site, it was suspected that the source of the acceleration errors was errors in the measurement of M, from which the R's are calculated. To test this assumption, values of M were calculated from the true lateral acceleration and speed values as recorded by the instrumented vehicle. The

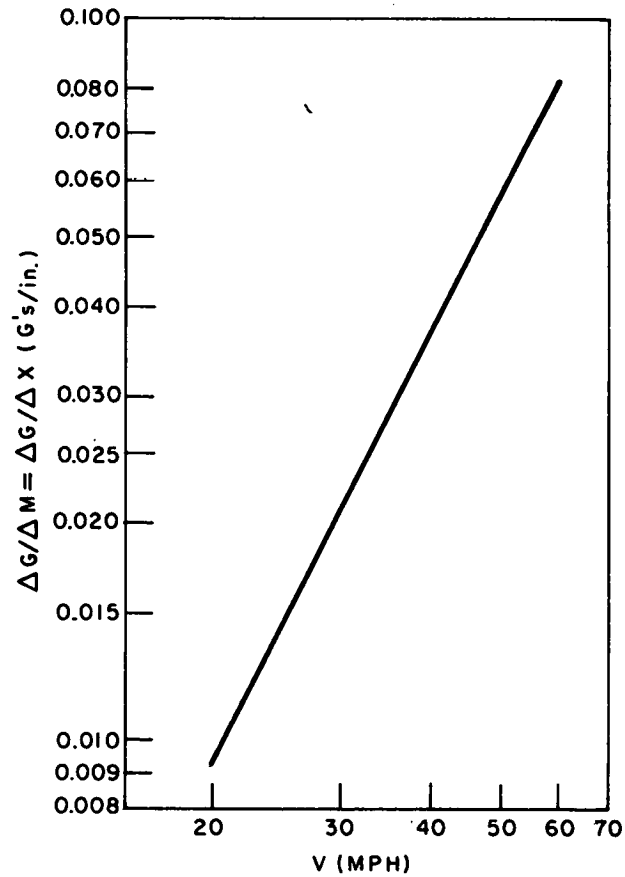

Figure C-4. Sensitivity of computations of lateral accelerations to errors in M *and* X_2 *as a function of speed.*

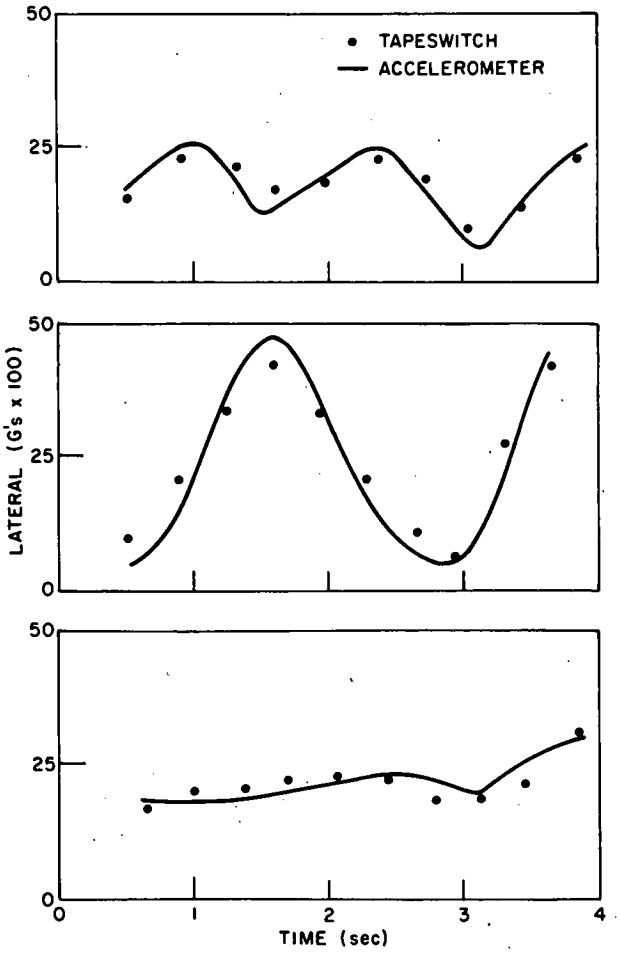

Figure C-5. Tapeswitch system output compared with vehicle accelerometer output.

new set of M's was then tested by using them to calculate lateral acceleration on a different run and comparing the output with the instrumented vehicle accelerometer data. The acceleration values computed from the corrected M's were generally within 0.03 g of the accelerometer value, and it was concluded that the major source of error lay in the measurement of M. Rather than attempt to develop a more accurate system of measurement, the instrumented vehicle was used to calibrate the system for all subsequent data collection at curved sites. The calibration procedure was as follows: A minimum of ten runs through the site was made with the instrumented vehicle at different speeds. On each run the driver attempted as well as he could to maintain constant lateral acceleration. Speed was automatically controlled at a preset level. The empirical accelerometer readings and the speed and X values from the Tapeswitch system were used to compute M's. The computation follows. The approximation formula for r is

$$r = \frac{S^2 + h^2 + 2hM}{2(M + h)} \qquad \text{(C-12)}$$

where h is defined in terms of X, as noted earlier. Since $S^2 >> h^2$ and $S^2 >> hM$, these terms can be neglected and the expression becomes

$$r \approx \frac{S^2}{2(M + h)} \qquad \text{(C-18)}$$

Then, by Eq. (C-18) and (C-1a),

$$G_r \approx \frac{2(M + h)}{15S^2} \qquad \text{(C-19)}$$

and

$$M \approx \frac{155^2\, G_r - h}{2V^2} \qquad \text{(C-20)}$$

The new values of M were then obtained by taking the mean of all of the M's thus computed for a given interval.

Operational Considerations

Installation

Installation of the detectors configured to measure lateral acceleration is similar to but somewhat more complex and time-consuming than the longitudinal configuration. The configuration is as depicted in Figure C-2.

The procedure requires that all of the radial detectors be placed before the diagonals because the latter are located with respect to the former. The first radial is placed near the center of the array. This detector is placed perpendicular to the center line such that its curb end extends 1 ft onto the shoulder (assuming the shoulder is paved). Each subsequent radial is then located with respect to the previous one using the measuring boards in the manner described in Chapter Two. The boards' measuring tapes are set so that the inside (of the curve) ends of the boards are S feet apart and the outside ends are $S + \Delta S$ feet apart. In all of the installations, S was set equal to 22 ft, and ΔS is given by the relationship

$$\Delta S/S = L/\bar{R} \qquad \text{(A-21)}$$

where L = length of the radial detectors, and $\bar{R}$ = the average radius of the instrumented section of the curve. This procedure ensures that each radial detector in fact closely approximates a true radial segment.

After all of the radials are in place, the measuring boards are used to locate the diagonals. The measuring tapes are set for the appropriate angle θ, as shown in Figure C-1. Each diagonal is placed with respect to the preceding radial. The leading edge of board 1 is butted against the trailing edge of a radial and the leading edge of board 2 is used as the guide for placing the diagonal. Since the first detector is a diagonal, it is necessary to lay a dummy radial at the beginning of the system. This is removed when the first diagonal is in place. The entire operation takes two men approximately an hour (see Fig. C-6).

Data Collection Operations

Data collection is largely automatic since the system is reset automatically once a vehicle passes over the last detector. However, the operator may intervene as necessary to exclude all vehicles other than automobiles and light trucks. Because only one vehicle at a time is tracked, the system automatically ensures a separation equal to the detector array length (265 ft) between a recorded vehicle and the

a) Placing the System

b) System in Operation

c) System in Operation

d) System in Operation

Figure C-6. Random photos showing the Tapeswitch system from the driver's viewpoint.

nearest preceding vehicle. Thus, none of the vehicles observed was impeded by a lead vehicle. Because almost all of the vehicles passing through the site were recorded, the data collection rate on curves was over twice as great as at intersections.

Reliability

Diagonal detectors failed with greater frequency than the radial detectors. Accordingly, diagonal detectors were used only once; thereafter, they were cut to 8 ft lengths and used as spare radials.

Influence on Driver Behavior

A study was conducted to determine whether the presence of the system had an important effect on driver behavior. Speeds were recorded at three sites where only the 9th and 10th diagonal switches were installed. These speeds were averaged and compared with the averaged speeds recorded by the corresponding switches in the full-system installations at the same sites. The results are summarized in Table C-1. Although there was a difference, it was too small to be of any practical significance,* and it was concluded that the presence of the Tapeswitch detectors has no meaningful influence on cornering behavior.

* Within the accuracy of the Tapeswitch system.

DRIVER DEMAND RESEARCH ON CURVES

Lateral Acceleration Measurements on Curves

Lateral acceleration data were collected on the ten curve sites given in Table C-2. The system of detectors was centered on the curve at each site. As a rule the system was allowed to reset itself automatically. This procedure ensured a minimum separation of 265 ft between a recorded vehicle and the immediately preceding vehicle.

Individual vehicle records were inspected for anomalies prior to further processing. A substantial number (about 30 percent) of poor records were found and discarded. Most of the anomalies were the result of the tracked wheel passing outside of the system as previously described.

Reliable records were subjected to further computer reduction to provide summary tables for each site. A sample summary output (for site No. 1) is shown in Figure C-7. RN is the local road edge radius defined by the system, VEL is vehicle speed in mph, ALAT is lateral acceleration in *g*'s, and ALNG is longitudinal acceleration in *g*'s. The statistics under "peak value" heading were computed from the distribution of peak values, where the peak is the highest value observed for a given vehicle in any of the ten intervals. The computation of lateral acceleration values assumes no superelevation.

Figure C-8 shows lateral acceleration percentile profiles

TABLE C-1

INFLUENCE OF TAPESWITCH SYSTEM ON OBSERVED SPEEDS

SITE NO.	POSTED SPEED LIMIT (MPH)	2-TAPESWITCH INSTALLATION		FULL-SYSTEM INSTALLATION		DIFFERENCE IN AVERAGE SPEEDS (MPH)
		NO. VEHICLES OBSERVED	AVERAGE SPEED (MPH)	NO. VEHICLES OBSERVED	AVERAGE SPEED (MPH)	
1	40	120	32.27	120	32.11	0.16
5	55	279	45.14	100	46.02	0.88
6	55	92	51.77	92	51.38	0.39

TABLE C-2

SITE CHARACTERISTICS FOR TWO-LANE CURVES, CLOVERLEAF INTERCHANGES, AND EXPRESSWAY CURVES

SITE NO.	DESCRIPTION	CURVE RADIUS (FT)	LENGTH OF CURVE (FT)	SUPER-ELEVATION (IN./FT)	AVERAGE INITIAL SPEED (MPH)	TOTAL NO. VEHICLES OBSERVED	POSTED SPEED LIMIT (MPH)
1	Two-lane rural	287	389	¾	31.3	396	40
2	Two-lane rural	573	545	1	35.2	298	45
3	Two-lane urban	319	412	1	31.9	326	40
4	Cloverleaf interchange	180	850	Variable	25.5	329	Not posted
5	Two-lane rural	1800	840	¾	47.1	436	55
6	Two-lane rural	880	700	Variable	51.7	316	55
7	Cloverleaf interchange	220	364.88	1	25.2	305	Not posted
8	Cloverleaf interchange	393	493.10	1	37.3	308	25
9	Cloverleaf interchange	540	639.86	1	37.2	716	25
10	Expressway curve	1432	1100	Variable	52.0	687	50

at one site. Also indicated are the mean speeds of the vehicles within 0.02 g of the indicated acceleration in each interval. At other sites the profiles were more variable because of local variations in the radius of curvature. In general, however, drivers tended to maintain constant speeds through the curves.

Table C-3 gives the single highest (maximum) as well as the 99th, 95th, and 50th percentile values of peak lateral acceleration (G_R*) and associated speeds at each of the ten sites. Peak lateral acceleration is simply the highest value observed for a vehicle across the ten intervals. The associated speed is the mean of speeds observed in the 124-ft

TABLE C-3

PERCENTILE LEVELS OF THE DISTRIBUTION OF THE PEAK LATERAL ACCELERATION OBSERVED FOR EACH VEHICLE AND THE MEAN SPEEDS OF THE VEHICLES IN THE VARIOUS PERCENTILE LEVELS

SITE NO.	TURN (L-R)	SITE TYPE	NO. VEHICLES	NOMINAL (AVERAGE) RADIUS	MAXIMUM		99TH PERCENTILE		95TH PERCENTILE		50TH PERCENTILE		
					G_R*	ASSO-CIATED SPEED	G_R*	ASSO-CIATED SPEED	G_R*	ASSO-CIATED SPEED	G_R*	ASSO-CIATED SPEED	SG_R*
1	L	1	266	279	0.49	39.8	0.43	35.9	0.38	37.9	0.28	32.1	0.062
2	R	1	189	534	0.46	45.7	0.45	37.5	0.30	40.9	0.20	36.7	0.064
3	R	1	147	333	0.48	43.8	0.47	33.6	0.42	35.9	0.26	33.9	0.078
4	R	2	281	188	0.49	35.1	0.43	32.4	0.34	30.0	0.27	26.0	0.049
5	R	1	366	1860	0.33	63.0	0.22	51.8	0.17	54.3	0.12	48.4	0.035
6	L	1	275	826	0.46	71.1	0.41	64.3	0.35	60.6	0.26	52.8	0.054
7	R	2	216	237	0.45	36.2	0.37	28.6	0.29	30.1	0.21	25.5	0.050
8	R	2	283	367	0.46	46.9	0.40	44.0	0.36	42.9	0.27	36.9	0.055
9	R	2	622	541	0.42	47.5	0.36	40.6	0.28	42.4	0.20	36.0	0.055
10	L	3	634	1551	0.41	69.0	0.29	60.3	0.23	59.2	0.16	51.7	0.041

SITE NO. 1 6/17/71 MATSONFORD RD. LEFT-HAND CURVE SITE TYPE 1 45 DEGREE ANGLE (DIAGONAL SWITCH)

	DISTANCE (FT.) OF RADIAL SWITCH ALONG CURVE										
	36	58	80	102	124	146	168	190	212	234	
RN	279.2	279.2	279.2	279.2	279.2	279.2	279.2	279.2	279.2	279.2	Peak Values
FREQ	262	266	266	265	265	261	258	252	247	247	266
VEL											
MAX	39.9	39.6	39.3	39.2	39.2	39.4	39.6	40.0	40.4	41.0	39.8
99	38.8	38.7	38.5	38.5	38.6	38.7	39.1	39.4	39.9	40.2	39.3
95	37.1	37.2	37.0	36.9	36.9	37.1	37.4	37.3	37.9	37.9	37.6
90	35.8	35.7	35.7	35.6	35.6	35.9	36.0	36.2	36.2	36.3	36.3
85	35.0	34.9	34.8	34.8	34.9	35.3	35.2	35.3	35.6	35.9	35.1
50	31.2	31.2	31.1	31.1	31.2	31.5	31.7	31.9	32.0	32.2	31.7
15	27.7	27.7	27.9	27.8	27.9	28.2	28.4	28.5	28.5	28.7	28.2
MEAN	31.3	31.3	31.3	31.2	31.3	31.5	31.6	31.8	31.9	32.2	31.7
S.D.	3.61	3.57	3.52	3.47	3.45	3.44	3.42	3.44	3.45	3.47	3.41
ALAT											
MAX	.49	.40	.42	.41	.45	.40	.43	.39	.42	.45	.49
99	.41	.38	.38	.37	.36	.38	.39	.37	.37	.36	.43
95	.35	.35	.36	.34	.34	.35	.35	.34	.35	.32	.38
90	.34	.33	.33	.33	.31	.32	.33	.32	.32	.29	.36
85	.31	.31	.32	.31	.30	.31	.30	.30	.30	.28	.35
50	.25	.25	.25	.25	.24	.24	.25	.24	.24	.22	.28
15	.20	.20	.20	.19	.19	.19	.19	.19	.19	.16	.22
MEAN	.26	.25	.26	.25	.24	.25	.25	.24	.25	.22	.28
S.D.	.060	.058	.060	.058	.058	.058	.057	.054	.054	.058	.062
FREQ	262	266	266	265	265	261	258	252	247	246	266
ALNG											
MAX	.10	.10	.14	.06	.06	.41	.06	.10	.06	.42	.42
99	.07	.07	.07	.06	.05	.06	.05	.06	.05	.19	.08
95	.05	.05	.05	.03	.02	.03	.03	.04	.02	.04	.05
90	.04	.04	.04	.02	.01	.02	.02	.02	.01	.02	.04
85	.03	.03	.03	.01	.01	.01	.01	.02	.00	.01	.03
50	.00	.00	.00	-.01	-.02	-.02	-.02	-.02	-.03	-.03	-.00
15	-.03	-.03	-.02	-.03	-.04	-.04	-.04	-.04	-.05	-.05	-.04
MEAN	.00	.00	.00	-.01	-.02	-.01	-.02	-.01	-.02	-.02	-.00
S.D.	.032	.030	.029	.025	.029	.038	.030	.028	.027	.049	.050

Figure C-7. Sample summary statistics for site No. 1.

interval of vehicles falling within a close range of the designated G_R* percentile level, which tabulated as:

G_R* PERCENTILE LEVEL	G_R* PERCENTILE RANGE
99th	97-100
95th	93-97
50th	48-52

Also, Table C-3 gives the site type, left- or right-hand turn, and the average radius of the curve. The average radius was estimated by finding the mean of the local radii in the ten intervals. In the field, average radius would be determined from engineering drawings or by measuring the curve as previously described [see Eq. (C-9) and Fig. C-3].

The single highest observed levels of G_R* at the ten sites ranged from 0.33 to 0.49 *g*, 99th percentile levels from 0.22 to 0.47 *g*, 95th percentile levels from 0.17 to 0.42 *g*, and median levels from 0.12 to 0.27 *g*. Note that the mean speed associated with G_{R99}* is not consistently greater than the mean speed associated with G_{R95}*. This indicates that the difference in lateral acceleration at these speeds was produced, at least in part, by differences in path.

It is difficult to compare site types because of site-to-site differences in radii. Site No. 2 (type 1) and site No. 9 (type 2) have essentially identical average radii and differ little in median and 95th percentile levels of lateral acceleration. On the other hand, site No. 3 (type 1) and site No. 8 (type 2), whose radii differ by only 10 percent, differ by 0.06 *g* at the 95th percentile. (Sites No. 2 and 3 have too few cases—189 and 147—for the empirical 99th percentile to be meaningful.) Nevertheless, these data provide no basis for treating type 1 and type 2 curves differently.

Peak 95th, 90th, and 50th percentile acceleration data are plotted against degree of curvature * in Figure C-9. Also plotted are Taragin's (*18*) cornering data.† Obviously, Taragin's data do not constitute a good model for the data from the present study. Lateral acceleration means and extremes from the ten sites are almost independent of radius. Because lateral acceleration on a curve of given radius is largely dependent on speed, the conclusion regarding the present sample of sites is that entry speed is dependent on other factors in addition to radius of curvature.

* Degree of curvature, $D = 5730/R$.

† Taragin's data were presented in terms of velocity and were converted to lateral acceleration values for the purposes of the comparison.

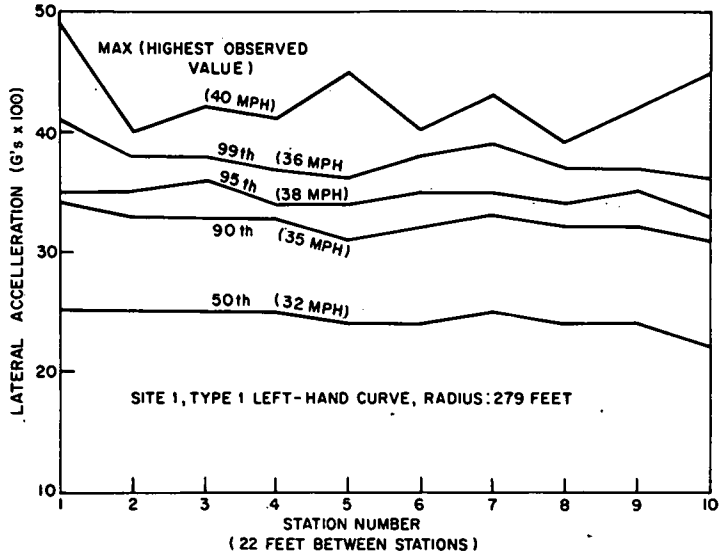

Figure C-8. Lateral acceleration percentile profiles and approximate associated speeds.

Taragin found a correlation of 0.81 between entry speed and radius in his sample of rural two-lane highways. The present sample was less homogeneous and included suburban roads and entrance ramps. Also, on mild curves (whose radius is greater than 1500 ft) designed for highway speeds, speeds will be determined largely by the speeds on the preceding section (i.e., drivers will not slow for the curve) and, therefore, entry speed is largely independent of radius.

Figure C-10 is a scattergram of a random selection of nominal versus observed lateral acceleration points from site No. 4, a freeway entrance ramp. Nominal lateral acceleration is computed by Eq. (6) using the observed speed at a point and average radius of curvature of the road, while the "observed" acceleration is computed from the observed speed at the same point and local radius of curvature of the vehicle's path at that point as determined by the Tapeswitch system. The relationship is clearly very strong at site No. 4. However, at other sites the relationship between nominal and observed acceleration was less consistent. The correlation coefficients between observed and nominal lateral acceleration ranged from 0.60 to 0.95 at the ten sites. Poor correspondence between the nominal and observed values arises because of deviations in vehicle path from the local radius of curvature of the road. In general, this occurred more frequently on curves whose degree of curvature varied across the instrumented section, and these were the sites with the lowest correlation coefficients. Although the path through a curve is ultimately bounded by the road, drivers do not attempt to follow every variation in local radius but tend to "smooth" the curve by following constant arcs.

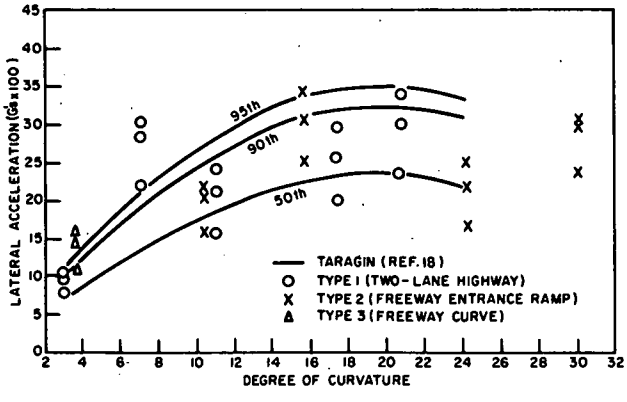

Figure C-9. Percentile levels of lateral acceleration as a function of degree of curvature from the present study and from Taragin (18).

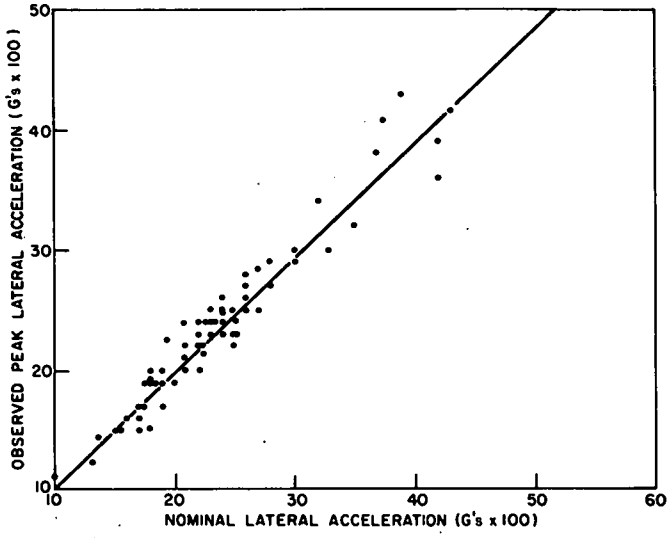

Figure C-10. Observed peak lateral acceleration as a function of nominal lateral acceleration.

Positive Longitudinal Acceleration on Curves

Longitudinal acceleration was also measured on the curves across each trio of radials. The highest single value of positive longitudinal acceleration observed was 0.43 g. However, a total of only five values of longitudinal acceleration in excess of 0.19 g was observed. Mean values were close to zero and 99th percentile values ranged from 0.07 to 0.19 g. Further, no combinations of high values of lateral acceleration (>0.30 g) and high longitudinal acceleration (>0.20 g) were observed.

Analysis of Curve Data

An approach similar to that used in the analysis of the intersection data was pursued in an attempt to develop a model for predicting lateral acceleration on curves. Because speed tends to remain constant through a curve, no attempt was made to predict acceleration profiles. Instead, the dependent variable was the peak lateral acceleration G_R* observed for each vehicle across the ten intervals.

As the first step, distributions of G_R* from each site were tested for significant deviations from normality at the 5-percent level by the Kolmogorov-Smirnov test. The normality assumption was upheld at each of the ten sites.

Accordingly, a series of multiple-regression analyses was performed to predict the:

1. Mean maximum lateral acceleration ($\bar{G}_R$*)
2. Standard deviation of G_R*, (S_{GR}*)
3. Mean speed associated with the 99th, 95th, and 90th percentile levels of G_R*, (V_{GR99}*, V_{GR95}*, V_{GR90}*).

The set of predictor variables included:

1. Average radius of curvature ($\bar{R}$)
2. $1/\bar{R}$
3. The 95th percentile speed at the 124-ft point ($V_{95_{124}}$)
4. Mean speed at the 124-ft point ($\bar{V}_{124}$)
5. Standard deviation of V_{124}, ($S_{V_{124}}$)
6. Mean nominal lateral acceleration at 124 ft ($\tilde{\bar{G}}_{R124}$)
7. Standard deviation of $\tilde{G}_{R124}$ ($\tilde{S}_{GR124}$)
8. Mean peak lateral acceleration $\bar{G}_R$*.

Average radius of curvature can be determined for the entire constant radius section of the curve (i.e., between PC and PT) from the cord length and the cord-to-arc distance [see Fig. C-3 and Eq. (C-9)]. Nominal lateral acceleration is given by

$$\tilde{G}_R = V^2_{124}/15\bar{R} \qquad \text{(C-1b)}$$

Variable $\bar{G}_R$*, the mean peak lateral acceleration, is a dependent variable; but, once determined, it is used as a predictor variable or S_{GR}*. Note that the only vehicle variable that must be measured is V_{124}, the speed of each vehicle in the middle of the curve.

The prediction equations that emerged from the analyses are:

$$\bar{G}_R{}^* = 0.073 + 0.824\,\tilde{\bar{G}}_{124} \qquad \text{(C-22)}$$

Standard error of prediction = 0.0175 g

$$S_{GR}{}^* = 0.011 + 2.042\,S_{\tilde{G}124} - 0.481\,\tilde{\bar{G}}_{124} + 0.218\,\bar{G}_{R\max} \qquad \text{(C-23)}$$

Standard error of prediction = 0.0055 g

$$V_{GR99}{}^* = -29.75 + 1.709\,\bar{V}_{124} + 3547\,(1/\bar{R}) \qquad \text{(C-24)}$$

Standard error of prediction = 1.6 mph

$$V_{GR95}{}^* = 1.512 + 1.121\,\bar{V}_{124} \qquad \text{(C-25)}$$

Standard error of prediction = 0.90 mph

$$V_{GR90}{}^* = -0.074 + 1.118\,\bar{V}_{124} \qquad \text{(C-26)}$$

Standard error of prediction = 1.2 mph

The prediction equations selected were the best equations obtainable using the predictor variables; that is, these equations represented the best tradeoff between the statistics measuring accuracy of prediction and the number of predictor variables required.

The standard error of prediction measures the equation's accuracy of prediction and is expressed in the same unit of measurement as the variable predicted. These standard errors were considered sufficiently small to permit the estimation of the key variables using the predictor variables in question.

The following analysis was performed to evaluate the accuracy of estimation of the acceleration percentiles. Peak lateral acceleration means and standard deviations were estimated for the various sites by substituting the predictor variable values (computed for the sites) into the equations. The calculated means and standard deviations were then used to estimate 99th, 95th, and 90th maximum lateral acceleration percentiles for each site (employing the relationship derived from the normality assumption, $X_p = \bar{x} + Z_p\,S_x$). The estimated percentiles were compared to the corresponding empirical percentiles. The comparison showed that the 99th percentiles predicted for two sites (sites No. 2 and 4) underestimated the corresponding empirical percentiles by more than 10 percent (of the value of the empirical percentiles). The 99th percentiles predicted for the other eight sites underestimated the corresponding empirical values, but by less than 10 percent. None of the predicted 95th or 90th percentiles underestimated the corresponding empirical percentiles by more than 10 percent. The percentile values and the differences between the estimated and empirical values are shown in Table C-4. Note the difference between the estimated and empirical 99th percentile values obtained for site No. 2. This difference was disregarded because the empirical 99th percentile obtained for site No. 2 appeared to be considerably higher than could reasonably be expected. The other differences given in Table C-4 were considered sufficiently small to warrant the conclusion that these percentiles can be estimated accurately using the prediction equations (and the normal-distribution relationship).

With the exception of the one extreme difference, all predicted values were within 0.04 g of the empirical values.

These values do not take into account the effects of superelevation. Lateral acceleration was computed assuming a flat pavement. According to Taragin (*18*), drivers do not adjust their curve speeds to compensate for or take

TABLE C-4

ESTIMATED AND EMPIRICAL VALUES AND THEIR DIFFERENCES FOR THE 99TH, 95TH, AND 90TH PERCENTILES

SITE NO.	99TH PERCENTILE			95TH PERCENTILE			90TH PERCENTILE		
	EST.	EMP.	DIFF.	EST.	EMP.	DIFF.	EST.	EMP.	DIFF.
1	0.42	0.43	−0.01	0.37	0.38	−0.01	0.35	0.36	−0.01
2	0.31	0.45	−0.14	0.27	0.30	−0.03	0.25	0.27	−0.02
3	0.44	0.47	−0.03	0.40	0.42	−0.02	0.37	0.37	0.00
4	0.39	0.43	−0.04	0.36	0.34	0.02	0.34	0.33	0.01
5	0.21	0.22	−0.01	0.19	0.17	0.02	0.17	0.16	0.01
6	0.37	0.41	−0.04	0.33	0.35	−0.02	0.31	0.33	−0.02
7	0.36	0.37	−0.01	0.32	0.29	0.03	0.30	0.26	0.04
8	0.39	0.40	−0.01	0.35	0.36	−0.01	0.33	0.35	−0.02
9	0.32	0.36	−0.04	0.28	0.28	0.00	0.27	0.26	0.01
10	0.27	0.29	−0.02	0.24	0.23	0.01	0.22	0.21	0.01
	Mean Diff.:		−0.035			−0.003			0.001

advantage of superelevation. Hence, the predicted percentile levels of lateral acceleration should be corrected by subtracting the superelevation (expressed in number of feet per foot).

LATERAL SKID TESTS

Determination of Skid Numbers

Skid numbers (SN) and cornering slip numbers (CSN) measured for six test curves, as described in Chapter Two, are given in Table C-5 and shown graphically in Figure C-11. Figure C-11 also shows the maximum lateral acceleration achieved by each vehicle/tire combination on each curve. In terms of the pad-to-pad relative values of the skid numbers, the trailer data are in good agreement. The NBS trailer produced the lowest values and the THD (external water) trailer, the highest. The MTT cornering slip number values are substantially higher than the trailer skid number values and do not discriminate between curves 3, 7, and 8 as do the trailer skid numbers.

Vehicle Cornering Test Procedure

The vehicle cornering test procedure used was similar to the methods developed by NBS tire testers. The vehicle is accelerated to its assigned speed well in advance of the curve, and the curve is negotiated at a constant speed with the steering wheel set in one position. This procedure is repeated at increasing speeds until rear-end breakaway occurs. When this procedure is followed, a small peak occurs in the lateral accelerometer trace coincident with breakaway. This value is taken as the maximum lateral acceleration (see Fig. C-12). If, during a trial, steering wheel cor-

TABLE C-5

SKID NUMBERS AND CORNERING SLIP NUMBERS FOR SEVERAL CURVES

SITE NO.	NBS SN_{40}	THD (INTERNAL) SN_{30}	THD (EXTERNAL) SN_{30}	MTT CSN_{40}
2	23	28	28	52
3	65	70	72	85
4	51	58	63	77
5	51	53	57	65
7	68	72	76	85
8	60	59	63	85

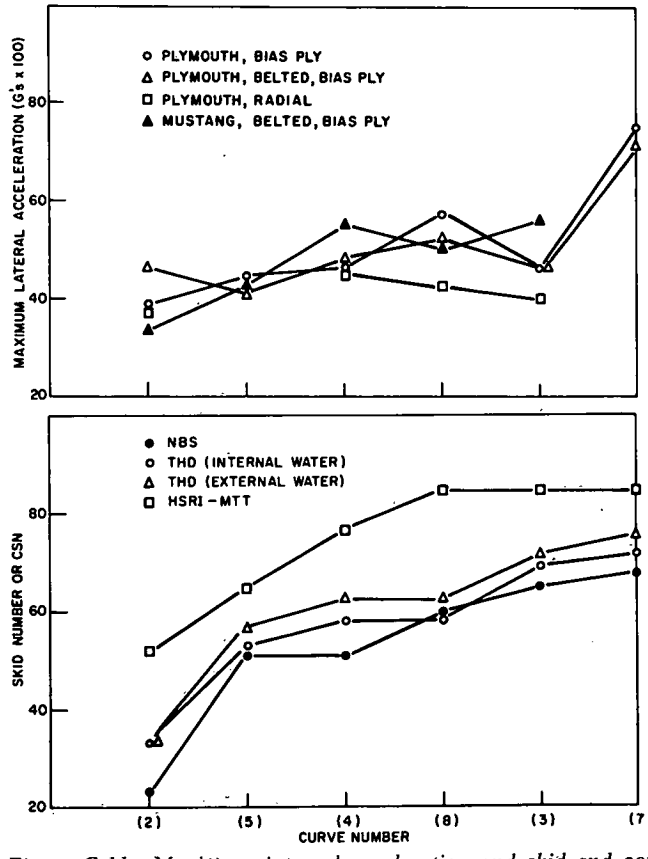

Figure C-11. Maximum internal acceleration and skid and cornering slip numbers on six curves.

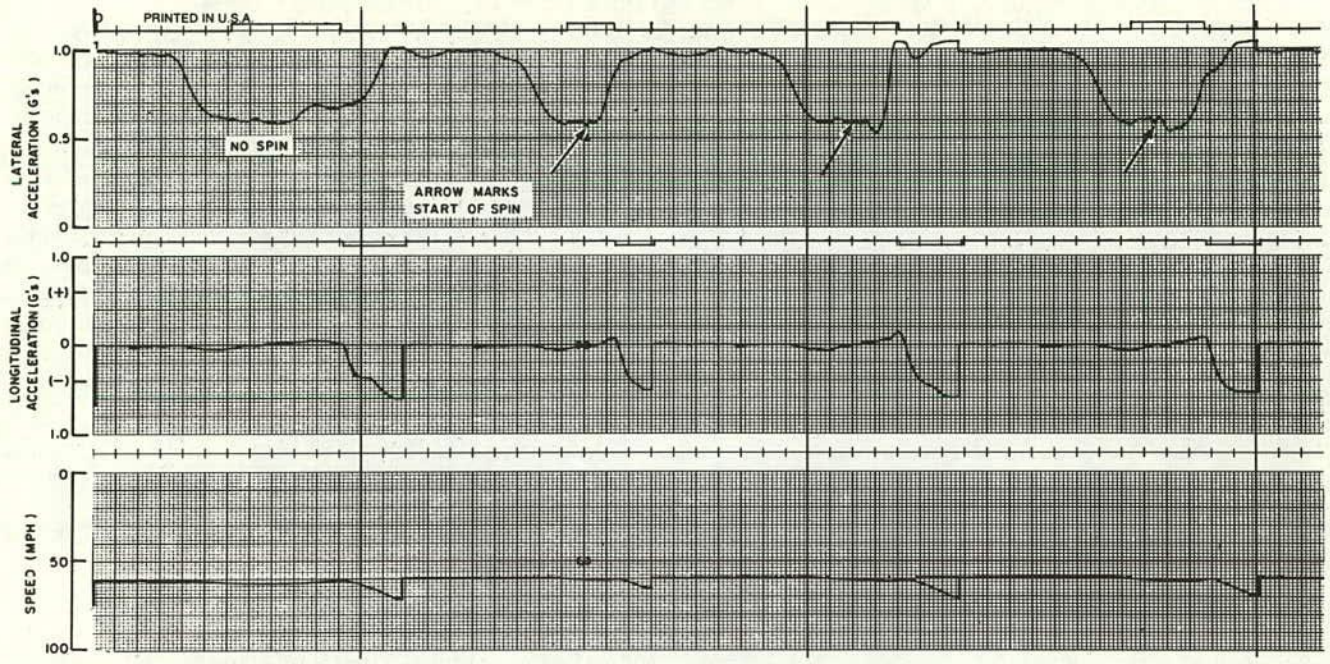

Figure C-12. Sample cornering limit data showing characteristic peak at start of spin.

rections were required to keep the vehicle on the curve, the trial was abandoned.

Although on some trials there is some uncertainty about exactly whether or not breakaway occurred, the speed difference between no loss of control and sharp breakaway is on the order of 1 or 2 mph.

Skid Test Results

The relationship between skid numbers and maximum lateral acceleration was not nearly so strong as that between skid numbers and braking deceleration. Correlation coefficients between skid numbers and locked-wheel deceleration were generally around 0.95, whereas the correlation coefficients between skid numbers and maximum lateral acceleration on the 20° curves ranged from less than 0.50 to 0.70. The HSRI's Mobile Tire Tester was no better a predictor of maximum cornering force than the skid trailers. Figure C-11 shows that there are strong interactions between the surfaces and the vehicle/tire combinations. The radial tire gave the lowest performance values on three of the four surfaces on which it was tested. Except for the Plymouth on belted bias-ply tires (whose worst performance was on curve 5), curves 2 and 7 yielded the lowest and highest lateral acceleration values, respectively. These two surfaces also had the lowest and highest skid numbers. It is this correspondence that is responsible for whatever apparent correlation exists between skid number and maximum cornering force because, on curves 3, 4, and 5, cornering force is essentially independent of skid number. Note also that although the difference in skid numbers between curves 3 and 4 was small (4 or less), the difference between the cornering forces that could be achieved on them were considerable (in excess of 0.2). Figure C-13 shows maxi-

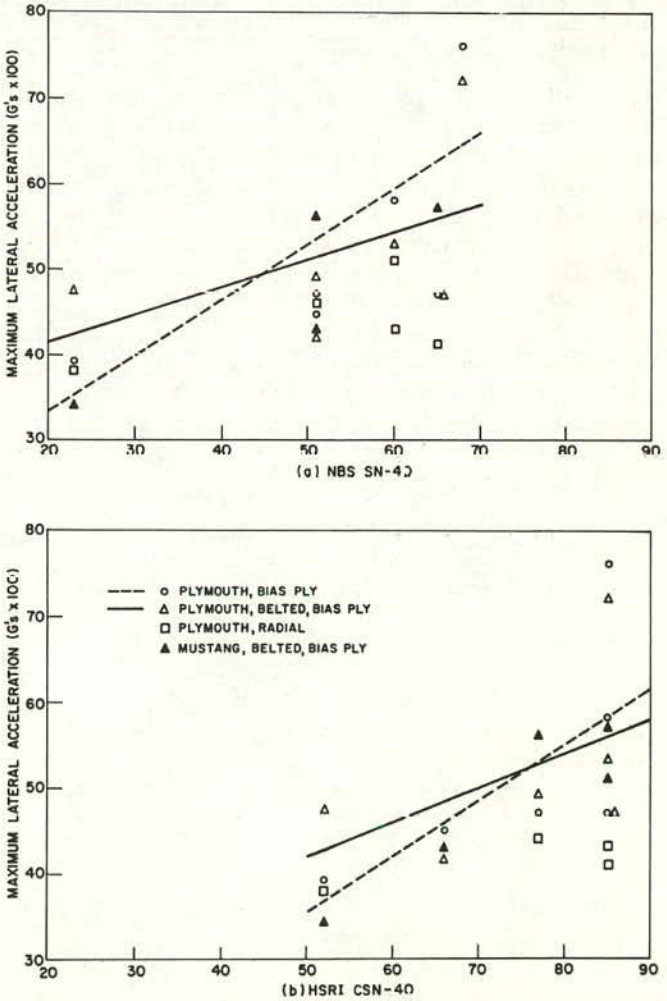

Figure C-13. Maximum lateral acceleration of four tire/vehicle combinations as function of (a) NBS SN_{40} and (b) HSRI CSN_{40}.

mum lateral acceleration plotted against the corresponding NBS SN_{40} and HSRI CSN_{40} values for the four vehicles. The best-fit lines for the Plymouth on bias-ply and belted bias-ply tires are also plotted. It is clear from these data that neither conventional locked-wheel skid trailer measurements nor rolling cornering slip numbers can provide accurate predictions of maximum vehicular cornering forces. It is not surprising that locked-wheel skid numbers predict cornering maxima poorly because the comparison is between the longitudinal force generated by a sliding tire at zero slip angle and the lateral force produced by a rolling tire at a high slip angle. However, since the MTT measures tire forces produced under conditions similar to those that obtain in a cornering vehicle, a better correlation between cornering slip number and cornering maxima was anticipated. Part of the problem arises from the obvious interactions between surfaces and tire/vehicle combinations. Because the ordering of the tire/vehicle combinations (in terms of cornering maxima) varies from surface to surface, it is clear that no single surface skid-resistance value will correlate well with all tire/vehicle combinations. In fact, the correlation between the different tire/vehicle combinations is low. Also, the ASTM tire used in the MTT differs considerably from any of the passenger car tires tested.

Published reports of the

NATIONAL COOPERATIVE HIGHWAY RESEARCH PROGRAM

are available from:

Highway Research Board
National Academy of Sciences
2101 Constitution Avenue
Washington, D.C. 20418

Rep. No.	*Title*
—*	A Critical Review of Literature Treating Methods of Identifying Aggregates Subject to Destructive Volume Change When Frozen in Concrete and a Proposed Program of Research—Intermediate Report (Proj. 4-3(2)), 81 p., $1.80
1	Evaluation of Methods of Replacement of Deteriorated Concrete in Structures (Proj. 6-8), 56 p., $2.80
2	An Introduction to Guidelines for Satellite Studies of Pavement Performance (Proj. 1-1), 19 p., $1.80
2A	Guidelines for Satellite Studies of Pavement Performance, 85 p.+9 figs., 26 tables, 4 app., $3.00
3	Improved Criteria for Traffic Signals at Individual Intersections—Interim Report (Proj. 3-5), 36 p., $1.60
4	Non-Chemical Methods of Snow and Ice Control on Highway Structures (Proj. 6-2), 74 p., $3.20
5	Effects of Different Methods of Stockpiling Aggregates—Interim Report (Proj. 10-3), 48 p., $2.00
6	Means of Locating and Communicating with Disabled Vehicles—Interim Report (Proj. 3-4), 56 p. $3.20
7	Comparison of Different Methods of Measuring Pavement Condition—Interim Report (Proj. 1-2), 29 p., $1.80
8	Synthetic Aggregates for Highway Construction (Proj. 4-4), 13 p., $1.00
9	Traffic Surveillance and Means of Communicating with Drivers—Interim Report (Proj. 3-2), 28 p., $1.60
10	Theoretical Analysis of Structural Behavior of Road Test Flexible Pavements (Proj. 1-4), 31 p., $2.80
11	Effect of Control Devices on Traffic Operations—Interim Report (Proj. 3-6), 107 p., $5.80
12	Identification of Aggregates Causing Poor Concrete Performance When Frozen—Interim Report (Proj. 4-3(1)), 47 p., $3.00
13	Running Cost of Motor Vehicles as Affected by Highway Design—Interim Report (Proj. 2-5), 43 p., $2.80
14	Density and Moisture Content Measurements by Nuclear Methods—Interim Report (Proj. 10-5), 32 p., $3.00
15	Identification of Concrete Aggregates Exhibiting Frost Susceptibility—Interim Report (Proj. 4-3(2)), 66 p., $4.00
16	Protective Coatings to Prevent Deterioration of Concrete by Deicing Chemicals (Proj. 6-3), 21 p., $1.60
17	Development of Guidelines for Practical and Realistic Construction Specifications (Proj. 10-1), 109 p., $6.00
18	Community Consequences of Highway Improvement (Proj. 2-2), 37 p., $2.80
19	Economical and Effective Deicing Agents for Use on Highway Structures (Proj. 6-1), 19 p., $1.20
20	Economic Study of Roadway Lighting (Proj. 5-4), 77 p., $3.20
21	Detecting Variations in Load-Carrying Capacity of Flexible Pavements (Proj. 1-5), 30 p., $1.40
22	Factors Influencing Flexible Pavement Performance (Proj. 1-3(2)), 69 p., $2.60
23	Methods for Reducing Corrosion of Reinforcing Steel (Proj. 6-4), 22 p., $1.40
24	Urban Travel Patterns for Airports, Shopping Centers, and Industrial Plants (Proj. 7-1), 116 p., $5.20
25	Potential Uses of Sonic and Ultrasonic Devices in Highway Construction (Proj. 10-7), 48 p., $2.00
26	Development of Uniform Procedures for Establishing Construction Equipment Rental Rates (Proj. 13-1), 33 p., $1.60
27	Physical Factors Influencing Resistance of Concrete to Deicing Agents (Proj. 6-5), 41 p., $2.00
28	Surveillance Methods and Ways and Means of Communicating with Drivers (Proj. 3-2), 66 p., $2.60
29	Digital-Computer-Controlled Traffic Signal System for a Small City (Proj. 3-2), 82 p., $4.00
30	Extension of AASHO Road Test Performance Concepts (Proj. 1-4(2)), 33 p., $1.60
31	A Review of Transportation Aspects of Land-Use Control (Proj. 8-5), 41 p., $2.00
32	Improved Criteria for Traffic Signals at Individual Intersections (Proj. 3-5), 134 p., $5.00
33	Values of Time Savings of Commercial Vehicles (Proj. 2-4), 74 p., $3.60
34	Evaluation of Construction Control Procedures—Interim Report (Proj. 10-2), 117 p., $5.00
35	Prediction of Flexible Pavement Deflections from Laboratory Repeated-Load Tests (Proj. 1-3(3)), 117 p., $5.00
36	Highway Guardrails—A Review of Current Practice (Proj. 15-1), 33 p., $1.60
37	Tentative Skid-Resistance Requirements for Main Rural Highways (Proj. 1-7), 80 p., $3.60
38	Evaluation of Pavement Joint and Crack Sealing Materials and Practices (Proj. 9-3), 40 p., $2.00
39	Factors Involved in the Design of Asphaltic Pavement Surfaces (Proj. 1-8), 112 p., $5.00
40	Means of Locating Disabled or Stopped Vehicles (Proj. 3-4(1)), 40 p., $2.00
41	Effect of Control Devices on Traffic Operations (Proj. 3-6), 83 p., $3.60
42	Interstate Highway Maintenance Requirements and Unit Maintenance Expenditure Index (Proj. 14-1), 144 p., $5.60
43	Density and Moisture Content Measurements by Nuclear Methods (Proj. 10-5), 38 p., $2.00
44	Traffic Attraction of Rural Outdoor Recreational Areas (Proj. 7-2), 28 p., $1.40
45	Development of Improved Pavement Marking Materials—Laboratory Phase (Proj. 5-5), 24 p., $1.40
46	Effects of Different Methods of Stockpiling and Handling Aggregates (Proj. 10-3), 102 p., $4.60
47	Accident Rates as Related to Design Elements of Rural Highways (Proj. 2-3), 173 p., $6.40
48	Factors and Trends in Trip Lengths (Proj. 7-4), 70 p., $3.20
49	National Survey of Transportation Attitudes and Behavior—Phase I Summary Report (Proj. 20-4), 71 p., $3.20

* Highway Research Board Special Report 80.

Rep. No.	Title
50	Factors Influencing Safety at Highway-Rail Grade Crossings (Proj. 3-8), 113 p., $5.20
51	Sensing and Communication Between Vehicles (Proj. 3-3), 105 p., $5.00
52	Measurement of Pavement Thickness by Rapid and Nondestructive Methods (Proj. 10-6), 82 p., $3.80
53	Multiple Use of Lands Within Highway Rights-of-Way (Proj. 7-6), 68 p., $3.20
54	Location, Selection, and Maintenance of Highway Guardrails and Median Barriers (Proj. 15-1(2)), 63 p., $2.60
55	Research Needs in Highway Transportation (Proj. 20-2), 66 p., $2.80
56	Scenic Easements—Legal, Administrative, and Valuation Problems and Procedures (Proj. 11-3), 174 p., $6.40
57	Factors Influencing Modal Trip Assignment (Proj. 8-2), 78 p., $3.20
58	Comparative Analysis of Traffic Assignment Techniques with Actual Highway Use (Proj. 7-5), 85 p., $3.60
59	Standard Measurements for Satellite Road Test Program (Proj. 1-6), 78 p., $3.20
60	Effects of Illumination on Operating Characteristics of Freeways (Proj. 5-2) 148 p., $6.00
61	Evaluation of Studded Tires—Performance Data and Pavement Wear Measurement (Proj. 1-9), 66 p., $3.00
62	Urban Travel Patterns for Hospitals, Universities, Office Buildings, and Capitols (Proj. 7-1), 144 p., $5.60
63	Economics of Design Standards for Low-Volume Rural Roads (Proj. 2-6), 93 p., $4.00
64	Motorists' Needs and Services on Interstate Highways (Proj. 7-7), 88 p., $3.60
65	One-Cycle Slow-Freeze Test for Evaluating Aggregate Performance in Frozen Concrete (Proj. 4-3(1)), 21 p., $1.40
66	Identification of Frost-Susceptible Particles in Concrete Aggregates (Proj. 4-3(2)), 62 p., $2.80
67	Relation of Asphalt Rheological Properties to Pavement Durability (Proj. 9-1), 45 p., $2.20
68	Application of Vehicle Operating Characteristics to Geometric Design and Traffic Operations (Proj. 3-10), 38 p., $2.00
69	Evaluation of Construction Control Procedures—Aggregate Gradation Variations and Effects (Proj. 10-2A), 58 p., $2.80
70	Social and Economic Factors Affecting Intercity Travel (Proj. 8-1), 68 p., $3.00
71	Analytical Study of Weighing Methods for Highway Vehicles in Motion (Proj. 7-3), 63 p., $2.80
72	Theory and Practice in Inverse Condemnation for Five Representative States (Proj. 11-2), 44 p., $2.20
73	Improved Criteria for Traffic Signal Systems on Urban Arterials (Proj. 3-5/1), 55 p., $2.80
74	Protective Coatings for Highway Structural Steel (Proj. 4-6), 64 p., $2.80
74A	Protective Coatings for Highway Structural Steel—Literature Survey (Proj. 4-6), 275 p., $8.00
74B	Protective Coatings for Highway Structural Steel—Current Highway Practices (Proj. 4-6), 102 p., $4.00
75	Effect of Highway Landscape Development on Nearby Property (Proj. 2-9), 82 p., $3.60
76	Detecting Seasonal Changes in Load-Carrying Capabilities of Flexible Pavements (Proj. 1-5(2)), 37 p., $2.00
77	Development of Design Criteria for Safer Luminaire Supports (Proj. 15-6), 82 p., $3.80
78	Highway Noise—Measurement, Simulation, and Mixed Reactions (Proj. 3-7), 78 p., $3.20
79	Development of Improved Methods for Reduction of Traffic Accidents (Proj. 17-1), 163 p., $6.40
80	Oversize-Overweight Permit Operation on State Highways (Proj. 2-10), 120 p., $5.20
81	Moving Behavior and Residential Choice—A National Survey (Proj. 8-6), 129 p., $5.60
82	National Survey of Transportation Attitudes and Behavior—Phase II Analysis Report (Proj. 20-4), 89 p., $4.00
83	Distribution of Wheel Loads on Highway Bridges (Proj. 12-2), 56 p., $2.80
84	Analysis and Projection of Research on Traffic Surveillance, Communication, and Control (Proj. 3-9), 48 p., $2.40
85	Development of Formed-in-Place Wet Reflective Markers (Proj. 5-5), 28 p., $1.80
86	Tentative Service Requirements for Bridge Rail Systems (Proj. 12-8), 62 p., $3.20
87	Rules of Discovery and Disclosure in Highway Condemnation Proceedings (Proj. 11-1(5)), 28 p., $2.00
88	Recognition of Benefits to Remainder Property in Highway Valuation Cases (Proj. 11-1(2)), 24 p., $2.00
89	Factors, Trends, and Guidelines Related to Trip Length (Proj. 7-4), 59 p., $3.20
90	Protection of Steel in Prestressed Concrete Bridges (Proj. 12-5), 86 p., $4.00
91	Effects of Deicing Salts on Water Quality and Biota—Literature Review and Recommended Research (Proj. 16-1), 70 p., $3.20
92	Valuation and Condemnation of Special Purpose Properties (Proj. 11-1(6)), 47 p., $2.60
93	Guidelines for Medial and Marginal Access Control on Major Roadways (Proj. 3-13), 147 p., $6.20
94	Valuation and Condemnation Problems Involving Trade Fixtures (Proj. 11-1(9)), 22 p., $1.80
95	Highway Fog (Proj. 5-6), 48 p., $2.40
96	Strategies for the Evaluation of Alternative Transportation Plans (Proj. 8-4), 111 p., $5.40
97	Analysis of Structural Behavior of AASHO Road Test Rigid Pavements (Proj. 1-4(1)A), 35 p., $2.60
98	Tests for Evaluating Degradation of Base Course Aggregates (Proj. 4-2), 98 p. $5.00
99	Visual Requirements in Night Driving (Proj. 5-3), 38 p., $2.60
100	Research Needs Relating to Performance of Aggregates in Highway Construction (Proj. 4-8), 68 p., $3.40
101	Effect of Stress on Freeze-Thaw Durability of Concrete Bridge Decks (Proj. 6-9), 70 p., $3.60
102	Effect of Weldments on the Fatigue Strength of Steel Beams (Proj. 12-7), 114 p., $5.40
103	Rapid Test Methods for Field Control of Highway Construction (Proj. 10-4), 89 p., $5.00
104	Rules of Compensability and Valuation Evidence for Highway Land Acquisition (Proj. 11-1), 77 p., $4.40

Rep. No. Title

105 Dynamic Pavement Loads of Heavy Highway Vehicles (Proj. 15-5), 94 p., $5.00
106 Revibration of Retarded Concrete for Continuous Bridge Decks (Proj. 18-1), 67 p., $3.40
107 New Approaches to Compensation for Residential Takings (Proj. 11-1(10)), 27 p., $2.40
108 Tentative Design Procedure for Riprap-Lined Channels (Proj. 15-2), 75 p., $4.00
109 Elastomeric Bearing Research (Proj. 12-9), 53 p., $3.00
110 Optimizing Street Operations Through Traffic Regulations and Control (Proj. 3-11), 100 p., $4.40
111 Running Costs of Motor Vehicles as Affected by Road Design and Traffic (Proj. 2-5A and 2-7), 97 p., $5.20
112 Junkyard Valuation—Salvage Industry Appraisal Principles Applicable to Highway Beautification (Proj. 11-3(2)), 41 p., $2.60
113 Optimizing Flow on Existing Street Networks (Proj. 3-14), 414 p., $15.60
114 Effects of Proposed Highway Improvements on Property Values (Proj. 11-1(1)), 42 p., $2.60
115 Guardrail Performance and Design (Proj. 15-1(2)), 70 p., $3.60
116 Structural Analysis and Design of Pipe Culverts (Proj. 15-3), 155 p., $6.40
117 Highway Noise—A Design Guide for Highway Engineers (Proj. 3-7), 79 p., $4.60
118 Location, Selection, and Maintenance of Highway Traffic Barriers (Proj. 15-1(2)), 96 p., $5.20
119 Control of Highway Advertising Signs—Some Legal Problems (Proj. 11-3(1)), 72 p., $3.60
120 Data Requirements for Metropolitan Transportation Planning (Proj. 8-7), 90 p., $4.80
121 Protection of Highway Utility (Proj. 8-5), 115 p., $5.60
122 Summary and Evaluation of Economic Consequences of Highway Improvements (Proj. 2-11), 324 p., $13.60
123 Development of Information Requirements and Transmission Techniques for Highway Users (Proj. 3-12), 239 p., $9.60
124 Improved Criteria for Traffic Signal Systems in Urban Networks (Proj. 3-5), 86 p., $4.80
125 Optimization of Density and Moisture Content Measurements by Nuclear Methods (Proj. 10-5A), 86 p., $4.40
126 Divergencies in Right-of-Way Valuation (Proj. 11-4), 57 p., $3.00
127 Snow Removal and Ice Control Techniques at Interchanges (Proj. 6-10), 90 p., $5.20
128 Evaluation of AASHO Interim Guides for Design of Pavement Structures (Proj. 1-11), 111 p., $5.60
129 Guardrail Crash Test Evaluation—New Concepts and End Designs (Proj. 15-1(2)), 89 p., $4.80
130 Roadway Delineation Systems (Proj. 5-7), 349 p., $14.00
131 Performance Budgeting System for Highway Maintenance Management (Proj. 19-2(4)), 213 p., $8.40
132 Relationships Between Physiographic Units and Highway Design Factors (Proj. 1-3(1)), 161 p., $7.20

Rep. No. Title

133 Procedures for Estimating Highway User Costs, Air Pollution, and Noise Effects (Proj. 7-8), 127 p., $5.60
134 Damages Due to Drainage, Runoff, Blasting, and Slides (Proj. 11-1(8)), 23 p., $2.80
135 Promising Replacements for Conventional Aggregates for Highway Use (Proj. 4-10), 53 p., $3.60
136 Estimating Peak Runoff Rates from Ungaged Small Rural Watersheds (Proj. 15-4), 85 p., $4.60
137 Roadside Development—Evaluation of Research (Proj. 16-2), 78 p., $4.20
138 Instrumentation for Measurement of Moisture—Literature Review and Recommended Research (Proj. 21-1), 60 p., $4.00
139 Flexible Pavement Design and Management—Systems Formulation (Proj. 1-10), 64 p., $4.40
140 Flexible Pavement Design and Management—Materials Characterization (Proj. 1-10), 118 p., $5.60
141 Changes in Legal Vehicle Weights and Dimensions—Some Economic Effects on Highways (Proj. 19-3), 184 p., $8.40
142 Valuation of Air Space (Proj. 11-5), 48 p., $4.00
143 Bus Use of Highways—State of the Art (Proj. 8-10), 406 p., $16.00
144 Highway Noise—A Field Evaluation of Traffic Noise Reduction Measures (Proj. 3-7), 80 p., $4.40
145 Improving Traffic Operations and Safety at Exit Gore Areas (Proj. 3-17) 120 p., $6.00
146 Alternative Multimodal Passenger Transportation Systems—Comparative Economic Analysis (Proj. 8-9), 68 p., $4.00
147 Fatigue Strength of Steel Beams with Welded Stiffeners and Attachments (Proj. 12-7), 85 p., $4.80
148 Roadside Safety Improvement Programs on Freeways—A Cost-Effectiveness Priority Approach (Proj. 20-7), 64 p., $4.00
149 Bridge Rail Design—Factors, Trends, and Guidelines (Proj. 12-8), 49 p., $4.00
150 Effect of Curb Geometry and Location on Vehicle Behavior (Proj. 20-7), 88 p., $4.80
151 Locked-Wheel Pavement Skid Tester Correlation and Calibration Techniques (Proj. 1-12(2)), 100 p., $6.00
152 Warrants for Highway Lighting (Proj. 5-8), 117 p., $6.40
153 Recommended Procedures for Vehicle Crash Testing of Highway Appurtenances (Proj. 22-2), 19 p., $3.20
154 Determining Pavement Skid-Resistance Requirements at Intersections and Braking Sites (Proj. 1-12), 64 p., $4.40

Synthesis of Highway Practice

No. Title

1 Traffic Control for Freeway Maintenance (Proj. 20-5, Topic 1), 47 p., $2.20
2 Bridge Approach Design and Construction Practices (Proj. 20-5, Topic 2), 30 p., $2.00
3 Traffic-Safe and Hydraulically Efficient Drainage Practice (Proj. 20-5, Topic 4), 38 p., $2.20
4 Concrete Bridge Deck Durability (Proj. 20-5, Topic 3), 28 p., $2.20
5 Scour at Bridge Waterways (Proj. 20-5, Topic 5), 37 p., $2.40
6 Principles of Project Scheduling and Monitoring (Proj. 20-5, Topic 6), 43 p., $2.40
7 Motorist Aid Systems (Proj. 20-5, Topic 3-01), 28 p., $2.40
8 Construction of Embankments (Proj. 20-5, Topic 9), 38 p., $2.40
9 Pavement Rehabilitation—Materials and Techniques (Proj. 20-5, Topic 8), 41 p., $2.80
10 Recruiting, Training, and Retaining Maintenance and Equipment Personnel (Proj. 20-5, Topic 10), 35 p., $2.80
11 Development of Management Capability (Proj. 20-5, Topic 12), 50 p., $3.20
12 Telecommunications Systems for Highway Administration and Operations (Proj. 20-5, Topic 3-03), 29 p., $2.80
13 Radio Spectrum Frequency Management (Proj. 20-5, Topic 3-03), 32 p., $2.80
14 Skid Resistance (Proj. 20-5, Topic 7), 66 p., $4.00
15 Statewide Transportation Planning—Needs and Requirements (Proj. 20-5, Topic 3-02), 41 p., $3.60
16 Continuously Reinforced Concrete Pavement (Proj. 20-5, Topic 3-08), 23 p., $2.80
17 Pavement Traffic Marking—Materials and Application Affecting Serviceability (Proj. 20-5, Topic 3-05), 44 p., $3.60
18 Erosion Control on Highway Construction (Proj. 20-5, Topic 4-01), 52 p., $4.00
19 Design, Construction, and Maintenance of PCC Pavement Joints (Proj. 20-5, Topic 3-04), 40 p., $3.60
20 Rest Areas (Proj. 20-5, Topic 4-04), 38 p., $3.60
21 Highway Location Reference Methods (Proj. 20-5, Topic 4-06), 30 p., $3.20
22 Maintenance Management of Traffic Signal Equipment and Systems (Proj. 20-5, Topic 4-03) 41 p., $4.00
23 Getting Research Findings into Practice (Proj. 20-5, Topic 11) 24 p., $3.20
24 Minimizing Deicing Chemical Use (Proj. 20-5, Topic 4-02), 58 p., $4.00
25 Reconditioning High-Volume Freeways in Urban Areas (Proj. 20-5, Topic 5-01), 56 p., $4.00
26 Roadway Design in Seasonal Frost Areas (Proj. 20-5, Topic 3-07), 104 p., $6.00

THE TRANSPORTATION RESEARCH BOARD is an agency of the National Research Council, which serves the National Academy of Sciences and the National Academy of Engineering. The Board's purpose is to stimulate research concerning the nature and performance of transportation systems, to disseminate information that the research produces, and to encourage the application of appropriate research findings. The Board's program is carried out by more than 150 committees and task forces composed of more than 1,800 administrators, engineers, social scientists, and educators who serve without compensation. The program is supported by state transportation and highway departments, the U.S. Department of Transportation, and other organizations interested in the development of transportation.

The Transportation Research Board operates within the Commission on Sociotechnical Systems of the National Research Council. The Council was organized in 1916 at the request of President Woodrow Wilson as an agency of the National Academy of Sciences to enable the broad community of scientists and engineers to associate their efforts with those of the Academy membership. Members of the Council are appointed by the president of the Academy and are drawn from academic, industrial, and governmental organizations throughout the United States.

The National Academy of Sciences was established by a congressional act of incorporation signed by President Abraham Lincoln on March 3, 1863, to further science and its use for the general welfare by bringing together the most qualified individuals to deal with scientific and technological problems of broad significance. It is a private, honorary organization of more than 1,000 scientists elected on the basis of outstanding contributions to knowledge and is supported by private and public funds. Under the terms of its congressional charter, the Academy is called upon to act as an official—yet independent—advisor to the federal government in any matter of science and technology, although it is not a government agency and its activities are not limited to those on behalf of the government.

To share in the tasks of furthering science and engineering and of advising the federal government, the National Academy of Engineering was established on December 5, 1964, under the authority of the act of incorporation of the National Academy of Sciences. Its advisory activities are closely coordinated with those of the National Academy of Sciences, but it is independent and autonomous in its organization and election of members.

TRANSPORTATION RESEARCH BOARD
National Research Council
2101 Constitution Avenue, N.W.
Washington, D.C. 20418

ADDRESS CORRECTION REQUESTED